5-2011

The Role of Albino3 and the Lipid Environment in Chloroplast Signal Recognition Particle Targeting

Nathan Lewis
University of Arkansas

THE ROLE OF ALBINO3 AND THE LIPID ENVIRONMENT IN CHLOROPLAST SIGNAL RECOGNITION PARTICLE TARGETING

THE ROLE OF ALBINO3 AND THE LIPID ENVIRONMENT IN CHLOROPLAST SIGNAL RECOGNITION PARTICLE TARGETING

A dissertation submitted in partial fulfillment
of the requirements for the degree of
Doctor of Philosophy in Cell and Molecular Biology

By

Nathaniel E. Lewis
Missouri State University
Bachelor of Science in Print Journalism, 2003

May 2011
University of Arkansas

ABSTRACT

Signal recognition particles (SRPs) in pro- and eukaryotes function in cotranslational targeting of nascent poplypeptides to an SRP receptor at the target membrane. A unique chloroplast SRP (cpSRP) functions post-translationally to direct light-harvesting chlorophyll-binding proteins (LHCPs) to the receptor cpFtsY at the thylakoid membrane for LHCP insertion in a process involving the integral membrane protein Albino3 (Alb3) and requiring GTP. Work here focuses on understanding cpSRP targeting events at the thylakoid membrane, specifically those involving Alb3 and the lipid environment.

We show an interaction between the novel cpSRP subunit cpSRP43 and the soluble, stromal-exposed C terminus of Albino3 (Alb3-Cterm). We determine that the site for this interaction is housed in an ankyrin repeat region of cpSRP43. Further, we provide functional relevance to this interaction within the overall targeting pathway. We also examine the role of lipids in cpSRP targeting and show the ability of artificial liposomes to support critical cpSRP functions. Work was also done in creating thylakoid-mimicking liposomes and using various microscopy techniques to visualize targeting components in a lipid environment. Finally, we report an interaction between Alb3 and the *Arabidopsis thaliana* large ribosomal subunit protein L23, which hints at a cotranslational function for Alb3.

This dissertation is approved for recommendation to the Graduate Council.

Dissertation Director:

_____

Dr. Robyn L. Goforth

Dissertation Committee:

_____

Dr. Ralph L. Henry

_____

Dr. Roger E. Koeppe, II

_____

Dr. Dan J. Davis

_____

Dr. Greg J. Salamo

DISSERTATION DUPLICATION RELEASE

I hereby authorize the University of Arkansas Libraries to duplicate this dissertation when needed for research and/or scholarship.

Agreed _____

Nathaniel E. Lewis

Refused _____

Nathaniel E. Lewis

ACKNOWLEDGEMENTS

I would like to thank my advisor, Dr. Robyn Goforth, for not just teaching me, but for showing me how to be a scientist. Few graduate students have the opportunity, as I did, to work beside their advisor throughout their career. The example you set and the guidance you provided every day were truly invaluable.

I would also like to thank Dr. Ralph Henry for taking a chance on a sports journalist with a smart wife. I literally would not be here if you had not made it possible for me to come back to science. And thank you for making science fun.

I would like to acknowledge my committee members – Dr. Roger Koeppe, Dr. Dan Davis, and Dr. Greg Salamo. Thank you for your time, editing, and guidance.

I owe a tremendous amount of thanks to all my coworkers and fellow graduate students I had the pleasure of working with over my graduate student career. In particular, Alicia Brown, who has an amazing ability to answer any question, both the first and the tenth time you ask; and Naomi Marty, who showed me how to organize and execute an assay.

Thanks to my family for all the love and support and for your very evident pride in my accomplishments.

And, I would like to thank my lovely wife Penny. You are my constant source of inspiration, support, and encouragement. Thank you for believing in me, always. And to my two boys – Isaac and Asher – "Dig-Dag" loves you more than you will ever know.

TABLE OF CONTENTS

TABLE OF FIGURES

ABBREVIATIONS

ΔpH – pH gradient across a membrane

ΔΨ – electrical gradient across a membrane

Alb3 – Albino3 protein

Alb3-50aa – 50 amino acid peptide from stromal facing loop of Alb3

AFM – atomic force microscope

ATP – adenosine triphosphate

BSA – bovine serum albumin

cDNA – complementary DNA

Chl or chl – chlorophyll

cpSec – chloroplast secretory

cpSRP – chloroplast signal recognition particle

cpSRP43 – 43 kDa subunit of the cpSRP

cpSRP54 – 54 kDa subunit of the cpSRP

cpFtsY – chloroplast FtsY homologue (cpSRP receptor)

cpSecA – chloroplast SecA

cpTat – chloroplast twin-arginine translocation

cpTatC – cpTat subunit C

CLSM – confocal laser scanning microscope

DNA – deoxyribonucleic acid

ER – endoplasmic reticulum

Ffh – fifty-four homologue

FtsY – SRα homologue in bacteria

GDP – guanosine diphosphate

GMP-PNP – 5'-guanyl-imidodiphosphate trisodium salt

GST – glutathione S-transferase

GTP – guanosine triphosphate

Hcf106 – cpTat translocon subunit homologous to bacterial TatB subunit

HKM – 10 mM HEPES-KOH pH 8, 10 mM $MgCl_2$

IB – import buffer, 50 mM HEPES-KOH pH 8, 0.33 M sorbitol

IBM – IB, 10mM $MgCl_2$

IgG – immunoglobulin G

ITC – isothermal titration calorimetry

K_d – dissociation constant

kDa/kD – kiloDalton

L23 – *Arabidopsis Thaliana* large ribosomal subunit protein L23

LHCP – light-harvesting chlorophyll-binding protein

Maltoside – n-Dodecyl β-D-Maltoside

min – minute

NMR – nuclear magnetic resonance

OE17 – 17 kDa component of the oxygen evolving complex

OE23 – 23 kDa component of the oxygen evolving complex

OE33 – 33 kDa component of the oxygen evolving complex

PBS – phosphate buffered saline

PCR – polymerase chain reaction

PI – preimmune

PMF – proton motive force

PsaG, PsaK – photosystem I reaction center proteins G, K

PsbX, PsbS, PsbW, PsbY – photosystem II reaction center proteins X, S, W, Y

PT – protease-treated

PVDF – polyvinylidene fluoride

RNA – ribonucleic acid

RNC – ribosome nascent chain complex

RT-PCR – reverse transcription PCR

SE – stromal extract

Sec – secretory

SecA – cytosolic chaperone in Sec pathway

SecB – cytosolic chaperone in Sec pathway

SecYEG – Y, E, G subunits of the bacterial Sec translocon

Sec61αγβ – α, γ, β subunits of the eukaryotic Sec translocon

SecGDFyajC – G, D, F, yajC subunits of the bacterial Sec translocon

SDS – sodium dodecylsulfate

SDS-PAGE – SDS-polyacrylamide gel electrophoresis

SR – SRP receptor

SRα, SRβ – α and β subunits of the SR

SRP – signal recognition particle

SW – salt-washed

Tat – twin-arginine translocation

TatA, TatB, TatC – A, B, C subunits of the bacterial Tat translocon

Tic – translocase at the inner membrane of the chloroplast

Tha4 – cpTat translocon subunit homologous to bacterial TatA

Toc – translocase at the outer membrane of the chloroplast

TEM – transmission electron microsocope

TM – transmembrane domain

TP – translation product

Trx-tag – thioredoxin tag

WT – wild-type

WORKS PUBLISHED

Marty, N. J., Rajalingam, D., Kight, A. D., **Lewis, N. E.**, Fologea, D., Kumar, T. K. S., Henry, R. L., and Goforth, R. L. (2009) The Membrane-binding Motif of the Chloroplast Signal Recognition Particle Receptor (cpFtsY) Regulates GTPase Activity, *J. Biol. Chem. 284*, 14891-14903.

Lewis, N. E., Marty, N. J., Kathir, K. M., Rajalingam, D., Kight, A. D., Daily, A., Kumar, T. K., Henry, R. L., and Goforth, R. L. (2010) A dynamic cpSRP43-Albino3 interaction mediates translocase regulation of chloroplast signal recognition particle (cpSRP)-targeting components, *J Biol Chem 285*, 34220-34230.

Lewis, N.E., Kight, A., Daily, A., Kumar, T.K.S., Henry, R.L., and Goforth R.L. (2010) Response to Falk and Sinning: The C Terminus of Alb3 Interacts with the Chromodomains 2 and 3 of cpSRP43, *J. Biol. Chem*. 285, le26-le28.

I

INTRODUCTION

INTRODUCTION

Sorting, routing and localization of proteins to specific sites within the cell are critical requirements that allow for compartmentalization of functionally diverse molecules into highly organized and specialized regions. The majority of proteins are synthesized in the cytosol and must then be trafficked to the appropriate membrane or organelle. Once proteins are routed to a specific organelle, such as mitochondria, endoplasmic reticulum, or chloroplasts, further targeting to an exact site of function, such as a specific membrane or soluble space, is necessary.

Work presented here focuses on protein targeting to the chloroplast thylakoid membrane by the chloroplast signal recognition particle (cpSRP) pathway. The aim of this work is to elucidate the role of the integral membrane cpSRP insertase Albino3 (Alb3) and the lipid environment of the targeted thylakoid membrane. This work identifies key membrane interactions and the function of those interactions in cpSRP targeting.

Protein targeting to membranes is accomplished by different pathways and components depending on the substrate and its targeted destination. However, despite the different routes, most targeting systems share basic components – a recognition element which identifies a particular substrate with its destination, an energy source to power the translocation event, a pore-complex which regulates substrate passage into and through membranes, and often soluble and membrane-bound protein components which aid in or are essential to targeting. The many variations of the basic targeting pathway theme show the high degree of specialization that exists both intracellularly and across different domains of life. Much of what is known about protein targeting comes from bacterial

export systems, which are the most heavily studied targeting pathways. Regardless of pathway or organism, however, the soluble targeting components and their functions are better characterized than the membrane components and membrane-associated steps.

CHLOROPLAST THYLAKOID TARGETING

Chloroplast proteins are derived from two distinct genomes, that of the nucleus and the plastid. The vast majority (> 95 %) of chloroplast proteins are encoded in the nucleus (*1*), synthesized in the cytosol, and then must be imported into the chloroplast. These proteins contain a transit peptide that minimally specifies chloroplast import and sometimes the final destination. Due to the post-translational nature of these imported proteins, many of which are integral membrane proteins, chaperones, including heat shock proteins among others, are heavily involved in order to maintain substrate solubility prior to chloroplast import. Not all chloroplast targeted proteins are routed to the thylakoid. There are two other potential chloroplast membrane destinations, the outer envelope and the inner envelope, but these are outside the scope of this research [for review see (*2*)]. For proteins destined for the thylakoid, they must first pass through the outer and inner chloroplast membranes. This translocation is accomplished by the translocon of the outer envelope membrane of chloroplasts (TOC) and the translocon of the inner envelope membrane of chloroplasts (TIC). Another subset of proteins, those encoded by the chloroplast genome, are cotranslationally targeted as a ribosome nascent chain complex (RNC). Regardless of genomic origin, stromal proteins continuing to the thylakoid membrane or lumen are targeted by one of four different pathways – the chloroplast secretory (cpSec) pathway, the chloroplast twin arginine translocation (cpTat) pathway, the spontaneous pathway, or the cpSRP pathway (Fig. 1.1). These pathways, except for the spontaneous pathway to which no proteinaceous or energy requirements have been reported, all utilize an integral membrane protein translocase/insertase and an energy source driving the event. A detailed overview of each pathway covering substrate

recognition elements, known substrates, soluble and membrane protein components, and energy requirements is given below and summarized in Fig. 1.1.

Secretory Pathway

Sec systems are found in the eukaryotic endoplasmic reticulum (*3*), the plasma membrane of both Archaea (*4*) and Eubacteria (*5-7*), and the chloroplast thylakoid membranes of plants and algae (*8-9*). All Sec systems involve soluble accessory proteins, which vary depending on the organism, and a protein conducting channel. One conserved, critical targeting factor is the GTPase SecA, which powers the Sec translocation event. The channel consists primarily of two membrane proteins, the multi-spanning SecY (Sec61α) and the single spanning SecE (Sec61γ), but bacterial channels also contain SecG.

Understanding of the cpSec pathway has greatly benefited from advances in the study of the related Sec protein machinery in *E. coli*. But while much homology between bacterial and chloroplast Sec components has been shown, much of the chloroplast system remains unclear. No homologs of the bacterial chaperone SecB have been found, nor have any stromal chaperone/accessory proteins been identified. Other components present in *Escherichia coli* Sec system, which exports proteins across the plasma membrane, but lacking in the chloroplast system are members of the membrane complex SecDFyajC [for review see (*10-12*)].

The most well studied role of the versatile cpSec system is the post-translational translocation of substrates across the thylakoid membrane into the lumen. It is estimated that half of all lumenal proteins are transported by the cpSec pathway, with the other half reaching the lumen via the cpTat pathway. However, a second function of the Sec

translocon is the cotranslational integration of membrane spanning proteins into the lipid bilayer of the thylakoid. One shared feature of all cpSec transported substrates is the requirement to be in an unfolded state. With the absence of identified soluble chaperone and accessory proteins in the cpSec pathway, it remains to be known how substrates are unfolded prior to translocation or, alternatively, how cpSec substrates are maintained in an unfolded state in the chloroplast stroma.

Post-translation substrates of the cpSec pathway, including the identified plastocyanin and a 33-kDa subunit of the oxygen evolving complex (OE33), are targeted to the thylakoid lumen (*8, 13*). All post-translational Sec substrates contain an N-terminal stroma-targeting transit peptide, which is cleaved by stromal processing peptidase (SPP) after import into the chloroplast. This cleavage reveals a second targeting peptide, the lumenal-targeting signal peptide. Signal peptides of both the Sec and TAT pathways contain a large, acidic N-domain, an internal hydrophobic domain, and a polar C-terminal domain ending with A-X-A, which is the cleavage site for the thylakoid processing peptidase (TPP) after lumenal entry (*14*).

Mechanistically, the chloroplast Sec system operates quite similarly to the *E. coli* system (*15-16*). Unfolded precursors, in the absence of ATP, can bind the thylakoid. This membrane binding is stimulated by cpSecA, and cross-linking experiments have revealed a membrane complex containing substrate, cpSecA, and cpSecY (*17*). The translocation event requires ATP and is driven by a bind and release mechanism involving the ATPase cpSecA (*17*). Translocation inhibition using azide (SecA inhibitor) (*8, 18*) or anti-cpSecY IgG pretreatment (*19*) has been demonstrated.

The cpSecYE translocase also participates in cotranslational integration of thylakoid membrane proteins. Less is known about the targeting of these plastid-encoded substrates due to the difficultly in recreating the pathway using isolated thylakoid assays. Not only does it require all the necessary components for an *in vitro* translation system, but these membrane proteins are often part of larger complexes, which greatly complicates reconstitution. Thus the evidence for the known cotranslational cpSec substrates, cytochrome F and photosystem 2 subunit D, is mainly indirect. Cytochrome F is inserted into the thylakoid membrane as a single transmembrane anchor with a large lumenal domain. Cytochrome F was first shown as a cpSec substrate when the precursor accumulated in a cpSecA null maize mutant (*20*). These results were verified by pathway reconstitution assays (*21*-*22*). This shows that cpSecA is critical in cotranslational cpSec targeting. The possibility exists that cpSRP54 is also bound to the cytochrome F RNC complex (*23*), but results have been unclear (*22*). A second cotranslational substrate of the cpSec pathway is D1. Pulse-chase radiolabel assays in intact chloroplasts have shown D1 associates with SecY as a RNC, not as a full-length protein (*24*). This work also showed an association between SecY and the chloroplast ribosome. *In vitro* translation of D1 has shown an interaction between the nascent chain and cpSRP54 (*25*-*26*). Further, *Chlamydomonas reinhardtii* Alb3 knockout mutants show production of D1, but a lack of assembly into PSII (*27*). Taken together, these results suggest cpSRP54 targets a D1 RNC to the cpSecYE translocase for integration. D1 is then assembled into PSII in a process involving Alb3, but not cpSecYE (*24*).

Twin Arginine Translocation Pathway

There are two features that distinguish substrates of the cpTAT pathway from cpSec substrates. Like Sec substrates, cpTat precursors contain a bipartite transit sequence. Upon import into the stroma, the transit sequence is cleaved, revealing a lumenal signal peptide with the same basic makeup as Sec substrates (N-domain, H-domain, and C-domain). cpTat precursors, however, are distinguished by two arginine residues in the N-domain of the signal peptide, which gives the pathway its name (*14*). A second difference from the cpSec pathway is the ability of the cpTAT pathway to translocate fully folded substrates. Folded cpTat transport was suggested based on the tight folding of natural cpTat substrates (*28-29*), and confirmed when internally cross-linked proteins fused to cpTat substrates were effectively transported (*30-31*). However, evidence exists that cpTat also has the ability to handle misfolded and unfolded proteins as well (*31*).

Unlike chloroplast Sec, where much of what is known comes from the homologous bacterial system, the first Tat pathway component was identified in thylakoid studies (*32-33*). A homolog of this initial component, High chlorophyll fluorescence 106 (Hcf106), was subsequently identified in prokaryotes (the Tat system is absent from fungi and animals) and advances in Tat pathway understanding have come from both bacterial and thylakoid work.

In addition to Hcf106 (TatB in bacteria), two other proteins makeup the cpTat translocase. Tha4 (TatA), like Hcf106, is a single span membrane protein (*34*). The third component, cpTatC (TatC) contains six transmembrane domains (*35*). All three components are required for cpTat function, as antibodies against any of the three

proteins abolishes the pathway (*19, 35*). The three integral membrane cpTat components exist in two distinct populations. cpTatC and Hcf106 exist in a ~700 kDa complex that contains multiple copies of the two proteins in a 1:1 ratio (*36*). Tha4 exists in a separate subpopulation as a homo-oligomer (*37-38*). The cpTatc-Hcf106 complex serves as the cpTat receptor, binding precursors in the absence of Tha4 (*36, 39*). Binding and cross-linking of the cpTat substrate OE17 precursor to the cpTat receptor complex revealed the signal peptide, near the double arginine residues, interacted with cpTatC, and the hydrophobic region of the signal peptide interacted with Hcf106 (*40-41*). This compliments other work showing the twin arginine motif and a continuous hydrophobic domain of the signal peptide are necessary and sufficient for cpTat receptor binding (*39, 41-42*). Results from the bacterial Tat pathway show two precursors can simultaneously bind one cpTatC-Hcf106 receptor complex (*43*). More recent work with cpTat shows as many as four precursors can bind a single receptor complex and be transported simultaneously with an efficiency near that of monomer translocation (*44*). The cpTat substrate OE17 binds first to the thylakoid lipid membrane, not the receptor complex (*29*). Similarly, a chimeric precursor called 16/23, bound thylakoids and produced a degradation fragment after proteolysis, indicating partial insertion into the lipid bilayer prior to translocation (*45*). These substrates are thought to interact with the receptor at a later stage.

The functional cpTat translocase is formed only in the presence of receptor-bound precursor and the establishment of a membrane ΔpH (*38-39*). Satisfaction of those two requirements triggers assembly of a cpTatC-Hcf106-Tha4 complex. The oligomerization state of Tha4 in the final cpTat translocase varies, ranging up to decamers (*37*). The

requirement of Tha4 recruitment to form the active translocase coupled with the varying number of Tha4 molecules present in said translocase have led to models predicting a central role for Tha4 in cpTat substrate translocation. Translocating folded proteins of various sizes across a membrane without membrane leaking is a difficult task. One model proposes that the number of Tha4 molecules in the translocase depends on the size of substrate (*46*). For larger substrates, more Tha4 would assist in forming a larger membrane pore through which the protein would pass. However, substrate size does not seem to correspond to increased oligomers of Tha4 (*37*). A second model proposes that recruitment of Tha4, followed by possible structural changes, locally weakens the membrane, allowing substrate to pass through in a Tha4-assisted manner (*38, 47*). Future work will help to further evaluate each model. Regardless of how the physical process happens, the energy required for cpTat translocation is supplied by the electrochemical potential, which is primarily in the form of a pH gradient. Initial investigations into the energy requirements of the cpTat pathway were *in vitro* transport assays using isolated chloroplasts or thylakoids. This work showed no requirement for nucleotide triphosphates, but that the proton gradient (ΔpH) is both essential and exclusive to drive cpTat transport (*48-49*). Later *in vivo* studies have shown ΔpH is not strictly required, and that the electric potential (Δψ) may be sufficient in place of ΔpH (*50-51*). Follow-up *in vivo* studies have shown that cpTat transport may be possible in the total absence of a ΔpH and an electric potential (*52*). Further work is needed to settle the seeming discrepancy between *in vitro* and *in vivo* results.

Spontaneous Pathway

A third thylakoid targeting pathway is unique to chloroplasts and is unlike the other plastid targeting pathways in that it has neither proteinaceous nor energy requirements [for review see (*53*)]. Many integral thylakoid proteins, ranging from single span to multi-spanning, seem to integrate via the spontaneous pathways, yet little is known about the mechanism of insertion. Spontaneous insertion was initially characterized for single-span, nuclear-encoded subunits of the ATP synthase complex (CFoII) (*54*) and photosystem II (PsbW and PsbX) (*55*). These proteins contain a Sec-like bipartite transit sequence, but isolated thylakoid integration experiments have shown insertion does not require stromal extract, nucleotide triphosphates or a known translocon (*54-58*). An insertion mechanism has been proposed whereby the thylakoid localization signal serves as a second hydrophobic region. The two hydrophobic domains insert and the hydrophilic region forms a lumen-exposed loop (*58*). Signal sequence cleavage by TPP forms the mature protein.

Nuclear-encoded photosystem I subunits PsaK and PsaG also spontaneously insert. These proteins contain two transmembrane domains, with an N and C terminus extending into the lumen and a positively-charged, stromal-exposed loop region (*59-60*). Unlike the spontaneous single-span proteins, whose insertion is proposed to be driven by hydrophobic interactions, the positive loop region of these double-span proteins is critical for integration (*60*).

A third class of spontaneously inserting proteins are nuclear-encoded and multi-spanning (PsbY, Elip2, PsbS, cpSecE, Tha4, and Hcf106) (*55, 61-63*). However, *in vitro* results seem to show insertion of Elip2 and PsbS is not always truly spontaneous and may

require stromal factors and nucleotide triphosphates (*61*). Interestingly, the third member of the cpTat translocase, cpTatC, does not insert spontaneously and requires additional targeting factors, but does not use any of the traditional translocons for insertion. Martin et al. (*64*) speculate that cpTatC, and possibly other translocase proteins, may insert by a yet unknown pathway involving the insertase Alb4 or SecY2, homologs of Alb3 and SecY respectively.

Signal Recognition Particle Pathway

The signal recognition particle (SRP) targeting pathway is present across all domains of life, targeting proteins to the endoplasmic reticulum, cytoplasmic membrane and chloroplast thylakoid membrane [for review see (*65*)]. Much conservation is observed across all SRP pathways, but key differences exist as well, particularly in the chloroplast system (Fig. 1.2). While other SRP systems target a host of substrates, cpSRP seems specific for a family of light-harvesting chlorophyll-binding proteins (LHCPs). LHCPs are synthesized in the cytosol and must then be imported through the chloroplast outer and inner envelope (via TOC and TIC) into the stroma before targeting to the thylakoid membrane. This highlights a main difference in cpSRP targeting compared to other systems – because LHCP is translated in the cytosol and must then be imported, cpSRP functions post-translationally. Mammalian and bacterial SRPs function cotranslationally, targeting the ribosome nascent chain complex (RNC) to the membrane for integration.

All SRPs contain a conserved 54-kDa GTPase subunit called SRP54 in mammals, fifty four homolog (ffh) in bacteria, and cpSRP54 in plants. The mammalian and bacterial SRP molecules also contain an RNA-moiety that is lacking in chloroplasts. The cpSRP

molecule, however, contains a unique 43-kDa subunit (cpSRP43) that is critical to cpSRP targeting (*66-67*) (Fig. 1.2). Conservation also exists between SRP receptor (SR) molecules. All hydrolyze GTP, although the mammalian SR contains a second integral membrane GTPase receptor subunit (SRβ) tethered to the membrane-associated subunit (SRα). SRα is homologous to the *E. coli* and chloroplast SR (FtsY and cpFtsY, respectively), which both partition between the membrane and soluble phase (Fig. 1.2). The mammalian and bacterial SRP pathways ultimately target to a Sec translocase, with YidC also functioning in integration of SRP-targeted substrates in bacteria (*65*). While preliminary evidence exists for cotranslational cpSRP54 targeting to a cpSec translocase (*24-26*), the most studied cpSRP insertase is the YidC family member Alb3 (*68*) (Fig. 1.2). Mitochondrial Oxa1 is a third member of the YidC/Alb3 family, and more recent work has identified a second family member in chloroplasts (Alb4) (*69*) and gram positive bacteria (YidC2) (*70*).

Like the mammalian and bacterial counterparts, cpSRP54 is composed of an NG-domain that binds and hydrolyzes GTP and a C-terminal M-domain (*71*). In cotranslational systems, the M-domain binds the ribosome, the RNA moiety, and samples peptides as they emerge from the ribosome, binding the hydrophobic signal sequence of SRP substrates (*65, 72-73*). In post-translational cpSRP targeting, which lacks a RNC and RNA moiety, the M-domain interacts with cpSRP43 to form the cpSRP heterodimer molecule (*74-76*). cpSRP43 is made up almost entirely of protein interaction domains. It is composed of three chromodomains (CD), one at the N terminus (CD1) and two at the C terminus (CD2 and CD3). The central region of the molecule is made up of four ankyrin (Ank) repeats (Ank1, Ank2, Ank3 and Ank4) (*74-76*). Using a variety of

methods including pepscan, yeast-two- hybrid, copurification, and ITC, CD2 was identified and confirmed as the interaction site with the M-domain of cpSRP54 (*75-78*). *In vitro* experiments have shown formation of the SRP heterodimer is a critical interaction and that absence of either subunit abolishes LHCP integration (*74, 79*). However, more recent *in vivo* results show that in the absence of cpSRP54 (and cpFtsY), LHCP is integrated via a cpSRP43 only pathway (*80*).

Interaction of the cpSRP dimer with LHCP, post stromal import, forms the targeting molecule termed transit complex, which maintains the highly hydrophobic LHCP in soluble, integration competent state (*81*). An 18 amino acid segment of LHCP (L18) located between transmembrane domains 2 and 3 interacts with the Ank region of cpSRP43, specifically Ank1 (*75, 82-83*), while the M-domain of cpSRP54 binds hydrophobic sequences. Recent work has shown cpSRP43 exhibits a unique chaperone ability for the substrate LHCP. cpSRP43, independent of cpSRP54 and ATP, can reverse aggregation of LHCP (*84-85*). However, the functional relevance of this disaggregase activity has not been shown. In addition to maintaining LHCP solubility, transit complex formation is thought to prime cpSRP54 for GTP binding, based on homologous systems (*86*).

At the thylakoid membrane, transit complex docks with the receptor cpFtY (*87-88*), which interacts with the NG-domain of cpSRP54 (*89*). cpFtsY partitions between the stroma and thylakoid (*88, 90*), but no evidence exists of a soluble cpFtsY-transit complex molecule. In addition, cpFtsY tethered to the thylakoid membrane is fully functional in LHCP integration suggesting that the partitioning is not required (*90*). cpFtsY contains a short N-terminal region responsible for membrane binding (*90*) and a conserved NG-

domain that house GTPase activity (*87*). Once membrane and GTP bound, cpFtsY is primed for interaction with cpSRP. Likewise, GTP-bound transit complex in the stroma targets to and interacts with GTP-bound FtsY at the thylakoid membrane. It is likely that this membrane complex forms and is then directed to Alb3, since formation at the membrane can take place in the absence of an available Alb3 (*91*) (See Fig. 1.3 for a model of cpSRP targeting).

Alb3 is known to play a role in the insertion of LHCP (*68*), however the mechanism is not known. Nor has it been shown that Alb3 acts as the insertase, although this is largely assumed. The possibility exists that Alb3 holds delivered LHCP in a competent state for chlorophyll attachment and downstream assembly, thereby acting as a chaperone (*92*). It is also possible that the cpSec translocase plays a role, as it is known to exist in a complex with Alb3 (*93*), and can be copurified with a cpSRP/cpFtsY membrane complex locked at Alb3 using non-hydrolyzable GTP analogs (*91*). However, the fact that antibodies to cpSecY do not affect LHCP integration argues against a role of the cpSec translocase in LHCP insertion (*19*).

As the lack of understanding about the role of Alb3 shows, the picture of cpSRP targeting begins to cloud at the membrane. Much is still unknown about the membrane-associated targeting steps and about the mechanism of LHCP insertion. Thus, we set out to answer important question concerning cpSRP membrane events. How does the SRP membrane complex associate with Alb3? What triggers/regulates membrane events including LHCP release and GTP hydrolysis? What role, if any, does the lipid environment play? Does Alb3 operate outside LHCP integration, perhaps in a cotranslational role like family members YidC and Oxa1? Work done here not only helps

answers those and other essential questions, but adds to the overall understanding of cpSRP targeting events that take place at the membrane interface.

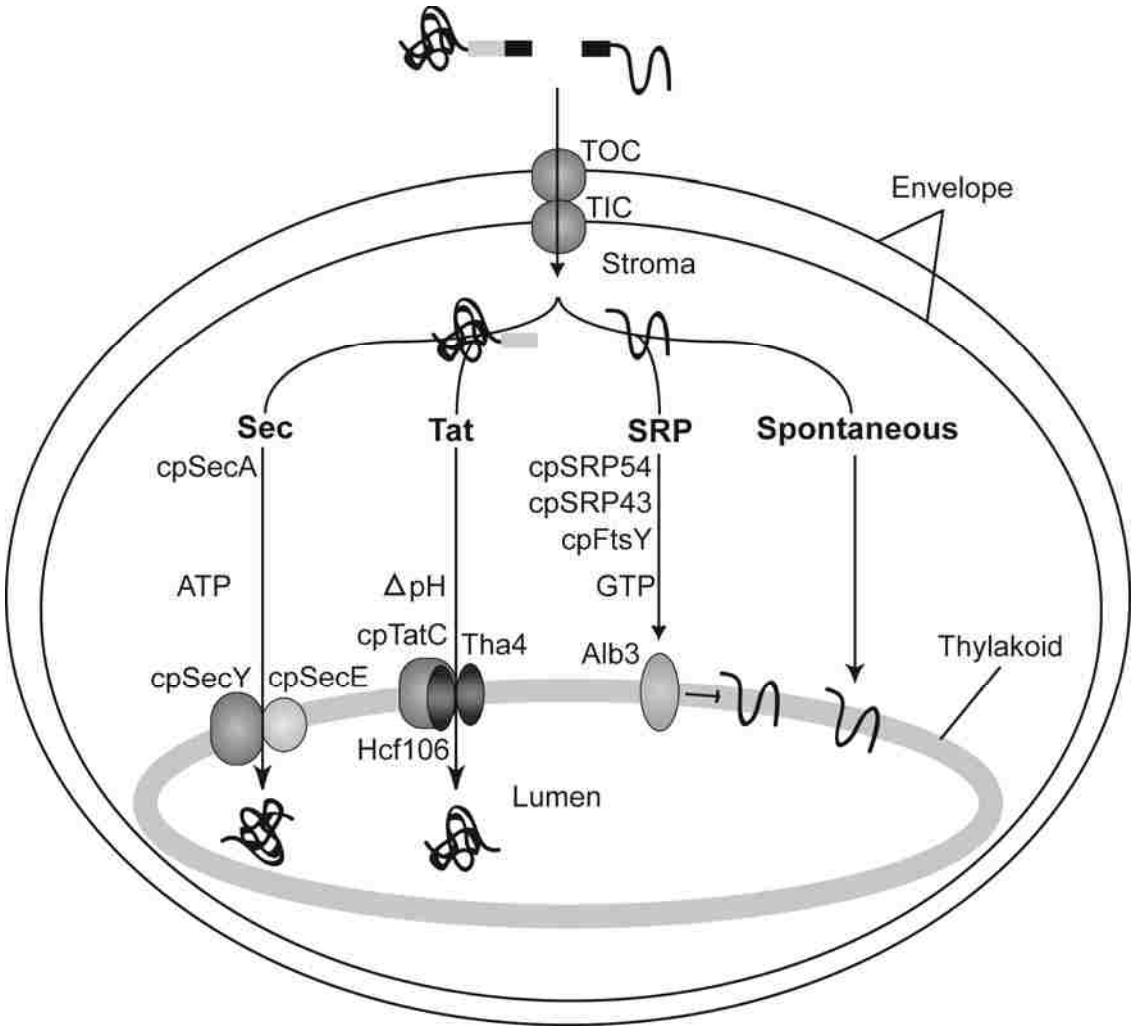

Figure 1.1. Model showing the four thylakoid targeting pathways.

Nuclear-encoded precursors are synthesized in the cytosol and contain an N-terminal chloroplast targeting sequence. Proteins targeting to the lumen contain a lumen targeting domain. After transport through the chloroplast envelopes via TOC/TIC, proteins enter one of four pathways. Soluble factors, energy requirements and membrane components are shown for each pathway.

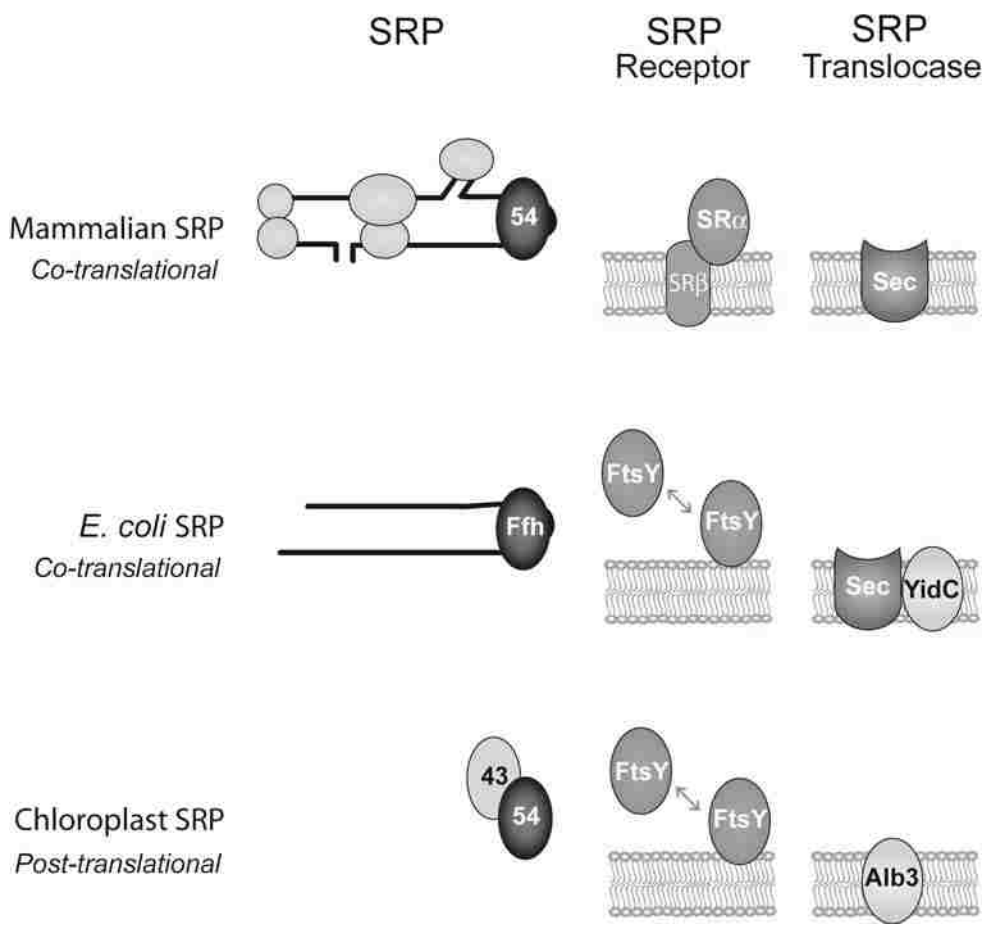

Figure 1.2. Comparison of SRP, SRP receptor, and SRP translocase from different organisms.

Components of the mammalian, *E. coli*, and chloroplast SRP systems are shown. Mammalian and bacterial SRPs contain an RNA moiety, while chloroplast SRP contains a unique 43-kDa protein subunit. All organisms utilize a homologous receptor protein, but mammals additionally have a transmembrane receptor subunit. Mammals and *E. coli* both use a Sec translocase, while *E. coli* and chloroplast have homologous insertase proteins YidC and Alb3. The possibility exists that additional membrane components exist for the chloroplast pathway.

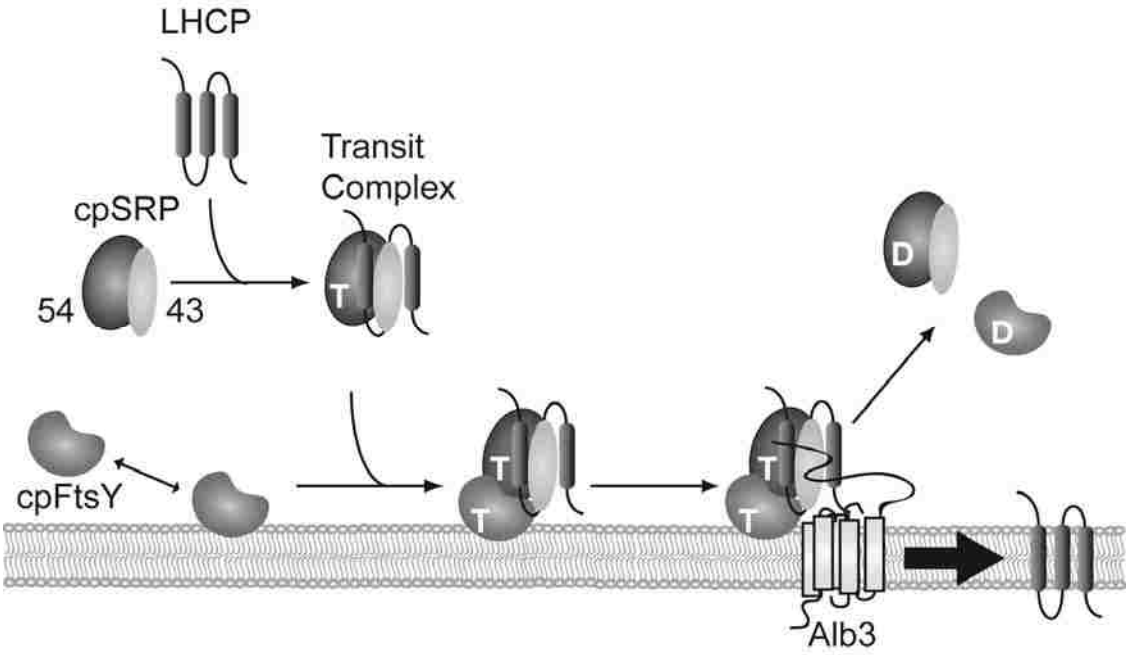

Figure 1.3. Model of chloroplast cpSRP targeting.

The cpSRP heterodimer (cpSRP54/cpSRP43) binds substrate LHCP to form the soluble transit complex. GTP-bound transit complex interacts with GTP-bound receptor cpFtsY at the thylakoid membrane. The membrane complex then targets to the integral membrane protein Alb3. In a series of poorly understood steps, LHCP is released from transit complex for integration, while cpSRP54 and cpFtsY hydrolyze GTP, promoting component release.

REFERENCES

1. Heazlewood, J. L., Tonti-Filippini, J., Verboom, R. E., and Millar, A. H. (2005) Combining Experimental and Predicted Datasets for Determination of the Subcellular Location of Proteins in Arabidopsis, *Plant Physiol. 139*, 598-609.

2. Cline, K., and Dabney-Smith, C. (2008) Plastid protein import and sorting: different paths to the same compartments, *Current Opinion in Plant Biology 11*, 585-592.

3. Osborne, A. R., Rapoport, T. A., and van den Berg, B. (2005) Protein translocation by the Sec61/SecY channel, *Annu Rev Cell Dev Biol 21*, 529-550.

4. Bolhuis, A. (2004) The archaeal Sec-dependent protein translocation pathway, *Philos Trans R Soc Lond B Biol Sci 359*, 919-927.

5. Veenendaal, A. K., van der Does, C., and Driessen, A. J. (2004) The protein-conducting channel SecYEG, *Biochim Biophys Acta 1694*, 81-95.

6. Dalbey, R. E., and Chen, M. (2004) Sec-translocase mediated membrane protein biogenesis, *Biochimica et Biophysica Acta 1694*, 37-53.

7. Vrontou, E., and Economou, A. (2004) Structure and function of SecA, the preprotein translocase nanomotor, *Biochim Biophys Acta 1694*, 67-80.

8. Yuan, J., Henry, R., McCaffery, M., and Cline, K. (1994) SecA homolog in protein transport within chloroplasts: evidence for endosymbiont-derived sorting, *Science 266*, 796-798.

9. Nakai, M., Goto, A., Nohara, T., Sugita, D., and Endo, T. (1994) Identification of the SecA protein homolog in pea chloroplasts and its possible involvement in thylakoidal protein transport, *J Biol Chem 269*, 31338-31341.

10. Cline, K., and Theg, S. M. (2007) The Sec and Tat Protein Translocation Pathways in Chloroplasts, In *The Enzymes* (Ross E. Dalbey, C. M. K., and Fuyuhiko, T., Eds.), pp 463-492, Academic Press.

11. Van Der Sluis, E. O., Nouwen, N., and Driessen, A. J. M. (2007) Sec Protein-Conducting Channel and SecA, In *The Enzymes* (Ross E. Dalbey, C. M. K., and Fuyuhiko, T., Eds.), pp 35-68, Academic Press.

12. Alken, M., and Hegde, R. S. (2007) The Translocation Apparatus of the Endoplasmic Reticulum, In *The Enzymes* (Ross E. Dalbey, C. M. K., and Fuyuhiko, T., Eds.), pp 207-243, Academic Press.

13. Keegstra, K., and Cline, K. (1999) Protein import and routing systems of chloroplasts, *Plant Cell 11*, 557-570.

14. Cline, K., and Henry, R. (1996) Import and routing of nucleus-encoded chloroplast proteins, *Annu Rev Cell Dev Biol 12*, 1-26.

15. Mitra, K., Frank, J., and Driessen, A. (2006) Co- and post-translational translocation through the protein-conducting channel: analogous mechanisms at work?, *Nat Struct Mol Biol 13*, 957-964.

16. Robson, A., and Collinson, I. (2006) The structure of the Sec complex and the problem of protein translocation, *EMBO Rep 7*, 1099-1103.

17. Haward, S. R., Napier, J. A., and Gray, J. C. (1997) Chloroplast SecA functions as a membrane-associated component of the Sec-like protein translocase of pea chloroplasts, *Eur J Biochem 248*, 724-730.

18. Knott, T. G., and Robinson, C. (1994) The secA inhibitor, azide, reversibly blocks the translocation of a subset of proteins across the chloroplast thylakoid membrane, *J Biol Chem 269*, 7843-7846.

19. Mori, H., Summer, E. J., Ma, X., and Cline, K. (1999) Component Specificity for the Thylakoidal Sec and Delta pH-dependent Protein Transport Pathways, *Journal of Cell Biology 146*, 45-56.

20. Voelker, R., Mendel-Hartvig, J., and Barkan, A. (1997) Transposon-disruption of a maize nuclear gene, tha1, encoding a chloroplast SecA homologue: in vivo role of cp-SecA in thylakoid protein targeting, *Genetics 145*, 467-478.

21. Mould, R. M., Kapazoglou, A., and Gray, J. C. (2001) Assembly of cytochrome f into the cytochrome bf complex in isolated pea chloroplasts, *Eur J Biochem 268*, 792-799.

22. Rohl, T., and van Wijk, K. J. (2001) In vitro reconstitution of insertion and processing of cytochrome f in a homologous chloroplast translation system, *Journal of Biological Chemistry 276*, 35465-35472.

23. High, S., Henry, R., Mould, R. M., Valent, Q., Meacock, S., Cline, K., Gray, J. C., and Luirink, J. (1997) Chloroplast SRP54 interacts with a specific subset of thylakoid precursor proteins, *Journal of Biological Chemistry 272*, 11622-11628.

24. Zhang, L., Paakkarinen, V., Suorsa, M., and Aro, E. M. (2001) A SecY homologue is involved in chloroplast-encoded D1 protein biogenesis, *Journal of Biological Chemistry 276*, 37809-37814.

25. Nilsson, R., Brunner, J., Hoffman, N. E., and van Wijk, K. J. (1999) Interactions of ribosome nascent chain complexes of the chloroplast- encoded D1 thylakoid membrane protein with cpSRP54, *EMBO Journal 18*, 733-742.

26. Nilsson, R., and van Wijk, K. J. (2002) Transient interaction of cpSRP54 with elongating nascent chains of the chloroplast-encoded D1 protein; 'cpSRP54 caught in the act', *FEBS Letters 524*, 127-133.

27. Ossenbuhl, F., Gohre, V., Meurer, J., Krieger-Liszkay, A., Rochaix, J. D., and Eichacker, L. A. (2004) Efficient assembly of photosystem II in Chlamydomonas reinhardtii requires Alb3.1p, a homolog of Arabidopsis ALBINO3, *Plant Cell 16*, 1790-1800.

28. Creighton, A. M., Hulford, A., Mant, A., Robinson, D., and Robinson, C. (1995) A monomeric, tightly folded stromal intermediate on the delta pH- dependent thylakoidal protein transport pathway, *J Biol Chem 270*, 1663-1669.

29. Musser, S. M., and Theg, S. M. (2000) Characterization of the early steps of OE17 precursor transport by the thylakoid DeltapH/Tat machinery, *Eur J Biochem 267*, 2588-2598.

30. Clark, S. A., and Theg, S. M. (1997) A folded protein can be transported across the chloroplast envelope and thylakoid membranes, *Mol Biol Cell 8*, 923-934.

31. Hynds, P. J., Robinson, D., and Robinson, C. (1998) The sec-independent twin-arginine translocation system can transport both tightly folded and malfolded proteins across the thylakoid membrane, *J Biol Chem 273*, 34868-34874.

32. Voelker, R., and Barkan, A. (1995) Two nuclear mutations disrupt distinct pathways for targeting proteins to the chloroplast thylakoid, *EMBO J 14*, 3905-3914.

33. Settles, A. M., Yonetani, A., Baron, A., Bush, D. R., Cline, K., and Martienssen, R. (1997) Sec-independent protein translocation by the maize Hcf106 protein, *Science 278*, 1467-1470.

34. Fincher, V., Dabney-Smith, C., and Cline, K. (2003) Functional assembly of thylakoid deltapH-dependent/Tat protein transport pathway components in vitro, *Eur J Biochem 270*, 4930-4941.

35. Mori, H., Summer, E. J., and Cline, K. (2001) Chloroplast TatC plays a direct role in thylakoid (Delta)pH-dependent protein transport, *FEBS Lett 501*, 65-68.

36. Cline, K., and Mori, H. (2001) Thylakoid DeltapH-dependent precursor proteins bind to a cpTatC-Hcf106 complex before Tha4-dependent transport, *J Cell Biol 154*, 719-729.

37. Dabney-Smith, C., and Cline, K. (2009) Clustering of C-Terminal Stromal Domains of Tha4 Homo-oligomers during Translocation by the Tat Protein Transport System, *Mol. Biol. Cell 20*, 2060-2069.

38. Dabney-Smith, C., Mori, H., and Cline, K. (2006) Oligomers of Tha4 Organize at the Thylakoid Tat Translocase during Protein Transport, *Journal of Biological Chemistry 281*, 5476-5483.

39. Mori, H., and Cline, K. (2002) A twin arginine signal peptide and the pH gradient trigger reversible assembly of the thylakoid [Delta]pH/Tat translocase, *J Cell Biol 157*, 205-210.

40. Alami, M., Luke, I., Deitermann, S., Eisner, G., Koch, H. G., Brunner, J., and Muller, M. (2003) Differential interactions between a twin-arginine signal peptide and its translocase in Escherichia coli, *Mol Cell 12*, 937-946.

41. Gerard, F., and Cline, K. (2006) Efficient twin arginine translocation (Tat) pathway transport of a precursor protein covalently anchored to its initial cpTatC binding site, *J Biol Chem 281*, 6130-6135.

42. Robinson, C., and Bolhuis, A. (2004) Tat-dependent protein targeting in prokaryotes and chloroplasts, *Biochim Biophys Acta 1694*, 135-147.

43. Tarry, M. J., Schafer, E., Chen, S., Buchanan, G., Greene, N. P., Lea, S. M., Palmer, T., Saibil, H. R., and Berks, B. C. (2009) Structural analysis of substrate binding by the TatBC component of the twin-arginine protein transport system, *Proc Natl Acad Sci U S A 106*, 13284-13289.

44. Ma, X., and Cline, K. (2010) Multiple precursor proteins bind individual Tat receptor complexes and are collectively transported, *EMBO J 29*, 1477-1488.

45. Hou, B., Frielingsdorf, S., and Klosgen, R. B. (2006) Unassisted membrane insertion as the initial step in DeltapH/Tat-dependent protein transport, *J Mol Biol 355*, 957-967.

46. Gohlke, U., Pullan, L., McDevitt, C. A., Porcelli, I., de Leeuw, E., Palmer, T., Saibil, H. R., and Berks, B. C. (2005) The TatA component of the twin-arginine protein transport system forms channel complexes of variable diameter, *Proc Natl Acad Sci U S A 102*, 10482-10486.

47. Bruser, T., and Sanders, C. (2003) An alternative model of the twin arginine translocation system, *Microbiol Res 158*, 7-17.

48. Mould, R. M., and Robinson, C. (1991) A proton gradient is required for the transport of two lumenal oxygen-evolving proteins across the thylakoid membrane, *J Biol Chem 266*, 12189-12193.

49. Cline, K., Ettinger, W. F., and Theg, S. M. (1992) Protein-specific energy requirements for protein transport across or into thylakoid membranes. Two lumenal proteins are transported in the absence of ATP, *J Biol Chem 267*, 2688-2696.

50. Finazzi, G., Chasen, C., Wollman, F.-A., and de Vitry, C. (2003) Thylakoid targeting of Tat passenger proteins shows no DpH dependence in vivo, *EMBO Journal 22*, 807-815.

51. Theg, S. M., Cline, K., Finazzi, G., and Wollman, F.-A. (2005) The energetics of the chloroplast Tat protein transport pathway revisited, *Trends in Plant Science 10*, 153-154.

52. Di Cola, A., Bailey, S., and Robinson, C. (2005) The thylakoid delta pH/delta psi are not required for the initial stages of Tat-dependent protein transport in tobacco protoplasts, *J Biol Chem 280*, 41165-41170.

53. Schleiff, E., and Klosgen, R. B. (2001) Without a little help from 'my' friends: direct insertion of proteins into chloroplast membranes?, *Biochim Biophys Acta 1541*, 22-33.

54. Michl, D., Robinson, C., Shackleton, J. B., Herrmann, R. G., and Klosgen, R. B. (1994) Targeting of proteins to the thylakoids by bipartite presequences: CFoII is imported by a novel, third pathway, *EMBO Journal 13*, 1310-1317.

55. Woolhead, C. A., Thompson, S. J., Moore, M., Tissier, C., Mant, A., Rodger, A., Henry, R., and Robinson, C. (2001) Distinct Albino3-dependent and -independent pathways for thylakoid membrane protein insertion, *J Biol Chem 276*, 40841-40846.

56. Robinson, D., Karnauchov, I., Herrmann, R. G., Klosgen, R. B., and Robinson, C. (1996) Protease-sensitive thylakoidal import machinery for the Sec-, Delta-pH- and signal recognition particle-dependent protein targeting pathways, but not for CFoII integration, *Plant Journal 10*, 149-155.

57. Kim, S. J., Robinson, C., and Mant, A. (1998) Sec/SRP-independent insertion of two thylakoid membrane proteins bearing cleavable signal peptides, *FEBS Letters 424*, 105-108.

58. Thompson, S. J., Kim, S. J., and Robinson, C. (1998) Sec-independent insertion of thylakoid membrane proteins. Analysis of insertion forces and identification of a loop intermediate involving the signal peptide, *J Biol Chem 273*, 18979-18983.

59. Mant, A., Woolhead, C. A., Moore, M., Henry, R., and Robinson, C. (2001) Insertion of PsaK into the thylakoid membrane in a "Horseshoe" conformation occurs in the absence of signal recognition particle, nucleoside triphosphates, or functional albino3, *Journal of Biological Chemistry 276*, 36200-36206.

60. Zygadlo, A., Robinson, C., Scheller, H. V., Mant, A., and Jensen, P. E. (2006) The Properties of the Positively Charged Loop Region in PSI-G Are Essential for Its \"Spontaneous\" Insertion into Thylakoids and Rapid Assembly into the Photosystem I Complex, *Journal of Biological Chemistry 281*, 10548-10554.

61. Kim, S. J., Jansson, S., Hoffman, N. E., Robinson, C., and Mant, A. (1999) Distinct "assisted" and "spontaneous" mechanisms for the insertion of polytopic chlorophyll-binding proteins into the thylakoid membrane, *Journal of Biological Chemistry 274*, 4715-4721.

62. Thompson, S. J., Robinson, C., and Mant, A. (1999) Dual signal peptides mediate the signal recognition particle/Sec- independent insertion of a thylakoid membrane polyprotein, PsbY, *J Biol Chem 274*, 4059-4066.

63. Steiner, J. M., Kocher, T., Nagy, C., and Loffelhardt, W. (2002) Chloroplast SecE: evidence for spontaneous insertion into the thylakoid membrane, *Biochem Biophys Res Commun 293*, 747-752.

64. Martin, J. R., Harwood, J. H., McCaffery, M., Fernandez, D. E., and Cline, K. (2009) Localization and integration of thylakoid protein translocase subunit cpTatC, *The Plant Journal 58*, 831-842.

65. Pool, M. (2005) Signal recognition particles in chloroplasts, bacteria, yeast and mammals, *Molecular Membrane Biology 22*, 3-15.

66. Klimyuk, V. I., Persello-Cartieaux, F., Havaux, M., Contard-David, P., Schuenemann, D., Meiherhoff, K., Gouet, P., Jones, J. D., Hoffman, N. E., and Nussaume, L. (1999) A chromodomain protein encoded by the Arabidopsis CAO gene is a plant- specific component of the chloroplast Signal Recognition Particle pathway that is involved in LHCP targeting, *Plant Cell 11*, 87-100.

67. Schuenemann, D., Gupta, S., Persello-Cartieaux, F., Klimyuk, V. I., Jones, J. D. G., Nussaume, L., and Hoffman, N. E. (1998) A novel signal recognition particle targets light-harvesting proteins to the thylakoid membranes, *Proceedings of the National Academy of Sciences of the United States of America 95*, 10312-10316.

68. Moore, M., Harrison, M. S., Peterson, E. C., and Henry, R. (2000) Chloroplast oxa1p homolog albino3 is required for post-translational integration of the light harvesting chlorophyll-binding protein into thylakoid membranes, *Journal of Biological Chemistry 275*, 1529-1532.

69. Gerdes, L., Bals, T., Klostermann, E., Karl, M., Philippar, K., Huenken, M., Soll, J., and Schuenemann, D. (2006) A second thylakoid membrane-localized Alb3/OxaI/YidC homologue is involved in proper chloroplast biogenesis in Arabidopsis thaliana, *Journal of Biological Chemistry 281*, 16632-16642.

70. Hasona, A., Crowley, P. J., Levesque, C. M., Mair, R. W., Cvitkovitch, D. G., Bleiweis, A. S., and Brady, L. J. (2005) Streptococcal viability and diminished stress tolerance in mutants lacking the signal recognition particle pathway or YidC2, *Proceedings of the National Academy of Sciences of the United States of America 102*, 17466-17471.

71. Eichacker, L. A., and Henry, R. (2001) Function of a chloroplast SRP in thylakoid protein export, *Biochimica et Biophysica Acta 1541*, 120-134.

72. Keenan, R. J., Freymann, D. M., Stroud, R. M., and Walter, P. (2001) The Signal Recognition Particle, *Annual Review of Biochemistry 70*, 755-775.

73. Luirink, J., and Sinning, I. (2004) SRP-mediated protein targeting: structure and function revisited, *Biochimica et Biophysica Acta 1694*, 17-35.

74. Groves, M. R., Mant, A., Kuhn, A., Koch, J., Dubel, S., Robinson, C., and Sinning, I. (2001) Functional characterization of recombinant chloroplast signal recognition particle, *Journal of Biological Chemistry 276*, 27778-27786.

75. Jonas-Straube, E., Hutin, C., Hoffman, N. E., and Schunemann, D. (2001) Functional analysis of the protein-interacting domains of chloroplast SRP43, *Journal of Biological Chemistry 276*, 24654-24660.

76. Goforth, R. L., Peterson, E. C., Yuan, J., Moore, M. J., Kight, A. D., Lohse, M. B., Sakon, J., and Henry, R. L. (2004) Regulation of the GTPase cycle in post-translational Signal Recognition Particle-based protein targeting involves cpSRP43, *Journal of Biological Chemistry 279*, 43077-43084.

77. Sivaraja, V., Kumar, T. K. S., Leena, P. S. T., Chang, A.-n., Vidya, C., Goforth, R. L., Rajalingam, D., Arvind, K., Ye, J.-L., Chou, J., Henry, R., and Yu, C. (2005) Three-dimensional solution structures of the chromodomains of cpSRP43, *Journal of Biological Chemistry 280*, 41465-41471.

78. Hermkes, R., Funke, S., Richter, C., Kuhlmann, J., and Schuenemann, D. (2006) The α-helix of the second chromodomain of the 43kDa subunit of the chloroplast signal recognition particle facilitates binding to the 54kDa subunit, *FEBS Letters 580*, 3107-3111.

79. Yuan, J., Kight, A., Goforth, R. L., Moore, M., Peterson, E. C., Sakon, J., and Henry, R. (2002) ATP stimulates signal recognition particle (SRP)/FtsY-supported protein integration in chloroplasts, *Journal of Biological Chemistry 277*, 32400-32404.

80. Tzvetkova-Chevolleau, T., Hutin, C., Noel, L. D., Goforth, R., Carde, J.-P., Caffarri, S., Sinning, I., Groves, M., Teulon, J.-M., Hoffman, N. E., Henry, R., Havaux, M., and Nussaume, L. (2007) Canonical signal recognition particle components can be bypassed for posttranslational protein targeting in chloroplasts, *Plant Cell 19*, 1635-1648.

81. Payan, L. A., and Cline, K. (1991) A stromal protein factor maintains the solubility and insertion competence of an imported thylakoid membrane protein, *Journal of Cell Biology 112*, 603-613.

82. DeLille, J., Peterson, E. C., Johnson, T., Moore, M., Kight, A., and Henry, R. (2000) A novel precursor recognition element facilitates posttranslational binding to the signal recognition particle in chloroplasts, *Proceedings of the National Academy of Sciences of the United States of America 97*, 1926-1931.

83. Tu, C. J., Peterson, E. C., Henry, R., and Hoffman, N. E. (2000) The L18 domain of light-harvesting chlorophyll proteins binds to chloroplast signal recognition particle 43, *Journal of Biological Chemistry 275*, 13187-13190.

84. Jaru-Ampornpan, P., Shen, K., Lam, V. Q., Ali, M., Doniach, S., Jia, T. Z., and Shan, S. O. (2010) ATP-independent reversal of a membrane protein aggregate by a chloroplast SRP subunit, *Nature Structural & Molecular Biology 17*, 696-702.

85. Falk, S., and Sinning, I. (2010) cpSRP43 is a novel chaperone specific for light-harvesting chlorophyll a,b-binding proteins, *J Biol Chem 285*, 21655-21661.

86. Wild, K., Rosendal, K. R., and Sinning, I. (2004) A structural step into the SRP cycle, *Molecular Microbiology 53*, 357-363.

87. Kogata, N., Nishio, K., Hirohashi, T., Kikuchi, S., and Nakai, M. (1999) Involvement of a chloroplast homologue of the signal recognition particle receptor protein, FtsY, in protein targeting to thylakoids, *FEBS Letters 447*, 329-333.

88. Tu, C. J., Schuenemann, D., and Hoffman, N. E. (1999) Chloroplast FtsY, chloroplast signal recognition particle, and GTP are required to reconstitute the soluble phase of light-harvesting chlorophyll protein transport into thylakoid membranes, *Journal of Biological Chemistry 274*, 27219-27224.

89. Jaru-Ampornpan, P., Chandrasekar, S., and Shan, S.-o. (2007) Efficient Interaction between Two GTPases Allows the Chloroplast SRP Pathway to Bypass the Requirement for an SRP RNA, *Mol. Biol. Cell 18*, 2636-2645.

90. Marty, N. J., Rajalingam, D., Kight, A. D., Lewis, N. E., Fologea, D., Kumar, T. K. S., Henry, R. L., and Goforth, R. L. (2009) The Membrane-binding Motif of the Chloroplast Signal Recognition Particle Receptor (cpFtsY) Regulates GTPase Activity, *Journal of Biological Chemistry 284*, 14891-14903.

91. Moore, M., Goforth, R. L., Mori, H., and Henry, R. (2003) Functional interaction of chloroplast SRP/FtsY with the ALB3 translocase in thylakoids: substrate not required, *Journal of Cell Biology 162*, 1245-1254.

92. Kuhn, A., Stuart, R., Henry, R., and Dalbey, R. E. (2003) The Alb3/Oxa1/YidC protein family: membrane-localized chaperones facilitating membrane protein insertion?, *Trends in Cell Biology 13*, 510-516.

93. Klostermann, E., Droste Gen Helling, I., Carde, J. P., and Schunemann, D. (2002) The thylakoid membrane protein ALB3 associates with the cpSecY-translocase in Arabidopsis thaliana, *Biochemical Journal 368*, 777-781.

II

A DYNAMIC CPSRP43-ALBINO3 INTERACTION MEDIATES TRANSLOCASE REGULATION OF CHLOROPLAST SINGAL RECOGNITION PARTICLE (CPSRP)-TARGETING COMPONENTS

Parts of this research accepted for publication as:

Lewis, N. E., Marty, N. J., Kathir, K. M., Rajalingam, D., Kight, A. D., Daily, A., Kumar, T. K., Henry, R. L., and Goforth, R. L. (2010) A dynamic cpSRP43-Albino3 interaction mediates translocase regulation of chloroplast signal recognition particle (cpSRP)-targeting components, *J Biol Chem 285*, 34220-34230.

SUMMARY

The chloroplast signal recognition particle (cpSRP) and its receptor, chloroplast FtsY (cpFtsY), form an essential complex with the translocase Albino3 (Alb3) during post-translational targeting of light-harvesting chlorophyll-binding proteins (LHCPs). Here, we describe a combination of studies that explore the binding interface and functional role of a functionally critical cpSRP43-Alb3 interaction. Using recombinant proteins corresponding to the C terminus of Alb3 (Alb3-Cterm) and various domains of cpSRP43, we identify the ankyrin repeat region of cpSRP43 as the domain primarily responsible for the interaction with Alb3-Cterm. Furthermore, we show Alb3-Cterm dissociates a cpSRP-LHCP targeting complex *in vitro* and stimulates GTP hydrolysis by cpSRP54 and cpFtsY in a strictly cpSRP43-dependent manner. These results support a model in which interactions between the ankyrin region of cpSRP43 and the C terminus of Alb3 promote distinct membrane-localized events, including LHCP release from cpSRP and release of targeting components from Alb3.

INTRODUCTION

Mitochondrial inner membranes and chloroplast thylakoid membranes are densely populated with protein complexes vital to the production of metabolic energy. For both membrane systems, biogenesis requires specialized protein sorting and integration systems, which localize nucleus- and organelle-encoded proteins to the target membrane. Consistent with the prokaryotic origin of mitochondria and chloroplasts, protein insertion into their energy-generating membranes is accomplished via the action of Oxa1p and Albino3 (Alb3), respectively, which belong to a family of protein insertases that includes YidC in bacteria (*1*-*6*).

Although YidC/Oxa1p/Alb3 homologues vary dramatically in length (225–795 residues), all share a conserved hydrophobic core of about 200 residues (*2*) that extends across five transmembrane domains leaving the C terminus exposed to the cytoplasm, matrix, or stroma, respectively (Fig. 2.1). Complementation studies demonstrated that the core regions of both Oxa1p and Alb3 functionally replace the core of YidC to insert membrane proteins via a "YidC only" pathway (*7*-*8*). Similarly, a chimera of YidC fused with a portion of the C terminus of Oxa1p was useful in demonstrating that the core region of YidC can functionally replace the core region of Oxa1p (*9*). These experimental results show that the core regions of YidC/Oxa1p/Alb3 are at least partially interchangeable and house the capacity for assisting membrane protein transition into adjacent bilayers. They also support the possibility that a conserved function of the YidC/Oxa1p/Alb3 C terminus is to bind soluble targeting machinery. For example, the hydrophilic C-terminal extension of Oxa1p forms an α-helical domain essential for interacting with the ribosome during cotranslational integration (*10*-*11*).

Like Oxa1p, Alb3 contains a hydrophilic C-terminal extension that may play a critical role in protein targeting (*12-13*). Alb3 works in conjunction with a post-translational chloroplast signal recognition particle (cpSRP) targeting system to integrate a family of nuclearly encoded light-harvesting chlorophyll-binding proteins (LHCPs) into thylakoid membranes where they are assembled with chlorophyll to form light-harvesting complexes (*14-17*). Antibody binding to the C terminus of Alb3 inhibits LHCP integration and prevents an Alb3-cpSRP interaction (*12*), suggesting interactions with the C terminus of Alb3 may be required in the cpSRP-dependent targeting reaction.

cpSRP is a heterodimer composed of a highly conserved 54-kDa GTPase (cpSRP54) and a 43-kDa protein (cpSRP43) unique to chloroplasts (*18-20*). LHCP precursors imported into the chloroplast stroma from the cytosol are N-terminally processed and bound by cpSRP to form a soluble cpSRP-LHCP complex, termed transit complex, which maintains mature-sized LHCP in an integration-competent state (*19, 21*). Transit complex interacts with a thylakoid membrane-associated SRP receptor GTPase (cpFtsY) prior to interaction with Alb3 (*12*). Although the membrane-localized steps are not well understood, a mechanism must exist for the regulated transfer of LHCP from cpSRP to Alb3 and most likely involves the cpSRP54/cpFtsY GTP hydrolysis cycle. By analogy to cotranslational SRP targeting mechanisms, LHCP release from cpSRP is presumably accompanied by reciprocal GTP hydrolysis by cpSRP54 and cpFtsY to stimulate their release from each other and from Alb3, ensuring their availability for subsequent rounds of targeting

cpSRP-dependent targeting of LHCPs is novel in that it functions post-translationally, targeting fully synthesized substrates. All other known SRP targeting

systems are cotranslational and utilize the translating ribosome as a regulator of substrate binding, GTP hydrolysis, and protein-protein interactions (*22-23*). The evolutionary acquisition of cpSRP43 appears critical for post-translational targeting of LHCPs (*24*). cpSRP43 not only binds targeting substrate (LHCP) but was recently shown to provide both novel and specific chaperone function, capable of independently reversing aggregation of the highly hydrophobic LHCPs (*25-26*). Furthermore, cpSRP43 interacts with cpSRP54 and specifically copurifies Alb3 from isolated thylakoid membranes (*24, 27-30*). More recently, we and others demonstrated that cpSRP43 binding to Alb3 is mediated by the Alb3 C terminus (*13, 31*). However, the physiological significance of this low affinity interaction (9.7 μM) remains uncertain.

cpSRP43 is composed of two types of characteristic protein-protein interaction domains: chromodomains (CD) and ankyrin (Ank) repeats (arranged CD1-Ank1-Ank2-Ank3-Ank4-CD2-CD3; Fig. 2.2) (*27, 30*). A conserved motif in LHCP, L18, is bound by the Ank repeat region of cpSRP43 (*27-28, 30, 32-33*), and cpSRP54 is bound by CD2 (*27, 34-35*). As expected, these regions are critical for formation of transit complex (Ank1-CD2), LHCP integration (CD1-CD2), and regulation of GTP hydrolysis (CD1) (*27*). Although Falk *et al.* (*13*) suggest that CD2-CD3 are responsible for cpSRP43 binding to the C terminus of Alb3, the physiological contribution of this interaction in the LHCP targeting mechanism is not known, and CD3 can be removed from cpSRP43 without consequence to the efficiency of transit complex formation or LHCP integration into isolated thylakoids (*27*).

Although key LHCP targeting/insertion components and transit of LHCP through the stroma to the thylakoids have been examined in detail, many questions remain

concerning the orchestration and timing of membrane-associated cpSRP-dependent targeting events. Results described in this study indicate that the Ank repeat domain of cpSRP43 is responsible for high affinity binding to Alb3-Cterm (97 nM) with CD2 contributing slightly to the binding interface. We show that this interaction is functionally critical for efficient assembly of a cpSRP-cpFtsY-Alb3 membrane complex and is used in LHCP targeting to regulate the timing of GTP hydrolysis by cpSRP54/cpFtsY. Our data also indicate that cpSRP43 binding to Alb3-Cterm affects the stability of transit complex, which supports a role of this interaction in promoting release of LHCP from cpSRP at the thylakoid membrane. Collectively, our results support a model whereby cpSRP43 targets available Alb3 via its C terminus and communicates this interaction to cpSRP/cpFtsY thereby triggering downstream events (*e.g.* GTP hydrolysis and substrate release) required to promote LHCP integration into the thylakoid membrane.

MATERIALS AND METHODS

All reagents, enzymes, and primers used were purchased commercially. Plasmids described previously were used for *in vitro* transcription and translation of pLHCP (*36*), cpSRP43 (*37*), and cpFtsY (*37*). Recombinant purified cpSRP43, GSTcpSRP43, GST, GST-Ank1-CD2, GST-CD1, GST-CD2, CD2, ΔCD1, ΔCD2, and ΔCD3 were prepared as described previously (*27*). His-cpSRP43 (*24*), Trx-His-Stag-cpFtsY (*12, 38*), and cpSRP54-His (*12*) were prepared as described with the exception of a new restriction site (XhoI) for cpFtsY (*39*). A peptide corresponding to the cpSRP43-binding site in LHCP, L18 (VDPLYPGGSFDPLGLASS), has been previously described (*33*). Antibodies to the following proteins have also been described as follows: Alb3-Cterm (*40*), Alb3–50 amino acids (*17*), cpSRP43 (*12*), cpFtsY (12), and cpSRP54(*12*). All cloned sequences were verified by sequencing.

Construction of Alb3-Cterm Clones

A cDNA clone for PPF1 (defined as Alb3 in *Pisum sativum*) was obtained by RT-PCR using total RNA from *P. sativum*. Forward and reverse primers matching the sequence for PPF1 (accession number Y12618) were designed to include EcoRI and XbaI sites, respectively, for ligation into pGEM-4Z (Promega). The coding sequence for PPF1-Cterm, a 124-amino acid segment of PPF1 beginning at NNVLSTA and ending at SKRKPVA, was amplified by PCR from PPF1-pGEM-4Z. The resulting PCR fragment was restricted with BamHI and XbaI and then ligated into similarly restricted pGEM-4Z to produce the plasmid Alb3-Cterm-pGEM-4Z. Forward and reverse primers were designed to match the beginning and ending of the Alb3-Cterm and to include SphI and HindIII sites, respectively, for ligation into pQE-80L (Qiagen). The forward primer also

included a two amino acid linker (SA), a FLAGTM tag, and a Thrombin cleavage site. The resulting PCR fragment was restricted with SphI and HindIII and then ligated into similarly restricted pQE-80L to create the plasmid His-FLAG-Alb3-Cterm-pQE-80L. This plasmid was transformed into BL21 Star (Invitrogen) and used for IPTG-induced expression of His-FLAG-Alb3-Cterm. All Alb3 constructs are from *P. sativum.*

To produce His-Stag-Alb3-Cterm, His-FLAG-Alb3-CtermpQE-80L was amplified by PCR with a reverse primer designed to match the ending of the Alb3-Cterm sequence and a forward primer designed to replace the FLAG tag (DYKDDDDK) with an S tag (KETAAAKFERQHMDS) resulting in a construct with a His6 tag, SA linker, Stag, thrombin cleavage site, and the 124-amino acid segment of PPF1 beginning at NNVLSTA and ending at SKRKPVA. This plasmid, referred to as His-Stag-Alb3-Cterm-pQE-80L, was transformed into BL21 Star and used for IPTG-induced expression of His-Stag-Alb3-Cterm.

Briefly, expressed Alb3-Cterm peptides were affinity-purified over Talon® Superflow metal affinity chromatography and either followed directly by desalting into HKMK (10mMHepes-KOH, pH 8.0, 10mM MgCl2, 100mM KCl) buffer or followed by a cation exchange step over Resource S (binding: 20mM Hepes, pH 8, 10mM KCl, and elution: 20mM Hepes, pH 8, 1 M KCl) and then desalting into HKMK buffer.

Construction of cpSRP43 Clones

Coding sequences for CD1 and CD2 were amplified by PCR from GST-CD1-pGEX-4T-2 and GST-CD2-pGEX-4T-2 (*27*) using forward primers designed to incorporate a BamHI restriction site and His6 tag and match the beginning of the CD1 (GEVNKII) or CD2 (QVFEYAE) coding sequences and reverse primers designed to

match a pGEX plasmid. Coding sequences for Ank1-CD2 were amplified by PCR from GST-ΔCD3 (*27*) using forward primers designed to incorporate a BamHI restriction site and a His6 tag and match the beginning of Ank1 (SEYETP) and reverse primers designed to match a pGEX plasmid. PCR products were restricted with BamHI and EcoRI (His-CD1 and His-Ank1-CD2) or XhoI (His-CD2) and ligated into similarly restricted pGEX-6P-2, producing GST-His-CD1-pGEX-6P-2, GST-His-CD2-pGEX-6P-2, and GST-His-Ank1-CD2-pGEX-6P-2. His-CD1, His-CD2, and His-Ank1-CD2 plasmids were transformed into BL21 Star and used for IPTG-induced expression of these constructs as described previously (*27*). The ΔCD2/CD3 cpSRP43 construct for expression in *Escherichia coli* was produced by PCR amplification of the entire mature cpSRP43-pGEX-6P-2 plasmid (*38*) minus the codons for amino acids to be deleted (Δ273–377; missing residues AEVDEI…QQPMNE). The use of phosphorylated primers corresponding to the flanking regions of the sequence to be deleted allowed for efficient ligation of the PCR products to re-circularize the plasmid and form the desired coding sequence for GST-ΔCD2/CD3-pGEX-6P-2. This plasmid was transformed into BL21 Star for IPTG-induced expression.

Briefly, expressed GST constructs were affinity-purified by using glutathione-Sepharose™ 4 Fast Flow resin (GE Healthcare) followed by a desalting step into HKM (10 mM Hepes-KOH, pH 8.0, 10mM MgCl2) buffer as described. Following the glutathione-Sepharose purification, cleaved constructs were brought to 50 mM Tris-HCl, 150 mM NaCl, 1 mM EDTA, 1 mM DTT, pH 7.0, and incubated with PreScission™ protease (GE Healthcare) overnight at 4 °C. Cleaved constructs were desalted into phosphate-buffered saline and passed over glutathione-Sepharose 4 Fast Flow resin for

removal of cleaved GST and PreScission™ protease followed by desalting into HKM buffer.

Ank1–4 was amplified from mature cpSRP43 in pGEM-4Z (37) using forward and reverse primers designed to match the beginning (EYETPWW) and ending (RRIGLEKVINV) of Ank1–4 and incorporate BamHI and SalI sites. PCR products were restricted with BamHI and SalI and ligated into similarly restricted pQE-80L, producing His-Ank1–4-pQE-80L. This plasmid was transformed into BL21 Star and used for IPTG induced expression of His-Ank1–4. His-Ank1– 4 was produced as inclusion bodies, solubilized in 8 M urea, and purified as a soluble protein with Talon® Superflow metal affinity resin. His-Ank-1– 4 containing 8 M urea was dialyzed against Tris-HCl, pH 7.5, and subsequently buffer exchanged into HKM.

Preparation of Chloroplasts and Radiolabeled Precursors

Intact chloroplasts were isolated from 10- to 12-day-old pea seedlings (*P. sativum* cv. Laxton's Progress) and used to prepare thylakoids and stroma as described previously (*41*). Chlorophyll (Chl) content was determined as described previously (*42*). Thylakoids were isolated from lysed chloroplasts by centrifugation and salt-washed (SW) two times with 1 M potassium acetate in import buffer (IB: 50 mM Hepes-KOH, pH 8.0, 0.33 M sorbitol) and two times with IB with 10 mM MgCl2 (IBM) prior to use. For protease treatment, SW thylakoids were diluted to 0.5 mg/ml Chl in IB with 0.2 mg/ml thermolysin and 1 mM CaCl2 and incubated for 40–60 min (*P. sativum*). Subsequently, samples were combined with EDTA in IB to 20 mM EDTA, and either washed or applied to a 7.5% Percoll™ (GE Healthcare) gradient in IB containing 10 mM EDTA. Pellets

from the Percoll gradient were washed once with IB containing 10 mM EDTA and twice with IBM. Protease-treated thylakoids were resuspended at 1 mg/ml Chl in IBM.

In vitro transcribed capped RNA was translated in the presence of [35S]methionine (*43*) using a wheat germ system to produce radiolabeled proteins (*41*). Precursor LHCP translation products were diluted 2-fold with 30 mM unlabeled Met in IB. cpSRP43, cpSRP54, and cpFtsY constructs were labeled with ratios of labeled and unlabeled Met such that an equal 35S signal represented equimolar protein as described previously (*37*). Constructs were quantified by comparing the 35S signal from a given protein band as analyzed by SDS-PAGE and phosphorimaging. Equimolar amounts of proteins were added to each experiment.

Thylakoid Binding Assay

P. sativum thylakoid binding assays included SW or protease-treated thylakoids (equal to 75 μg of Chl) in IBM and radiolabeled cpSRP43 or cpFtsY. Reactions were incubated for 30 min in light at 25 °C. Thylakoids were centrifuged at 3200 × *g* for 6 min, washed in 1 ml of IBM, and transferred to clean tubes. Thylakoids were then pelleted, solubilized in SDS buffer, and heated. Amounts equivalent to 7.5 μg of Chl per sample were analyzed by SDS-PAGE and phosphorimaging.

Protein Binding Assays

Alb3 coprecipitation by cpSRP components was examined by incubating SW thylakoids (equal to 75 μg of Chl) with 10 μg of His-tagged protein and in the presence or absence of 0.5 μM GMP-PNP at 25 °C for 30 min in light. Thylakoids were washed with 600 μl of IBM and solubilized with 2% *n*-dodecyl-β-D-maltoside (maltoside) in IB for 10 min. Samples were centrifuged at 70,000 × *g* for 12 min, and soluble material was

incubated with 50 µl of a 50% Talon Superflow metal affinity resin slurry in IB for 30 min while shaking. Resin was washed three times with 0.1% maltoside in IB and once with IB before elution in 50 µl of SDS sample buffer. Eluted proteins were separated by 12.5% SDS-PAGE and Western blotted for cpSRP43, cpSRP54, cpFtsY, and Alb3. The protein loading control lane is equivalent to 1/100th of the available Alb3 as based on the total amount of thylakoids used.

GST-cpSRP43 constructs/Alb3-Cterm binding assays were performed by incubating 350 pmol (4.7 µM final concentration) of GST-fused cpSRP43 or construct with 1500 pmol (20 µM final concentration) of His-Stag-Alb3-Cterm for 15 min at 25 °C and adding 30 µl of a 50% glutathione-Sepharose 4 Fast Flow slurry in 10 mM Hepes-KOH, pH 8.0, 10 mM MgCl2 (HKM), in a final volume of 75 µl. Samples were allowed to mix for 30 min at 4 °C and then transferred to a 0.8-ml centrifuge column (Pierce) and washed three times with 0.75 ml of 20 mM HK, 300 mM KCl, 10 mM MgCl2, 2% Tween 20, three times with 0.75 ml of 0.1% maltoside in IB, and three times with 0.75 ml of HKM. Coprecipitating proteins were eluted in 75 µl of SDS-PAGE solubilization buffer. Eluted proteins were separated by 12.5% SDS-PAGE and visualized by staining with Coomassie Blue.

Coprecipitation of cpSRP43 and constructs by His-Stag-Alb3-Cterm was accomplished by incubating 800 pmol (8 µM final concentration) of Alb3-Cterm with 30 µl of 50% S-protein/agarose slurry (Novagen) in IB and shaking gently for 15 min at 25 °C. After addition of 1500 pmol (15 µM final concentration) of cpSRP43 or construct, in a final volume of 100 µl, samples were allowed to mix for 30 min at 4 °C and then transferred to a 0.8-ml centrifuge column and washed three times with 0.1% maltoside in

IB. Coprecipitating proteins were eluted in 75 µl of SDS-PAGE solubilization buffer. Eluted proteins were separated by 12.5% SDS-PAGE and visualized by staining with Coomassie Blue. For his-Flag-Alb3-Cterm coprecipitation of cpSRP43, 800 pmol of his-Flag-Alb3-Cterm were incubated with 1500 pmol of cpSRP43 in a final volume of 75 µl while shaking gently for 15 min at 25 °C. After addition of 20 µl 50% Talon Superflow metal affinity resin slurry in 10 mM HK, 10 mM $MgCl_2$, samples were allowed to mix 30 min at 4 °C and then transferred to a 0.8 ml Centrifuge Column and washed three times with a buffer containing 50 mM Na_2HPO_4, 300 mM NaCl, and 10 mM imidazole, pH 7. Coprecipitating proteins were eluted in 75 µl of a buffer containing 50 mM Na_2HPO_4, 300 mM NaCl, and 150 mM imidazole, pH 7. Eluted proteins were separated by 12.5% SDS-PAGE and visualized by staining with Coomassie Blue and Western blotting for cpSRP43 (see Analysis of Samples section below for detailed protocol).

Isothermal Titration Calorimetry (ITC)

ITC experiments were performed by Dr. Suresh Kumar's lab using a VP-ITC titration microcalorimeter (MicroCal Inc.). All solutions were degassed under vacuum and equilibrated at 25 °C prior to titration. Protein or peptide (50–200 µM) was loaded into the sample cell (1.4 ml), and the titration syringe was loaded with another protein or peptide at 10–30-fold higher concentration. Titrations were routinely carried out using 40–50 injections of 6-µl aliquots using the injection rate of 5–7-min intervals with a stirring rate of 340 rpm. Solutions were prepared either in a buffer containing 10 mM Tris, 100 mM NaCl, pH 7.5, or in HKM. Titration curves were corrected for protein-free buffer and analyzed using Origin ITC software (MicroCal Inc.) (*44*).

Transit Complex Formation Assays

Transit complex was formed in 60-µl assays by mixing 25 pmol (0.4 µM final concentration) each cpSRP43 and cpSRP54 with 10 µl of diluted translation product similar to assays described previously (*33*, *45*). Assays were incubated for 20 min at 25 °C, and then 0–2000 pmol (0–33.3 µM) of either His-Stag-Alb3-Cterm peptide in 20 µl of HKMK, CD3 in HKM, or GST in HKM was added as indicated. Assays were incubated for 20 min at 25 °C and then centrifuged at 70,000 × *g* for 1 h. The top 30-µl supernatant was removed, cooled on ice, and prepared for native PAGE by the addition of 5 µl of 50% glycerol.

In moving radiolabel assays, transit complex components (cpSRP43, cpSRP54, and LHCP) were all produced by *in vitro* transcription/translation via a wheat germ system. Indicated protein component was translated in the presence of [35S]methionine to produce the radiolabeled protein. The other two components were translated in the presence of nonradioactive Met. Proteins (10 µl of each TP) were then treated as above to form transit complex prior to the addition of 0–5000 pmol (0–83.3 µM) of His-Stag-Alb3-Cterm and analysis by native PAGE.

Analysis of Samples

A portion of each sample from each assay was analyzed by SDS-PAGE (or native PAGE as indicated) followed by Western blotting or phosphorimaging. GE Healthcare image analysis software (ImageQuant) was used for quantification of radiolabeled protein from phosphorimages obtained using a Typhoon 8600. Horseradish peroxidase-labeled mouse IgG (Southern Biotech) was used as secondary antibody, and blots were developed with SuperSignal® West Pico chemiluminescent substrate (Pierce). Western

blots were imaged using an Alpha Innotech FluorChem IS-8900 using chemiluminescent detection. AlphaEase FC Stand Alone software (Alpha Innotech) was used for quantification. SDS-PAGE standards (Invitrogen) were used to calculate molecular weights (MagicMark™ XP Western Standard for Western blots; Benchmark™ Protein Ladder for Coomassie-stained gels). Protein concentrations were estimated by Coomassie Blue staining.

GTPase Assays

Recombinant cpSRP54 and cpFtsY were assayed for GTPase activity alone or in the presence of recombinant cpSRP43, recombinant cpSRP43 deletion constructs, and/or His-Stag-Alb3-Cterm as described previously (*27, 46*). GTPase activity was measured in solution by determining the amount of inorganic phosphate released by GTP hydrolysis. Assays containing 150 pmol (1 μM final concentration) of cpSRP43 (or indicated construct), cpSRP54, cpFtsY, the indicated amount of His-Stag-Alb3-Cterm (0–40 μM, 0–6000 pmol), and 2 mM GTP were brought to a final volume of 150 μl in HKM and incubated at 30 °C for 1 h. After incubation, SDS was added to a final concentration of 6% to denature protein components and prevent subsequent GTPase activity. The addition of ascorbic acid and ammonium molybdate (to 6 and 1%, respectively) was followed by a 5-min incubation, and subsequently each assay was brought to 1% sodium citrate, sodium (meta)arsenite, and acetic acid for a final volume of 1.05 ml. The absorbance of each sample was then measured at 850 nm. Throughout the duration of the experiment, the amount of GTP hydrolyzed increased linearly. Furthermore, a standard curve of inorganic phosphate (Pi) was linear from 2 to 75 nmol of Pi and was used to determine the amount of Pi released in each assay. A substrate control that lacked protein

components and a zero time control with the protein denatured by the addition of 6% SDS prior to the addition of GTP varied from 0.0 to 2.3 nmol of Pi between experiments and were used to correct for nonspecific hydrolysis and background hydrolysis for each assay.

RESULTS

cpSRP43 Interacts with the Thylakoid Membrane Protein Alb3

We previously demonstrated that His-tagged cpSRP43 binds SW *P. sativum* thylakoid membranes and copurifies Alb3 (*24*). More recently, it was published that cpSRP43 alone or as a heterodimer with cpSRP54 binds Alb3 through interactions between chromodomains (CDs) at the C terminus of cpSRP43 (CD2 and CD3) and the stroma-exposed C terminus of Alb3 (*13*). However, the physiological role of cpSRP43 binding to Alb3 is not known. In this context, we asked whether cpSRP43 plays a role in promoting Alb3 association with a cpSRP-cpFtsY complex, which forms at the thylakoid membrane (*12*). His-tagged cpSRP43, cpSRP54, and cpFtsY constructs shown to be active in reconstituting LHCP integration into isolated thylakoids and able to form a stable complex with Alb3 (*12*) were incubated with SW thylakoids in the presence or absence of GMP-PNP. Membranes were solubilized with maltoside and then mixed with Talon® Superflow metal affinity resin to repurify His-tagged constructs and associated proteins (Fig. 2.3). Samples were probed for His-tagged constructs and coprecipitating Alb3 (*P. sativum* PPF1). Assays containing cpSRP54, cpFtsY, or both copurify ~6% or less of the available Alb3, which is slightly above background binding (~2%) to the resin (Fig. 2.3, A and B). In contrast, assays containing cpSRP43 copurify ~15% of the available Alb3 (Fig. 2.3, A and B). Similar amounts of each added His-tagged construct were repurified indicating that changes in the amount of copurified Alb3 are not due to inaccessible His tags. The requirement for cpSRP43 to copurify Alb3 suggests that cpSRP43 functions as the bridge that connects cpSRP and cpFtsY to Alb3.

Copurification of Alb3 could stem from interaction of cpSRP43 with an unknown Alb3-associated thylakoid protein or could stem from binding of cpSRP43 to the Alb3 C terminus, an interaction reported recently using recombinant cpSRP43 and protein corresponding to the C terminus of Alb3 (Alb3-Cterm) (*13*). However, the reported affinity between cpSRP43 and Alb3-Cterm (*Kd* ~10 μM) seems insufficient to support specific molecular interactions expected for efficient protein targeting and approaches affinity values observed for nonspecific protein interactions (*47*). To investigate these possibilities further, we tested the ability of cpSRP43 to bind thylakoids lacking the C terminus of Alb3. Alb3 contains five transmembrane domains with its N terminus facing the thylakoid lumen (*6*). Thermolysin treatment of thylakoid membranes removes the C terminus of Alb3, but otherwise it has no effect on Alb3 integrity as judged by the size of the protease-resistant fragment (~30 kDa), which is detectable with antisera to a protease-resistant, stroma-exposed loop (anti-50 amino acids) and undetectable using antibody against the Alb3 C terminus Fig. 2.4 B). Although binding of cpFtsY to protease-treated thylakoids is unaffected because of its affinity for thylakoid lipids (*37*), the ability of cpSRP43 to bind protease-treated thylakoids is diminished by ~80% (Fig. 2.4 A), further supporting a role of the Alb3 C terminus in cpSRP43 binding to thylakoids. Taken together with the results of Fig. 2.3, these data suggest that one role of cpSRP43 binding to the Alb3 C terminus is to promote efficient formation of a cpSRP-cpFtsY-Alb3 complex.

cpSRP43 and Alb3-Cterm Interact with High Affinity

To better understand how a low affinity interaction is used to support cpSRP43-Alb3 association, we used ITC and copurification assays to reexamine the binding of

cpSRP43 to recombinant Alb3-Cterm expressed and pufiried from E. coli. As expected, cpSRP43 and Alb3-Cterm coprecipiate using a variety of resins and recombinant tags (Fig. 2.5 A-C). Surprisingly, however, ITC demonstrated that the affinity of cpSRP43 for His-FLAG-Alb3-Cterm was in the nanomolar range (94 nM; Fig. 2.5 D) as opposed to the micromolar (~10 μM) affinity reported earlier (*13*). Although the reason(s) for the observed discrepancy in the binding affinity is not clear, systematic examination of the buffer components used by Falk *et al.* (*13*) to observe micromolar affinity revealed that glycerol (at 5% v/v concentration) contributes significantly to the heat of the reaction and consequently influences the ability to accurately measure the *Kd* values using binding isothermogram (Fig. 2.6).

Ankyrin Region of cpSRP43 Provides the Primary Interface for Binding Alb3-Cterm

Because ITC conducted in the presence of glycerol had also been used to demonstrate that CD2 and CD3 of cpSRP43 provide the binding interface for Alb3-Cterm (*13*), the role of cpSRP43 domains in binding Alb3-Cterm was examined using both ITC in the absence of glycerol and copurification assays. cpSRP43 domain deletions (Fig. 2.2) were examined by ITC for their ability to interact with His-FLAG-Alb3-Cterm (Fig. 2.7). Similar to cpSRP43 ($K_{d(\text{app})}$ ~94 nM), His-Ank1-CD2 interacts with a near 1:1 stoichiometry and exhibits a high binding affinity for Alb3-Cterm (*Kd*(app) ~64 nM; Fig. 2.7 A). The binding affinity of Alb3-Cterm for His-Ank1–4 (Fig. 2.7 B) is marginally lower (*Kd*(app) ~205 nM) than that observed for cpSRP43 or His-Ank1-CD2, but remains in the nanomolar range. In contrast, Alb3-Cterm interaction with CD2 exhibits negligible binding affinity (*Kd*(app) ~350 μM; Fig. 2.7 C) as compared with that observed for Alb3-Cterm binding to cpSRP43, His-Ank1-CD2, or His-Ank1–4. In

contrast to Falk *et al.* (*13*), these observations indicate that the binding site for Alb3-Cterm lies in the ankyrin repeat region of cpSRP43 with the second chromodomain possibly adding to the interaction face based on comparison of the affinity of Alb3-Cterm for His-Ank1–4 and His-Ank1-CD2.

Copurification assays were conducted to confirm and extend the results obtained using ITC. Equimolar concentrations of GST, GST-cpSRP43, GST-Ank1-CD2, GST-CD2, GST-ΔCD2/CD3, or GST-CD1 (refer to Fig. 2.7 D) were incubated with His-Stag-Alb3-Cterm and recovered using glutathione-Sepharose. Bound proteins were eluted, separated by SDS-PAGE, and visualized directly by staining with Coomassie Blue. GST-cpSRP43 specifically coprecipitates Alb3-Cterm (apparent molecular mass ~20 kDa) at a ratio of ~0.85 pmol of Alb3-Cterm copurified per pmol of cpSRP43 (Fig. 2.8 A). GST-tagged constructs containing the ankyrin repeat region of cpSRP43 are also capable of copurifying Alb3-Cterm; GST-Ank1-CD2 and GST-CD2/CD3 both copurified Alb3-Cterm at a ratio greater than 0.6 pmol of Alb3-Cterm per pmol of construct. Those constructs lacking the ankyrin repeats (CD1 and CD2) exhibit strong decreases in the amount of Alb3-Cterm copurified (less than 0.07 pmol of Alb3-Cterm per pmol of construct).

Likewise, we utilized a His-Stag-Alb3-Cterm construct to verify an interaction between Alb3-Cterm and the ankyrin region of cpSRP43. cpSRP43 and constructs His-Ank1-CD2, ΔCD2/CD3, His-Ank1–4, and His-CD2 were incubated with His-Stag-Alb3-Cterm and repurified using S-protein-agarose (Fig. 2.8 B). Eluted proteins were separated by SDS-PAGE and visualized directly by staining with Coomassie Blue. Fig. 2.8 B shows that cpSRP43, His-Ank1-CD2, ΔCD2/CD3, and His-Ank1–4 are specifically

copurified with Alb3-Cterm, albeit to a lesser extent in the case of ΔCD2/CD3 and His-Ank1–4. Quantification from four separate assays shows that His-Stag-Alb3-Cterm coprecipitates His-Ank1-CD2 at ~90% the level of cpSRP43. His-Ank1–4 is coprecipitated at ~70% of the level of cpSRP43. CD2/CD3 was copurified at ~50% of cpSRP43, whereas copurification of His-CD2 is only ~15% of cpSRP43. Decreased copurification of His-Ank1–4 by Alb3-Cterm is likely due to the absence of CD2, which, in agreement with ITC (Fig. 2.7) and previous copurifications (Fig. 2.8 A), provides minor additional strength to the interaction. The presence of CD1 reduces the amount of cpSRP43 construct copurified by Alb3-Cterm (~70% by Ank1–4 compared with ~50% by ΔCD2/CD3). It is interesting to speculate that CD1 may serve as a negative regulator of cpSRP43 binding to Alb3.

Alb3-Cterm Stimulates GTP Hydrolysis by cpSRP GTPases in a cpSRP43-dependent Manner

GTP binding and hydrolysis by cpSRP54/cpFtsY are critical for LHCP integration into the thylakoid membrane (*12, 16*). Given that the timing of GTP hydrolysis is carefully synchronized in SRP targeting to the endoplasmic reticulum as part of a mechanism to ensure that SRP is released from its receptor only after encountering an available translocase, it seems plausible that a similar mechanism to promote GTP hydrolysis only when Alb3 is available may involve cpSRP43 binding to Alb3-Cterm. To examine a possible influence of Alb3 on the GTP hydrolysis activity of cpSRP54/cpFtsY, we utilized a colorimetric assay that measures the release of Pi by GTP hydrolysis as described previously (*27, 46*). The amount of Pi released by 150 pmol each of cpSRP54 and cpFtsY (9.3 nmol of Pi per h) does not appear to be changed by the addition of His-

Stag-Alb3-Cterm. However, in the presence of cpSRP43, GTP hydrolysis by cpSRP54 and cpFtsY is stimulated in a linear fashion with increasing amounts of Alb3-Cterm (Fig. 2.9). The addition of 6000 pmol of Alb3-Cterm to 150 pmol each of cpSRP43/cpSRP54/cpFtsY (40 mol of Alb3-Cterm, 1 mol of cpSRP43/cpSRP54/cpFtsY) results in a 5-fold stimulation in GTP hydrolysis (from 12.7 to 51.3 nmol of Pi). It is important to note that GTP hydrolysis assays were conducted in the absence of the signal peptide-mimicking detergent Nikkol, which is known to elevate the GTP hydrolysis activities of SRP/SRP receptor (*48-49*) as well as cpSRP/cpFtsY (*50*). Regardless, our data demonstrate the ability of Alb3-Cterm to stimulate GTPase activity of cpSRP54 and cpFtsY is absolutely dependent on the presence of cpSRP43, which points to the cpSRP43-Alb3 interaction as representing a critical step in the recycling of cpSRP and its receptor.

cpSRP43 Ankyrin Repeats and Chromodomain 2, but Not Chromodomain 3, Are Necessary for the Alb3-Cterm Stimulation of GTP Hydrolysis by the cpSRP GTPases

A construct corresponding to the Ank1-CD2 region of cpSRP43 substitutes for full-length cpSRP43 in promoting stimulation of GTP hydrolysis by Alb3-Cterm (Fig. 2.10). Moreover, only cpSRP43 constructs containing both the Ank repeat domain and CD2 (ΔCD1, ΔCD3, and Ank1-CD2) were able to replace cpSRP43 in the ability to respond to the addition of Alb3-Cterm. Binding of the Ank repeat domain of cpSRP43 to Alb3-Cterm is likely communicated to cpSRP54/cpFtsY through interaction of the CD2 domain of cpSRP43 with cpSRP54 (*34-35, 51*). It is noteworthy that cpSRP43 constructs lacking CD1 (ΔCD1, His-Ank1-CD2) exhibit elevated levels of GTP hydrolysis in the absence of Alb3-Cterm such that stimulation of GTP hydrolysis by addition of Alb3-

Cterm is less pronounced. These observations are consistent with our previous work showing that CD1 serves as a negative regulator of GTP hydrolysis (*27*). Taken together, the data presented in Figs. 2.8 and 2.10 argue for a model in which Alb3 binding to the cpSRP43 Ank region is communicated by CD2 to cpSRP GTPases via a mechanism that reverses the negative GTPase regulation associated with CD1.

cpSRP43/Alb3-Cterm Interaction Plays a Role in the Separation of LHCP from cpSRP

It is well established that regulation of the GTPase cycle is a primary means of ensuring highly efficient and unidirectional SRP targeting. Membrane-bound ribosome-nascent chains associated with SRP and SRP receptor remain in the GTP-bound conformation in the absence of an active translocation channel (*52*), suggesting that the interaction with the translocon and release of the signal sequence are prerequisite for GTP hydrolysis. Similarly, the interaction of signal peptides with SRP-SRP receptor complex inhibits GTPase activity in the absence of an available Sec translocase (*53-54*). We also observe a reduction in GTP hydrolysis by cpSRP54 and cpFtsY in the presence of cpSRP43 and L18.5 Like cotranslationally targeted nascent polypeptides, LHCP must be released from cpSRP prior to or simultaneous with the recycling of the targeting components. The question lingers as to the events that initiate LHCP release from cpSRP. We took advantage of the fact that radiolabeled LHCP in complex with cpSRP43 and cpSRP54 can be detected as a soluble complex (termed transit complex) on nondenaturing gels (*21, 33*). If Alb3-Cterm binding to cpSRP43 is part of the mechanism to initiate LHCP release from cpSRP, we predict that transit complex formation and stability would be sensitive to the presence of Alb3-Cterm.

Fig. 2.11 A and B shows that incubation of radiolabeled pLHCP with cpSRP43 and cpSRP54 reconstitutes formation of a cpSRP-LHCP transit complex, which migrates as a distinct band when examined using nondenaturing PAGE. In the absence of cpSRP, pLHCP remains in the sample well (not shown) as documented previously (*33*). The addition of His-Stag-Alb3-Cterm to the transit complex assay following complex formation results in an upward shift in the radiolabeled LHCP signal such that most of the LHCP is found in the well at the highest concentration of Alb3-Cterm. To understand whether upward migration of LHCP stems from a shift of the entire LHCP-cpSRP transit complex or reflects an Alb3-Cterm induced instability of transit complex, we used radiolabeled cpSRP43 or cpSRP54 to follow their relative migration. Whereas the migration of cpSRP43 and cpSRP54 in native gels was similarly shifted at all concentrations of Alb3-Cterm examined, increasing Alb3-Cterm concentrations caused LHCP to separate from the cpSRP components and accumulate in the well (Fig. 2.11 A). Both the shift in migration of cpSRP components and the accumulation of LHCP in the well appeared specific to the influence of Alb3-Cterm because neither GST nor the CD3 domain of cpSRP43 as a recombinant protein affected transit complex migration (Fig. 2.11 B). This destabilization effect appears to involve formation of a slow migrating intermediate complex, which contains cpSRP54/cpSRP43/LHCP. Presumably, the slow migration of this intermediate represents transit complex bound to Alb3-Cterm. However, this remains to be confirmed. Another possibility is that binding of Alb3-Cterm to cpSRP43 in a transit complex state induces a conformational change, either in cpSRP43 individually or the transit complex as a species, leading to a shape/charge change that affects the migration of the complex into the nondenaturing gel.

Although the level of Alb3-Cterm required to observe changes in the transit complex are higher than anticipated, this could be expected if affinity of Alb3-Cterm for cpSRP43 is influenced by the lipid environment normally surrounding Alb3 or by cpSRP43 interaction partners, which differ at each step of the targeting pathway (*e.g.* affinity of Alb3-Cterm for cpSRP43 alone may be different from its affinity for cpSRP43 in transit complex with cpSRP54 and LHCP or in a cpSRP54-LHCP-cpFtsY complex at the membrane). Related to this possibility, Alb3-Cterm binding to cpSRP43 may also influence the affinity of cpSRP43 for its interaction partners (*e.g.* LHCP) as part of the mechanism that leads to unidirectional targeting of LHCP to Alb3. The ability of Alb3-Cterm to affect transit complex stability suggests there may be downstream effects on LHCP integration. However, studies involving the use of Alb3-Cterm to examine its influence on LHCP integration were inconclusive because of the ability of Alb3-Cterm to influence thylakoid membrane integrity (unpublished data).

DISCUSSION

Previous work has established that the unique post-translational activities of an SRP targeting system in chloroplasts enable cpSRP to bind imported LHCP targeting substrates in the stroma and direct them to the thylakoid membrane, resulting in formation of a membrane complex containing cpSRP/cpFtsY, bound substrate, and Alb3 (*12, 17, 55*). However, many of the mechanistic features underlying formation and disassembly of the membrane complex are not well understood. A possible role of cpSRP43 in membrane-localized targeting events was suggested by our previous work showing that cpSRP43 alone binds thylakoid membranes and is recovered in association with Alb3 (*24*). Data presented in this study indicate that the cpSRP43 binding of cpSRP54, LHCP, and Alb3 at distinct steps in the targeting pathway is used to communicate pathway progression of the targeting substrate to the evolutionarily conserved GTPases (cpSRP54/cpFtsY) such that GTPase activity is repressed until cpSRP43 interacts with an available Alb3 translocase. Together, our results support a model in which cpSRP43 serves as a translocon-sensing component to regulate the timing of membrane-associated steps in the post-translational cpSRP-dependent targeting pathway, *e.g.* transfer of substrate from cpSRP and recycling of SRP-targeting components.

Details of a cpSRP43-Alb3 interaction were reported recently and indicated that cpSRP43 chromodomains (CD2-CD3) form the binding interface with Alb3-Cterm (*13*). However, the low affinity reported between Alb3-Cterm and cpSRP43 (*Kd* 9.7_M) or CD2-CD3 (*Kd*_25_M) led us to re-examine this interaction using a combination of approaches. Although our data confirm an interaction between cpSRP43 and Alb3-Cterm,

the affinity appears to be in the nanomolar (*Kd*_94 nM), not micromolar, range. The disparity between our findings and those reported likely emanate, in part, from the use of glycerol by Falk *et al.* (*13*) in ITC experiments, which contributes significantly to the heats of dilution and thereby influences the binding constant *Kd* calculation(s) (Fig. 2.6). Furthermore, although CD2 may contribute to the binding interface, our data (Figs. 2.5 and 2.7) comparing affinity of Alb3-Cterm for cpSRP43, Ank1-CD2, and CD2 suggest that the ankyrin repeats provide the primary interface for binding to Alb3-Cterm (*Kd*_205 nM). In addition, although Falk *et al.* (*13*) state that the interaction with Alb3-Cterm requires both CD2 and CD3, it should be noted that CD3 is not required for integration of LHCP (*27*). *In vivo* data also indicates that CD2 does not play a critical role in targeting to Alb3, but instead it is restricted to SRP dimer formation and cpSRP43 chaperone activity (*24-26*).

Physiological significance of the interaction between cpSRP43 and Alb3-Cterm is supported by the ability of Alb3-Cterm peptide to stimulate GTP hydrolysis by cpSRP54/cpFtsY only in the presence of cpSRP43 and to promote release of LHCP from cpSRP in transit complex. cpSRP43 therefore appears to function as a mediator, linking the translocon, substrate, and cpSRP GTPases. *In vivo* studies have shown that LHCPs are predominantly routed via a cpSRP54 (cpFtsY)-dependent pathway but can be routed by a cpSRP54 (cpFtsY)-independent pathway in the absence of cpSRP54 (*15*). The cpSRP54-independent mechanism relies on cpSRP43, which is consistent with the ability of cpSRP43 to bind LHCP (28), function as an LHCP family-specific chaperone (*25-26*), and interact with the Alb3 insertase (*13, 24*). It should be noted that although there are several possible roles for cpSRP54 in LHCP localization, *e.g.* substrate release from

cpSRP43 or recycling of cpSRP43 from the membrane, it remains a possibility that cpSRP54-dependent differences in LHCP accumulation observed *in vivo* (*56*) occur at the level of targeting to Alb3.

It is also important to consider that the Ank region of cpSRP43 functions to bind the L18 motif in LHCP, an event critical to formation of a cpSRP-LHCP transit complex in stroma (*27-28, 30, 32-33*). This raises the possibility that binding of Alb3-Cterm to the Ank region of cpSRP43 is part of a mechanism to reduce cpSRP43 affinity for LHCP, thereby serving to promote release of LHCP from cpSRP only in the presence of an available Alb3. The ability of Alb3-Cterm peptide to destabilize the transit complex is consistent with this hypothesis (Fig. 2.11). Although our data support a model in which the Alb3 C terminus interacts with cpSRP43 to initiate LHCP release from cpSRP at the membrane, binding of the released targeting substrate to Alb3 remains to be demonstrated. However, the levels of Alb3-Cterm, relative to the level of cpSRP in the assay, required to destabilize the transit complex were higher than expected, based on the high affinity of Alb3-Cterm for cpSPR43 (Fig. 2.5 D). This may stem from Alb3-Cterm exhibiting a lower affinity for cpSRP43 in transit complex relative to cpSRP43 alone or in a cpSRP-LHCP-cpFtsY complex at the membrane. Affinity of Alb3-Cterm for cpSRP43 in cpSRP heterodimer was reported to be considerably reduced relative to cpSRP43 alone (*13*). Furthermore, release of LHCP in an *in vivo* environment is likely directly coupled to integration and would therefore require full-length Alb3 and lipid components. Regardless, the concentration-dependent ability of Alb3-Cterm (but not GST or CD3; Fig. 2.11) to destabilize the transit complex appears to take place through formation of a slow migrating intermediate containing at least cpSRP54/cpSRP43/LHCP.

The formation and disappearance of this intermediate relative to the disappearance of transit complex and appearance of LHCP in the sample well (free from cpSRP) is consistent with the idea that formation of an intermediate is a required step during LHCP release from cpSRP. Considering the data shown here and the current model for GTPase regulation of cytosolic SRPs (*57*), we propose the following model for cpSRP GTPase regulation (Fig. 2.12). Binding of cpSRP to LHCP to form transit complex primes cpSRP54 for binding GTP. Interactions with thylakoid membranes prime cpFtsY for binding cpSRP54 and GTP (*37*). The GTP-bound cpSRP43-LHCP-cpSRP54 transit complex in stroma associates with GTP-bound cpFtsY on thylakoid membranes. The membrane-associated complex is directed to Alb3 via an interaction between the Ank1–4 region of cpSRP43 and the C terminus of Alb3, which initiates LHCP release from cpSRP and GTP hydrolysis by cpSRP54/cpFtsY. In the absence of available Alb3, cpSRP/LHCP/cpFtsY remains in a membrane-associated complex because of an affinity of cpFtsY for lipids (*37*). GTP hydrolysis by cpSRP54 and cpFtsY leads to dissociation of cpSRP43/cpSRP54 and cpFtsY from Alb3. Our model, which incorporates general features from cotranslational SRP targeting systems, emphasizes a central role of cpSRP43 in soluble and membrane-targeting events because of its ability to bind Alb3 and initiate steps that stimulate GTP hydrolysis as well as reduce cpSRP affinity for LHCP targeting substrate. We are currently working toward a greater understanding of the steps critical for LHCP release from cpSRP and recycling of soluble targeting components.

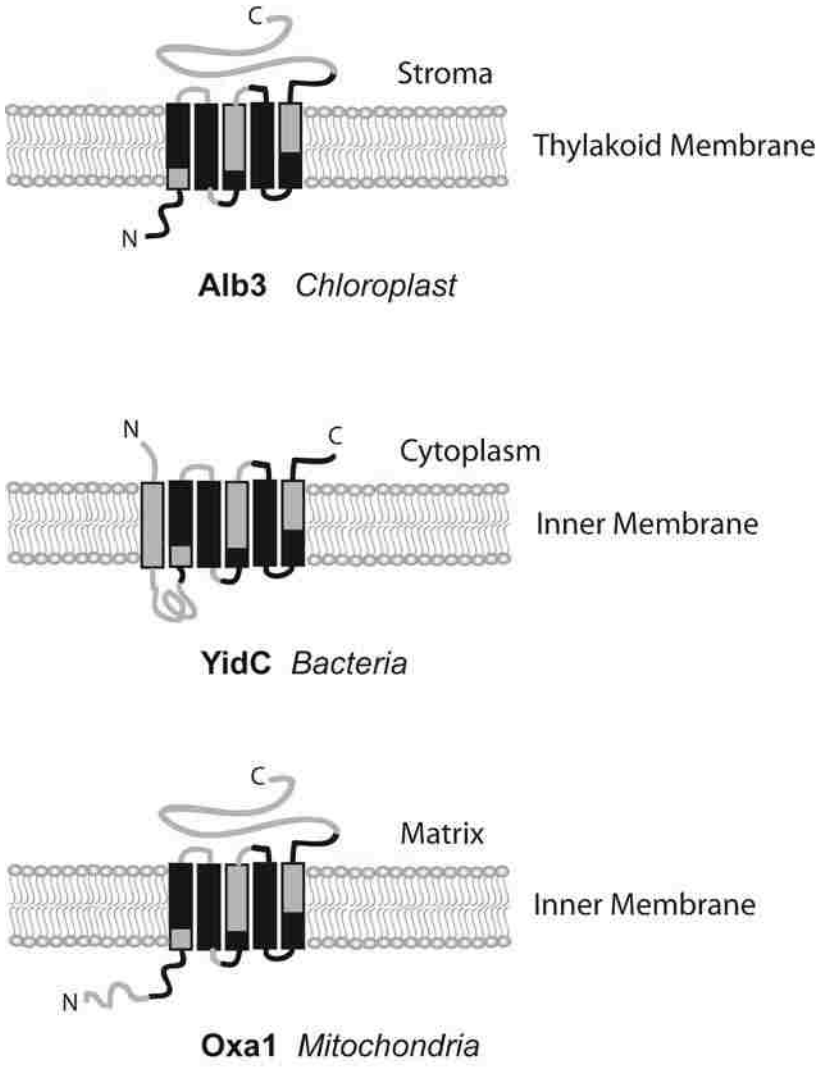

Figure 2.1. Representation of the conservation among the Alb3, YidC, and Oxa1 family members.

Conserved regions of the Alb3, YidC, and Oxa1 membrane proteins are shown in black and non-conserved regions in gray. Alb3 of the thylakoid membrane and Oxa1 of the inner mitochondrial membrane are polytopic membrane proteins with five transmembrane domains. The N-terminus of Alb3 faces the interior thylakoid lumen while the C-terminus extends into the stroma. Oxa1 is arranged with the N-terminus in the intermembrane space and the C-terminus facing the matrix. YidC has a sixth transmembrane spanning domain so that both the N- and C-termini extend into the cytoplasm. Figure adapted from van Bloois *et al*., 2005 (*8*).

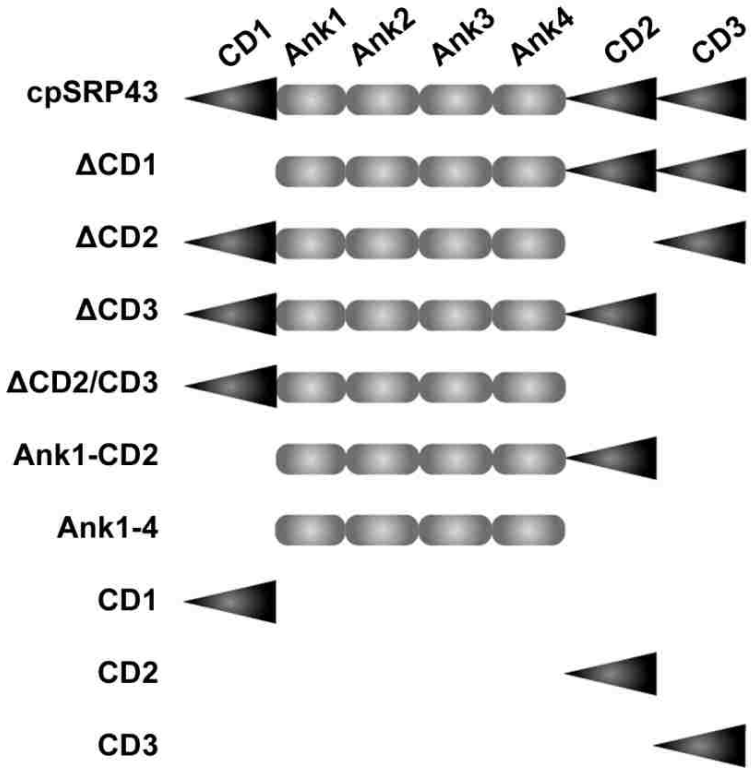

Figure 2.2. Model of the domain organization of cpSRP43 and cpSRP43 constructs.

Depiction of the domain organization of cpSRP43, with triangles representing chromodomains and rounded rectangles representing ankyrins. Domains are listed in the N to C termini order across the top. Protein constructs described in this study are shown as listed on the left.

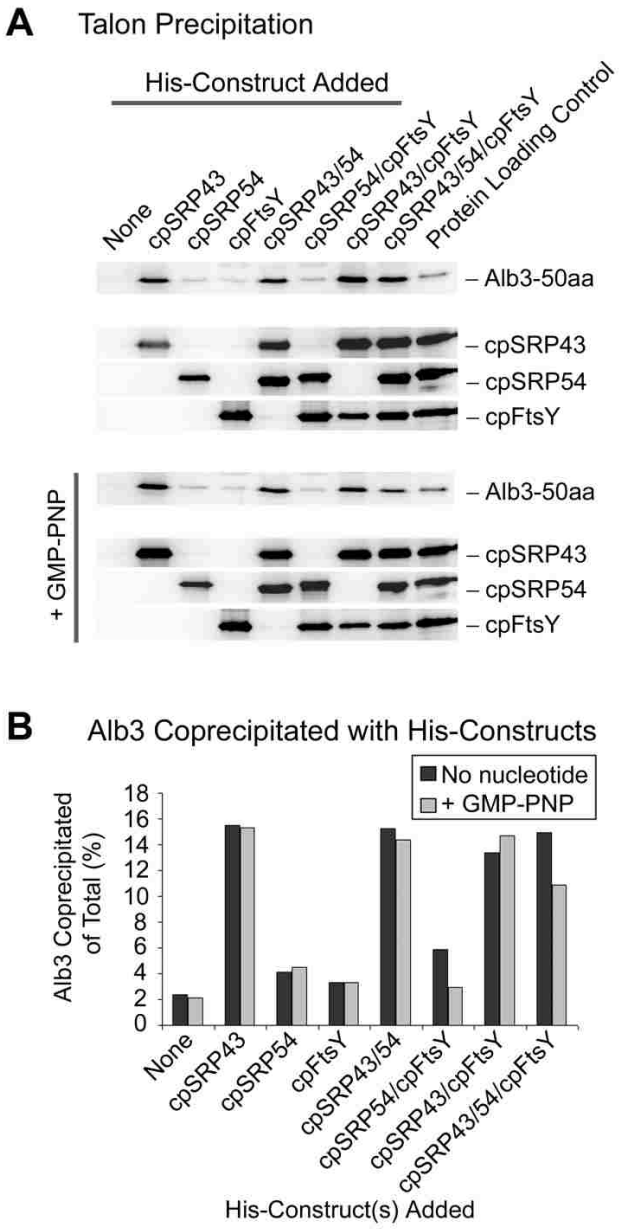

Figure 2.3. cpSRP43 is the predominant interacting partner with the translocase Alb3 in thylakoids.

A) SW thylakoids (75 μg of Chl) were incubated with 10 μg of His-tagged constructs as indicated. Membranes were solubilized and used for purification with Talon Superflow metal affinity resin. Western blots of copurified proteins are shown probed for proteins indicated to the *right. Protein Loading Control* lanes contain thylakoid membranes or 50 ng of His-tagged construct for comparing relative amounts precipitated. *aa*, amino acids. **B)** *Graph* depicts the amount of Alb3 copurified with His-tagged constructs. Total precipitated Alb3 was calculated from the relative signal of total thylakoid lane and eluate lanes in ***A***. Data obtained by Naomi Marty.

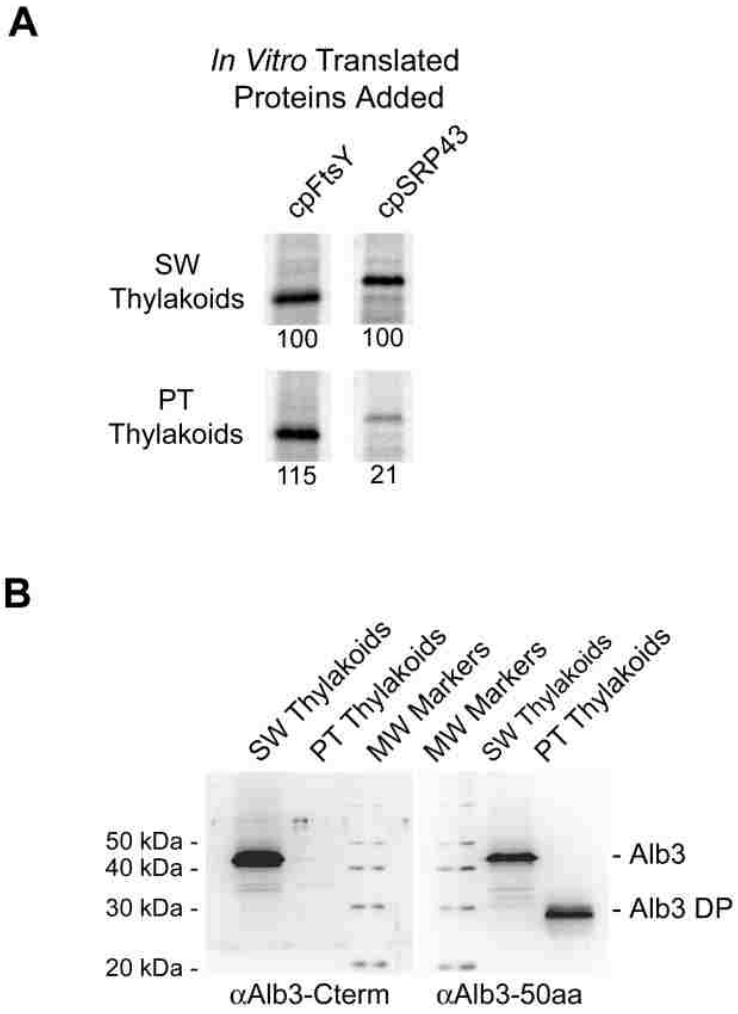

Figure 2.4. cpSRP43 binding to thylakoid membranes is protease sensitive.

A) Thylakoid membrane binding of radiolabeled cpSRP43 or cpFtsY was examined by incubation with salt-washed (SW) or protease-treated (PT) thylakoids. Thylakoids were re-isolated, washed and analyzed by SDS-PAGE and phosphorimaging. *In vitro* translation products were labeled differentially with S^{35}-Met and unlabeled Met such that equal signal represents equal molar quantities. S^{35} signal for individual components binding to SW thylakoids was set to 100 % and used for comparison and quantification of all other signals. **B)** Protease-treatment removes the soluble Alb3 C-terminus. Samples of both SW and PT thylakoids used in **A** were examined for complete protease-treatment of the membranes. Protease-treatment should result in conversion of Alb3 to Alb3-DP (detected by αAlb3-50aa), which indicates removal of the ~13 kD C-terminus (detected by αAlb3-Cterm). Data obtained by Naomi Marty.

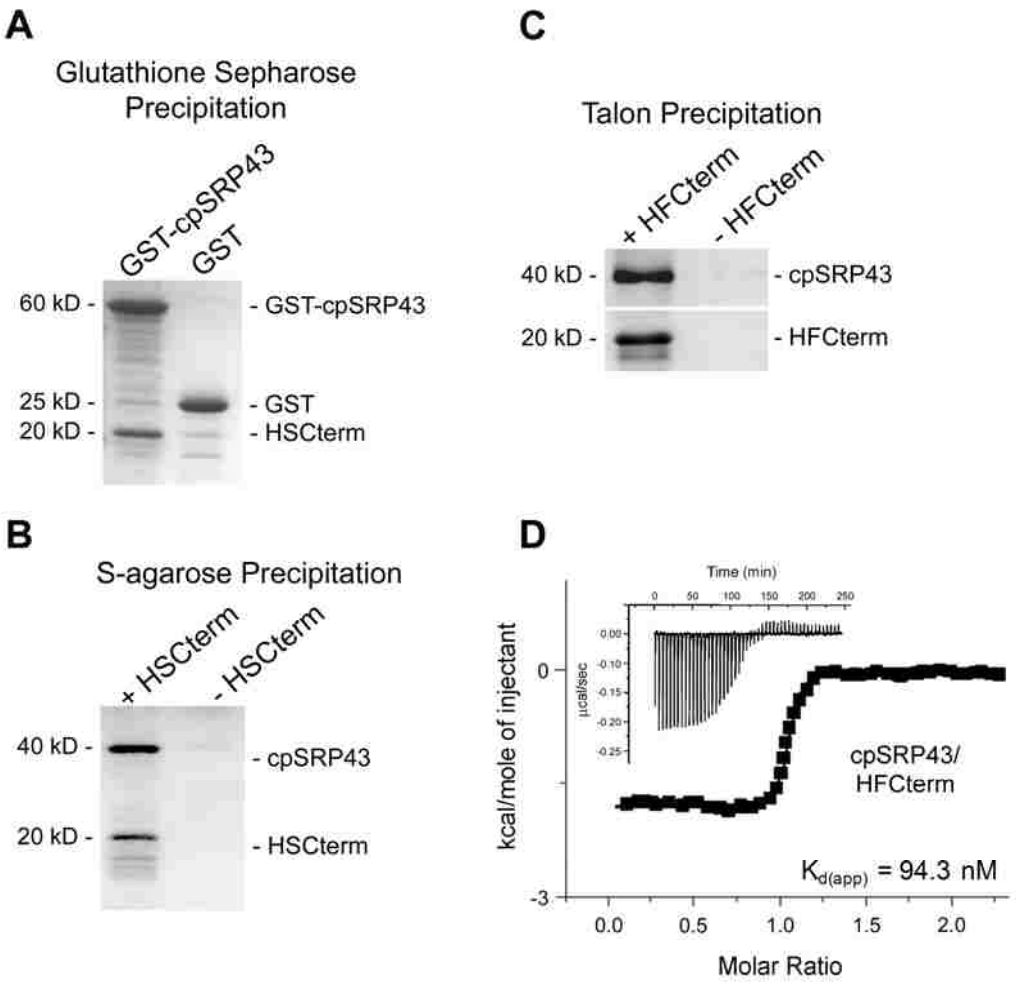

Figure 2.5. cpSRP43 and Alb3-Cterm interact with high affinity.

A) Equimolar concentrations of GST or GST-cpSRP43 were incubated with recombinant his-S_{tag}-Alb3-Cterm (HSCterm) and then recovered using Glutathione Sepharose resin and eluted with SDS buffer. The eluates were analyzed by SDS-PAGE and Coomassie blue staining. **B)** His-S_{tag}-Alb3-Cterm (HSCterm) was incubated with recombinant cpSRP43 and then recovered using S-protein agarose resin and eluted with SDS solubilization buffer. Eluates were analyzed as in **A**. **C**) His-Flag-Alb3-Cterm (HFCterm) was incubated with recombinant cpSRP43 and then recovered using Talon Superflow metal affinity resin and eluted with buffer containing imidazole. Eluates were analyzed as in **B** or by Western blotting for cpSRP43. **D)** ITC curve showing data characterizing interactions between His-FLAG-Alb3-Cterm with cpSRP43. All experiments were done at 25 °C. The insets and larger panels show the raw and integrated data, respectively, of the titration of cpSRP43 with Alb3-Cterm. The solid line in the larger panels represents the best fit curve of the data (Microcal Origin). Data obtained by Dakashinamurthy Rajalingam.

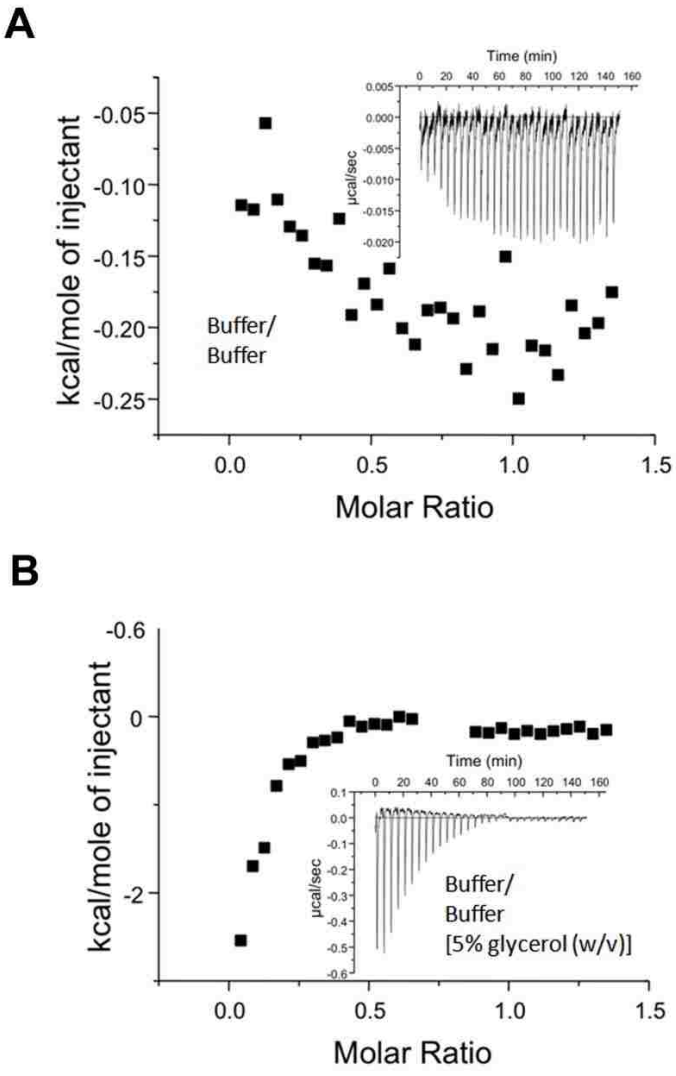

Figure 2.6. ITC data characterizing effect of glycerol.

ITC curves showing data characterizing the influence of 5% glycerol on the heats of dilution. All experiments were done at 25 °C. The insert and larger panels show the raw and integrated data, respectively, of the titration of buffer consisting of 20 mM HEPES 200 mM NaCl 2 mM MgCl2 1mM EDTA. The solid line in the larger panels represents the best-fit curve of the data (Microcal Origin). **A**) Depiction of buffer vs. buffer without glycerol. **B)** Depiction of buffer vs. buffer with 5% glycerol (w/v) included in both the cell and syringe. Significant heats of dilution are observed in the presence of glycerol. Data obtained by Anna Daily.

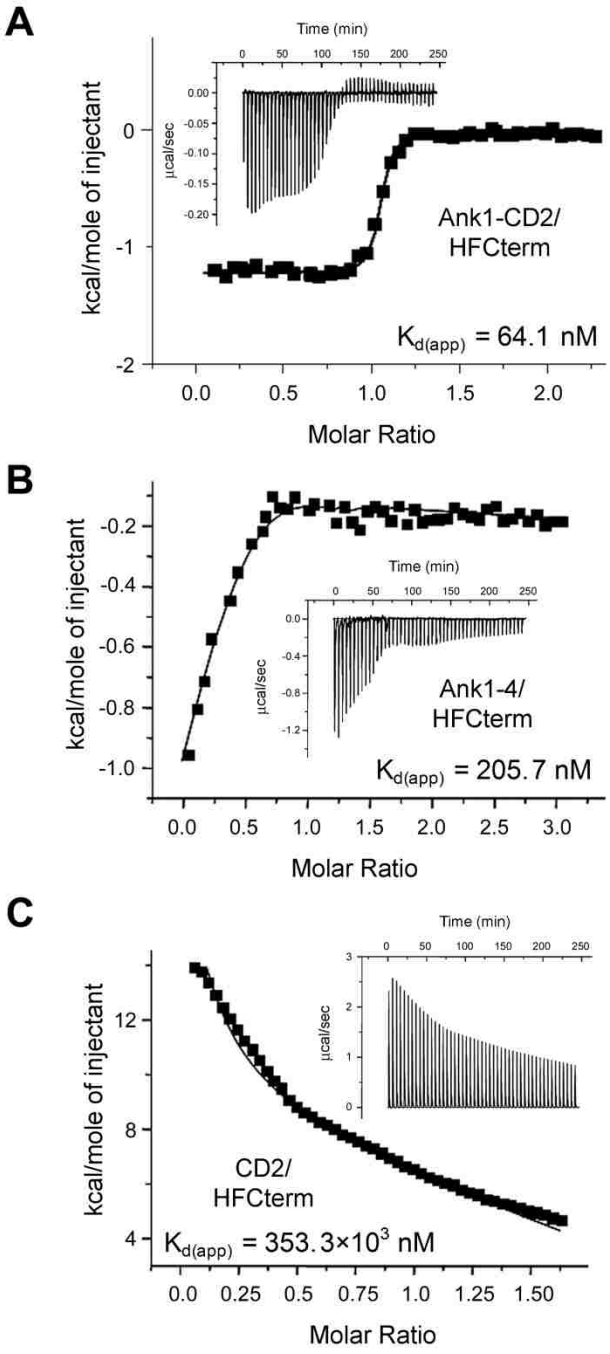

Figure 2.7. Ankyrin region of cpSRP43 is the interacting domain with the C terminus of Alb3.

A, B, C) ITC curves showing data characterizing interactions between His-FLAG-Alb3-Cterm with cpSRP43 constructs as indicated. All experiments were done at 25 °C. The insets and larger panels show the raw and integrated data, respectively, of the titration of cpSRP43 construct with Alb3-Cterm as indicated. The solid line in the larger panels represents the best fit curve of the data (Microcal Origin). Data obtained by Dakshinamurthy Rajalingam.

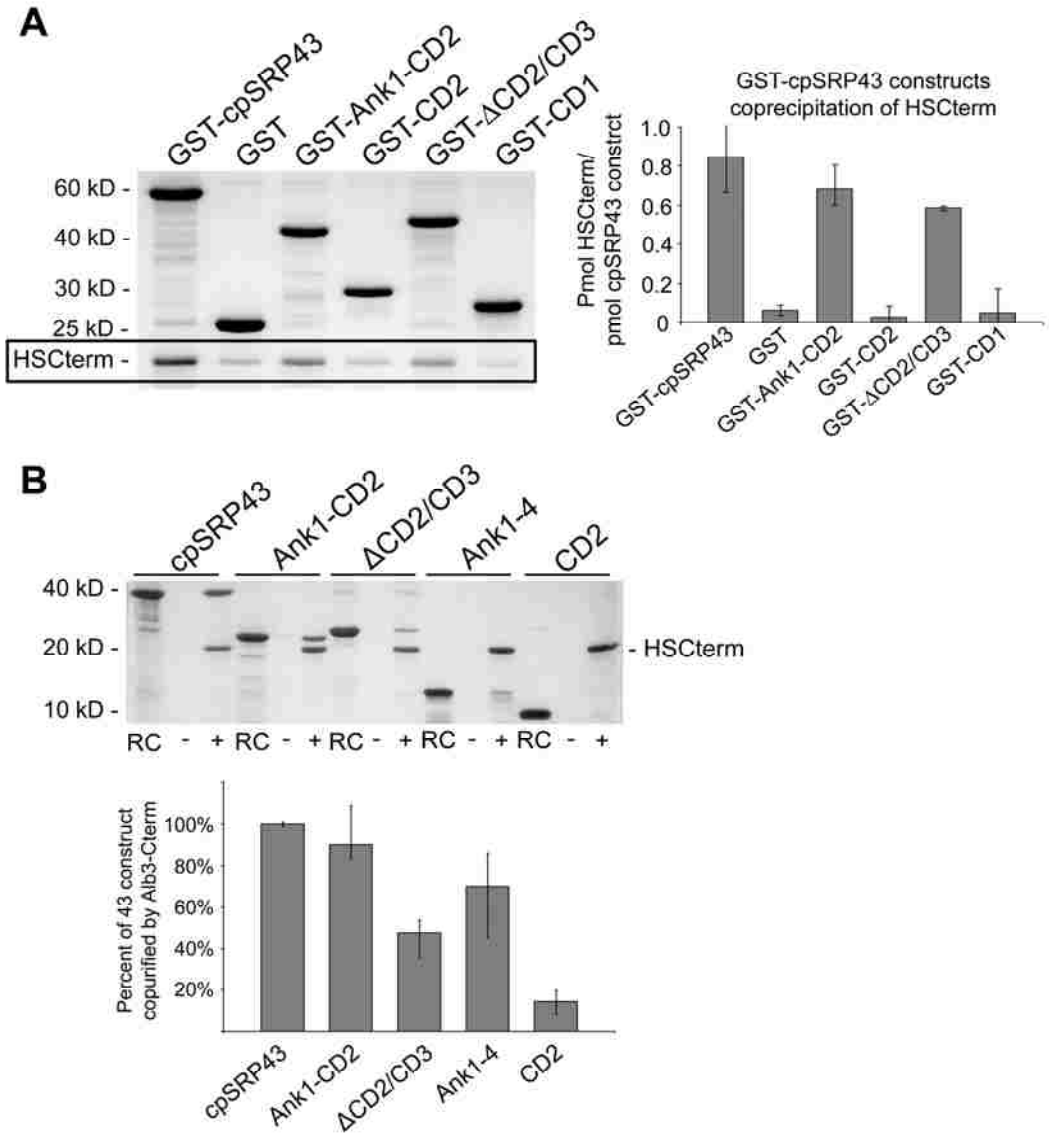

Figure 2.8. Ankyrin region of cpSRP43 and Alb3-Cterm coprecipitate.

A) Equimolar concentrations of GST or GST-43 construct were incubated with His-S_{tag}-Alb3-Cterm and then recovered using glutathione-Sepharose resin and eluted with SDS buffer. Eluates were analyzed by SDS-PAGE and Coomassie Blue staining. **B)** Equimolar concentrations of His-S_{tag}-Alb3-Cterm were incubated with cpSRP43, His-Ank1-CD2, ΔCD2/CD3, His-Ank1–4, or His-CD2 and then recovered using S-protein-agarose resin and eluted with SDS buffer. Lanes show proteins precipitated by His-S_{tag}-Alb3-Cterm (+) compared with background binding to resin alone (−). Lanes labeled RC (recombinant control) show appropriate migration distance of each cpSRP43 construct into the gel. Eluates were analyzed as in **A**.

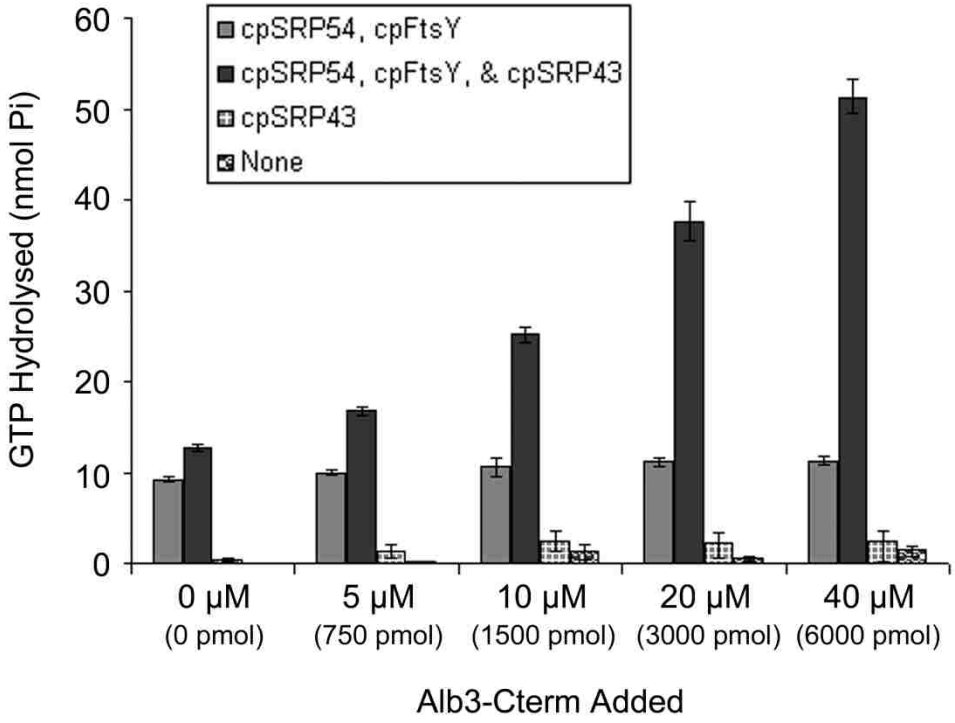

Figure 2.9. Alb3-Cterm binding to cpSRP43 stimulates GTP hydrolysis by the cpSRP GTPases.

The effect of Alb3-Cterm on the GTP hydrolysis activity of cpSRP54 and cpFtsY was examined in the presence or absence of cpSRP43. Assays contained 150 pmol (1 µm final concentration) of cpSRP43, cpSRP54, and cpFtsY and 0–6000 pmol (0–40 µm final concentration) of His-S_{tag}-Alb3-Cterm as indicated with 2 mm GTP as described under "Materials and Methods." GTPase activity resulting in the release of P_i was determined according to González-Romo *et al.* (44) using known phosphate standards. The average and standard deviation were calculated from three separate experiments.

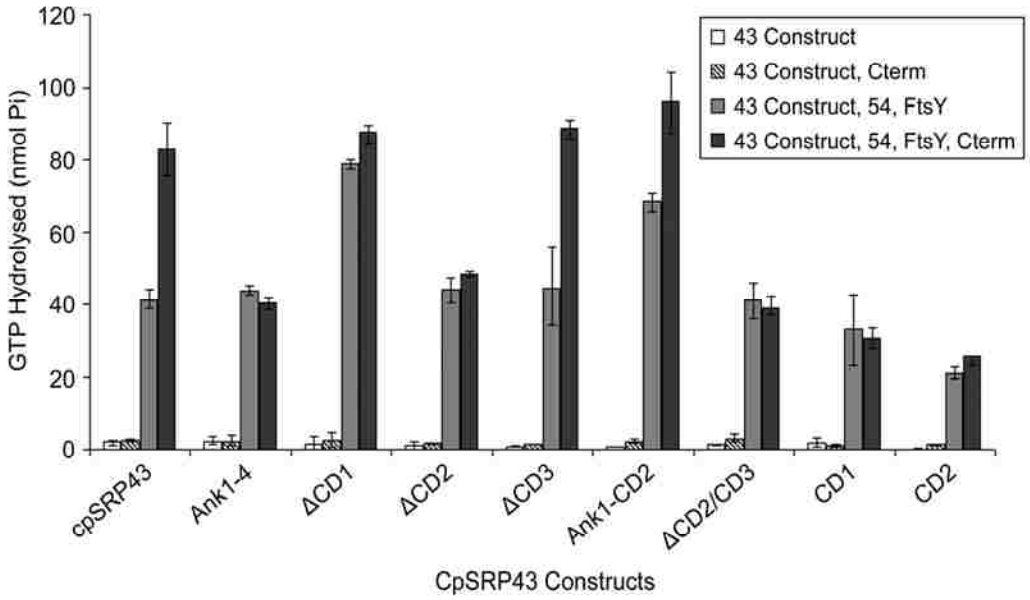

Figure 2.10. Ankyrin region of cpSRP43 and chromodomain 2 are necessary for Alb3-Cterm stimulation of GTP hydrolysis by the cpSRP GTPases.

The effect of Alb3-Cterm on the GTP hydrolysis activity of cpSRP54 and cpFtsY was examined in the presence or absence of cpSRP43, His-Ank1–4, ΔCD1, ΔCD2, ΔCD3, His-Ank1-CD2, ΔCD2/CD3, His-CD1, and His-CD2. Assays contained 150 pmol (1 μm final concentration) of cpSRP43 construct, cpSRP54, and cpFtsY and 4000 pmol (27 μm final) of His-S_{tag}-Alb3-Cterm as indicated with 2 mm GTP. GTPase activity resulting in the release of P_i was determined according to González-Romo *et al.* (44) using known phosphate standards. The average and standard deviation were calculated from three separate experiments.

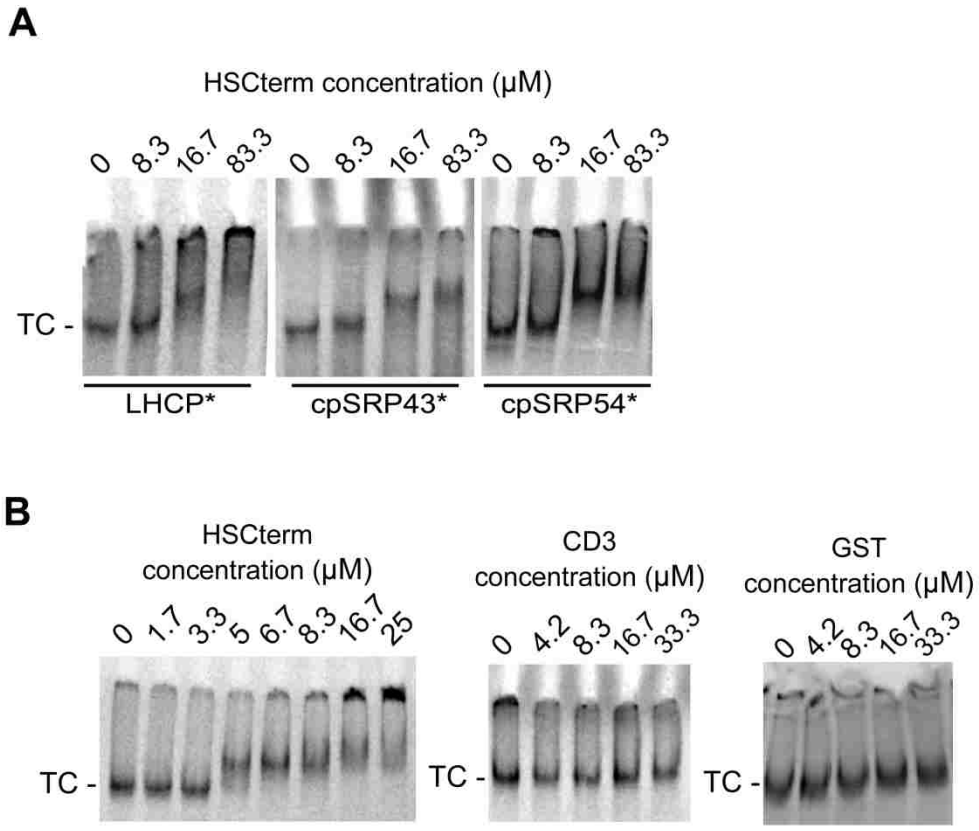

Figure 2.11. Interaction of cpSRP43 and Alb3-Cterm destabilizes transit complex.

A) *In vitro* translated transit complex components (pLHCP, cpSRP43, and cpSRP54) were incubated in the presence of increasing concentrations (0–83.3 μm and 0–5000 pmol) of His-S_{tag}-Alb3-Cterm as indicated. Transit complex formation was examined using native PAGE and phosphorimaging for the radiolabeled component as indicated (*). TC indicates transit complex band. **B)** Recombinant cpSRP43 and cpSRP54, in combination with *in vitro* translated and radiolabeled pLHCP, were used to form transit complex, which was monitored as in *A* after the addition of increasing concentrations (0–33.3 μm and 0–2000 pmol) of His-S_{tag}-Alb3-Cterm, GST, or CD3 as indicated. TC indicates transit complex band.

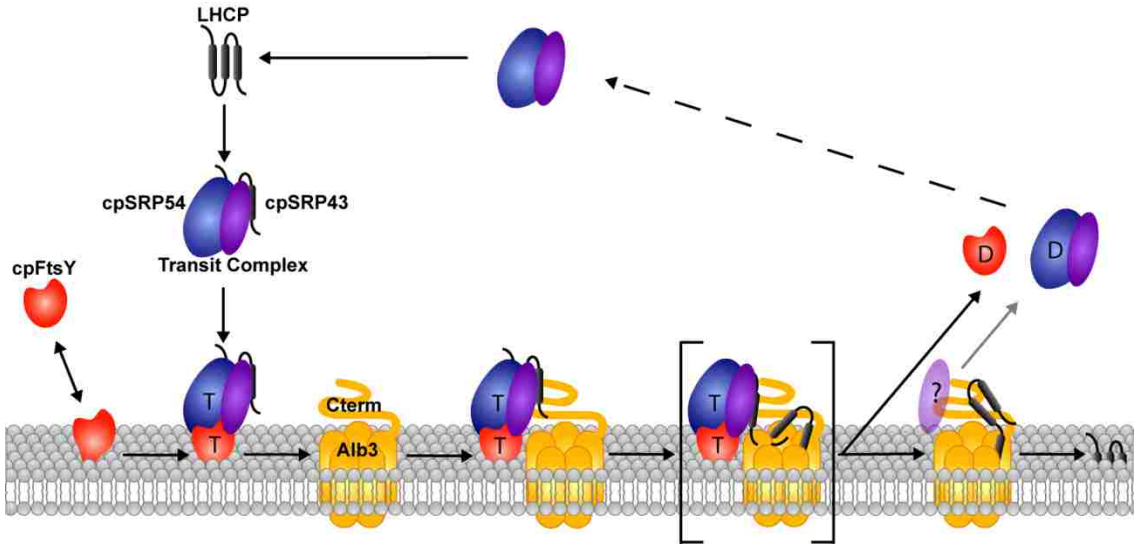

Figure 2.12. Current cpSRP43-dependent targeting model.

Interactions with thylakoid membranes prime cpFtsY for binding cpSRP54 and GTP. Interactions with cpSRP43/LHCP prime cpSRP54 for binding GTP. The GTP-bound cpSRP43-LHCP-cpSRP54 complex associates with GTP-bound cpFtsY on thylakoid membranes. The membrane-associated complex is directed to Alb3 via an interaction between the Ank1–4 region of cpSRP43 and the C terminus of Alb3. cpSRP43 binding to the C terminus of Alb3 initiates LHCP release from cpSRP. LHCP, which acts as a negative regulator of hydrolysis, is released from cpSRP for insertion into thylakoids. In the absence of LHCP, interactions with thylakoid membranes, cpSRP43, and Alb3 trigger reciprocal stimulation of GTP hydrolysis by cpSRP54 and cpFtsY. GTP hydrolysis leads to dissociation of cpSRP43/54 and cpFtsY components from Alb3 and the thylakoid membrane. cpSRP43 may remain associated with Alb3 following departure of the GTPases from the membrane.

REFERENCES

1. Luirink, J., Samuelsson, T., and de Gier, J. W. (2001) YidC/Oxa1p/Alb3: evolutionarily conserved mediators of membrane protein assembly, *FEBS Lett. 501*, 1-5.

2. Yen, M.-R., Harley, K. T., Tseng, Y.-H., and Saier, M. H., Jr. (2001) Phylogenetic and structural analyses of the oxa1 family of protein translocases, *FEMS Microbiol. Lett. 204*, 223-231.

3. Stuart, R. A. (2002) Insertion of proteins into the inner membrane of mitochondria: the role of the Oxa1 complex, *Biochim. Biophys. Acta 1592*, 79-87.

4. Dalbey, R. E., and Chen, M. (2004) Sec-translocase mediated membrane protein biogenesis, *Biochim. Biophys. Acta 1694*, 37-53.

5. Yi, L., and Dalbey, R. (2005) Oxa1/Alb3/YidC system for insertion of membrane proteins in mitochondria, chloroplasts and bacteria (Review), *Mol. Membr. Biol. 22*, 101-111.

6. Kuhn, A., Stuart, R., Henry, R., and Dalbey, R. E. (2003) The Alb3/Oxa1/YidC protein family: membrane-localized chaperones facilitating membrane protein insertion?, *Trends in Cell Biology 13*, 510-516.

7. Jiang, F., Yi, L., Moore, M., Chen, M., Rohl, T., Van Wijk, K. J., De Gier, J. W., Henry, R., and Dalbey, R. E. (2002) Chloroplast YidC homolog Albino3 can functionally complement the bacterial YidC depletion strain and promote membrane insertion of both bacterial and chloroplast thylakoid proteins, *J. Biol. Chem. 277*, 19281-19288.

8. van Bloois, E., Nagamori, S., Koningstein, G., Ullers, R. S., Preuss, M., Oudega, B., Harms, N., Kaback, H. R., Herrmann, J. M., and Luirink, J. (2005) The Sec-independent function of Escherichia coli YidC is evolutionary-conserved and essential, *J Biol Chem 280*, 12996-13003.

9. Preuss, M., Ott, M., Funes, S., Luirink, J., and Herrmann, J. M. (2005) Evolution of mitochondrial oxa proteins from bacterial YidC. Inherited and acquired functions of a conserved protein insertion machinery, *J Biol Chem 280*, 13004-13011.

10. Jia, L., Dienhart, M., Schramp, M., McCauley, M., Hell, K., and Stuart, R. A. (2003) Yeast Oxa1 interacts with mitochondrial ribosomes: the importance of the C-terminal region of Oxa1, *EMBO J. 22*, 6438-6447.

11. Szyrach, G., Ott, M., Bonnefoy, N., Neupert, W., and Herrmann, J. M. (2003) Ribosome binding to the Oxa1 complex facilitates co-translational protein insertion in mitochondria, *EMBO J. 22*, 6448-6457.

12. Moore, M., Goforth, R. L., Mori, H., and Henry, R. (2003) Functional interaction of chloroplast SRP/FtsY with the ALB3 translocase in thylakoids: substrate not required, *J. Cell Biol. 162*, 1245-1254.

13. Falk, S., Ravaud, S., Koch, J., and Sinning, I. (2010) The C terminus of the Alb3 membrane insertase recruits cpSRP43 to the thylakoid membrane, *J Biol Chem 285*, 5954-5962.

14. Asakura, Y., Hirohashi, T., Kikuchi, S., Belcher, S., Osborne, E., Yano, S., Terashima, I., Barkan, A., and Nakai, M. (2004) Maize mutants lacking chloroplast FtsY exhibit pleiotropic defects in the biogenesis of thylakoid membranes, *Plant Cell 16*, 201-214.

15. Hutin, C., Havaux, M., Carde, J. P., Kloppstech, K., Meiherhoff, K., Hoffman, N. E., and Nussaume, L. (2002) Double mutation cpSRP43/cpSRP54 is necessary to abolish the cpSRP pathway required for thylakoid targeting of the light-harvesting chlorophyll proteins., *Plant Journal 29*, 531-543.

16. Tu, C. J., Schuenemann, D., and Hoffman, N. E. (1999) Chloroplast FtsY, chloroplast signal recognition particle, and GTP are required to reconstitute the soluble phase of light-harvesting chlorophyll protein transport into thylakoid membranes, *J. Biol. Chem. 274*, 27219-27224.

17. Moore, M., Harrison, M. S., Peterson, E. C., and Henry, R. (2000) Chloroplast oxa1p homolog albino3 is required for post-translational integration of the light harvesting chlorophyll-binding protein into thylakoid membranes, *J. Biol. Chem. 275*, 1529-1532.

18. Klimyuk, V. I., Persello-Cartieaux, F., Havaux, M., Contard-David, P., Schuenemann, D., Meiherhoff, K., Gouet, P., Jones, J. D., Hoffman, N. E., and Nussaume, L. (1999) A chromodomain protein encoded by the Arabidopsis CAO gene is a plant- specific component of the chloroplast Signal Recognition Particle pathway that is involved in LHCP targeting, *Plant Cell 11*, 87-100.

19. Schuenemann, D., Gupta, S., Persello-Cartieaux, F., Klimyuk, V. I., Jones, J. D. G., Nussaume, L., and Hoffman, N. E. (1998) A novel signal recognition particle targets light-harvesting proteins to the thylakoid membranes, *Proc. Natl. Acad. Sci. U. S. A. 95*, 10312-10316.

20. Schuenemann, D. (2004) Structure and function of the chloroplast signal recognition particle, *Curr. Genet. 44*, 295-304.

21. Li, X., Henry, R., Yuan, J., Cline, K., and Hoffman, N. E. (1995) A chloroplast homologue of the signal recognition particle subunit SRP54 is involved in the posttranslational integration of a protein into thylakoid membranes, *Proc. Natl. Acad. Sci. U. S. A. 92*, 3789-3793.

22. Bacher, G., Lutcke, H., Jungnickel, B., Rapoport, T. A., and Dobberstein, B. (1996) Regulation by the ribosome of the GTPase of the signal-recognition particle during protein targeting [see comments], *Nature 381*, 248-251.

23. Mandon, E. C., Jiang, Y., and Gilmore, R. (2003) Dual recognition of the ribosome and the signal recognition particle by the SRP receptor during protein targeting to the endoplasmic reticulum, *J. Cell Biol. 162*, 575-585.

24. Tzvetkova-Chevolleau, T., Hutin, C., Noel, L. D., Goforth, R., Carde, J.-P., Caffarri, S., Sinning, I., Groves, M., Teulon, J.-M., Hoffman, N. E., Henry, R., Havaux, M., and Nussaume, L. (2007) Canonical signal recognition particle components can be bypassed for posttranslational protein targeting in chloroplasts, *Plant Cell 19*, 1635-1648.

25. Falk, S., and Sinning, I. (2010) cpSRP43 is a novel chaperone specific for light-harvesting chlorophyll a,b-binding proteins, *J Biol Chem 285*, 21655-21661.

26. Jaru-Ampornpan, P., Shen, K., Lam, V. Q., Ali, M., Doniach, S., Jia, T. Z., and Shan, S. O. (2010) ATP-independent reversal of a membrane protein aggregate by a chloroplast SRP subunit, *Nat. Struct. Mol. Biol. 17*, 696-702.

27. Goforth, R. L., Peterson, E. C., Yuan, J., Moore, M. J., Kight, A. D., Lohse, M. B., Sakon, J., and Henry, R. L. (2004) Regulation of the GTPase cycle in post-translational Signal Recognition Particle-based protein targeting involves cpSRP43, *J. Biol. Chem. 279*, 43077-43084.

28. Tu, C. J., Peterson, E. C., Henry, R., and Hoffman, N. E. (2000) The L18 domain of light-harvesting chlorophyll proteins binds to chloroplast signal recognition particle 43, *J. Biol. Chem. 275*, 13187-13190.

29. Groves, M. R., Mant, A., Kuhn, A., Koch, J., Dubel, S., Robinson, C., and Sinning, I. (2001) Functional characterization of recombinant chloroplast signal recognition particle, *J. Biol. Chem. 276*, 27778-27786.

30. Jonas-Straube, E., Hutin, C., Hoffman, N. E., and Schunemann, D. (2001) Functional analysis of the protein-interacting domains of chloroplast SRP43, *J. Biol. Chem. 276*, 24654-24660.

31. Lewis, N. E., Marty, N. J., Kathir, K. M., Rajalingam, D., Kight, A. D., Daily, A., Kumar, T. K., Henry, R. L., and Goforth, R. L. (2010) A dynamic cpSRP43-Albino3 interaction mediates translocase regulation of chloroplast signal recognition particle (cpSRP)-targeting components, *J Biol Chem 285*, 34220-34230.

32. Stengel, K. F., Holdermann, I., Cain, P., Robinson, C., Wild, K., and Sinning, I. (2008) Structural Basis for Specific Substrate Recognition by the Chloroplast Signal Recognition Particle Protein cpSRP43, *Science 321*, 253-256.

33. DeLille, J., Peterson, E. C., Johnson, T., Moore, M., Kight, A., and Henry, R. (2000) A novel precursor recognition element facilitates posttranslational binding to the signal recognition particle in chloroplasts, *Proc. Natl. Acad. Sci. U. S. A. 97*, 1926-1931.

34. Hermkes, R., Funke, S., Richter, C., Kuhlmann, J., and Schuenemann, D. (2006) The α-helix of the second chromodomain of the 43kDa subunit of the chloroplast signal recognition particle facilitates binding to the 54kDa subunit, *FEBS Lett. 580*, 3107-3111.

35. Kathir, K. M., Rajalingam, D., Sivaraja, V., Kight, A., Goforth, R. L., Yu, C., Henry, R., and Kumar, T. K. S. (2008) Assembly of Chloroplast Signal Recognition Particle Involves Structural Rearrangement in cpSRP43, *J. Mol. Biol. 381*, 49-60.

36. Cline, K., Fulsom, D. R., and Viitanen, P. V. (1989) An imported thylakoid protein accumulates in the stroma when insertion into thylakoids is inhibited, *J Biol Chem 264*, 14225-14232.

37. Marty, N. J., Rajalingam, D., Kight, A. D., Lewis, N. E., Fologea, D., Kumar, T. K. S., Henry, R. L., and Goforth, R. L. (2009) The Membrane-binding Motif of the Chloroplast Signal Recognition Particle Receptor (cpFtsY) Regulates GTPase Activity, *J. Biol. Chem. 284*, 14891-14903.

38. Yuan, J., Kight, A., Goforth, R. L., Moore, M., Peterson, E. C., Sakon, J., and Henry, R. (2002) ATP stimulates signal recognition particle (SRP)/FtsY-supported protein integration in chloroplasts, *J. Biol. Chem. 277*, 32400-32404.

39. Jaru-Ampornpan, P., Chandrasekar, S., and Shan, S.-o. (2007) Efficient Interaction between Two GTPases Allows the Chloroplast SRP Pathway to Bypass the Requirement for an SRP RNA, *Mol. Biol. Cell 18*, 2636-2645.

40. Woolhead, C. A., Thompson, S. J., Moore, M., Tissier, C., Mant, A., Rodger, A., Henry, R., and Robinson, C. (2001) Distinct Albino3-dependent and -independent pathways for thylakoid membrane protein insertion, *J Biol Chem 276*, 40841-40846.

41. Cline, K., Henry, R., Li, C., and Yuan, J. (1993) Multiple pathways for protein transport into or across the thylakoid membrane, *EMBO J. 12*, 4105-4114.

42. Arnon, D. I. (1949) Copper enzymes in isolated chloroplasts. Polyphenoloxidase in Beta vulgaris, *Plant Physiol. 24*, 1-15.

43. Chu, F., Shan, S. O., Moustakas, D. T., Alber, F., Egea, P. F., Stroud, R. M., Walter, P., and Burlingame, A. L. (2004) Unraveling the interface of signal recognition particle and its receptor by using chemical cross-linking and tandem mass spectrometry, *Proc Natl Acad Sci U S A 101*, 16454-16459.

44. Jelesarov, I., and Bosshard, H. R. (1999) Isothermal titration calorimetry and differential scanning calorimetry as complementary tools to investigate the energetics of biomolecular recognition, *J. Mol. Recognit. 12*, 3-18.

45. Payan, L. A., and Cline, K. (1991) A stromal protein factor maintains the solubility and insertion competence of an imported thylakoid membrane protein, *J. Cell Biol. 112*, 603-613.

46. Gonzalez-Romo, P., Sanchez-Nieto, S., and Gavilanes-Ruiz, M. (1992) A modified colorimetric method for the determination of orthophosphate in the presence of high ATP concentrations, *Anal Biochem 200*, 235-238.

47. Roselin, L. S., Lin, M.-S., Lin, P.-H., Chang, Y., and Chen, W.-Y. (2010) Recent trends and some applications of isothermal titration calorimetry in biotechnology, *Biotechnology Journal 5*, 85-98.

48. Bradshaw, N., Neher, S. B., Booth, D. S., and Walter, P. (2009) Signal sequences activate the catalytic switch of SRP RNA, *Science 323*, 127-130.

49. Zhang, X., Schaffitzel, C., Ban, N., and Shan, S.-o. (2009) Multiple conformational switches in a GTPase complex control co-translational protein targeting, *Proc. Natl. Acad. Sci. U. S. A.*, 1-6.

50. Jaru-Ampornpan, P., Nguyen, T. X., and Shan, S. O. (2009) A distinct mechanism to achieve efficient signal recognition particle (SRP)-SRP receptor interaction by the chloroplast srp pathway, *Mol Biol Cell 20*, 3965-3973.

51. Sivaraja, V., Kumar, T. K. S., Leena, P. S. T., Chang, A.-n., Vidya, C., Goforth, R. L., Rajalingam, D., Arvind, K., Ye, J.-L., Chou, J., Henry, R., and Yu, C. (2005) Three-dimensional solution structures of the chromodomains of cpSRP43, *J. Biol. Chem. 280*, 41465-41471.

52. Song, W., Raden, D., Mandon, E. C., and Gilmore, R. (2000) Role of Sec61alpha in the regulated transfer of the ribosome-nascent chain complex from the signal recognition particle to the translocation channel, *Cell 100*, 333-343.

53. Miller, J. D., and Walter, P. (1993) A GTPase cycle in initiation of protein translocation across the endoplasmic reticulum membrane, *Ciba Found Symp 176*, 147-159.

54. Rapiejko, P. J., and Gilmore, R. (1997) Empty site forms of the SRP54 and SR alpha GTPases mediate targeting of ribosome-nascent chain complexes to the endoplasmic reticulum [see comments], *Cell 89*, 703-713.

55. Kogata, N., Nishio, K., Hirohashi, T., Kikuchi, S., and Nakai, M. (1999) Involvement of a chloroplast homologue of the signal recognition particle receptor protein, FtsY, in protein targeting to thylakoids, *FEBS Lett. 447*, 329-333.

56. Rutschow, H., Ytterberg, A. J., Friso, G., Nilsson, R., and van Wijk, K. J. (2008) Quantitative Proteomics of a Chloroplast SRP54 Sorting Mutant and Its Genetic Interactions with CLPC1 in Arabidopsis, *Plant Physiol. 148*, 156-175.

57. Shan, S. O., and Walter, P. (2005) Co-translational protein targeting by the signal recognition particle, *FEBS Lett. 579*, 921-926.

APPENDIX A

RESPONSE TO FALK AND SINNING: THE C TERMINUS OF ALB3 INTERACTS WITH THE CHROMODOMAINS 2 AND 3 OF CPSRP43

Accepted for publication as:

Lewis, N.E., Kight, A., Daily, A., Kumar, T.K.S., Henry, R.L., and Goforth R.L. (2010) Response to Falk and Sinning: The C Terminus of Alb3 Interacts with the Chromodomains 2 and 3 of cpSRP43, *J. Biol. Chem*. 285, le26-le28.

This is a response to a letter by Falk and Sinning (1)

We recently identified the ankyrin region of cpSRP43 as the primary domain responsible for binding Alb3-Cterm during light-harvesting chlorophyll-binding protein (LHCP) targeting, an interaction shown to facilitate cpSRP43-dependent stimulation of cpSRP GTPases by Alb3-Cterm (*2*). Falk et al. (*3*), using only protein interaction assays, report that CD2CD3 of cpSRP43 forms the Alb3-Cterm binding interface, which appears inconsistent with the fact that CD3 is not required for LHCP integration (*4*) and that CD2 is not required for LHCP integration by a cpSRP54/cpFtsY-independent pathway that relies on cpSRP43/Alb3 (*5*).

We suggested that buffer choice, including the use of glycerol, may play a role in why Falk et al. (*3*) observed μM rather than nM affinity for cpSRP43 constructs (*2*). The use of high concentrations of glycerol in isothermal titration calorimetry (ITC) is known to cause experimental artifacts (*6*). Our control experiments clearly show that the use of glycerol, even at 5% v/v, causes significant background heat changes (Fig. A.1). In their letter, Sinning and Falk report a 13 μM affinity even in the absence of glycerol, suggesting glycerol may not be the primary cause for the reported differences. Although species-specific differences in Alb3-Cterm could explain the observed affinity differences, comparing GTPase stimulation by Arabidopsis and Pisum sativum Alb3-Cterm does not support this possibility (Fig. A.2).

Published reports (*2*, *4*-*5*) supporting the physiological relevance of high affinity protein interactions still suggest that the low affinity of cpSRP43 for Alb3-Cterm reported by Falk et al. (*3*) stems from assay conditions unfavorable for observing the primary targeting interaction that takes place between Alb3-Cterm and the Ank region of

cpSRP43. Importantly, buffers used by Falk et al. (*3*) in ITC and size-exclusion experiments do not support LHCP integration (Fig. A.3). In addition, Ank-containing cpSRP43 constructs, including those that lack CD2 and/or CD3, are able to prevent binding of radiolabeled cpSRP43 to Alb3 in salt-washed thylakoids whereas chromodomains do not (Fig. A.4).

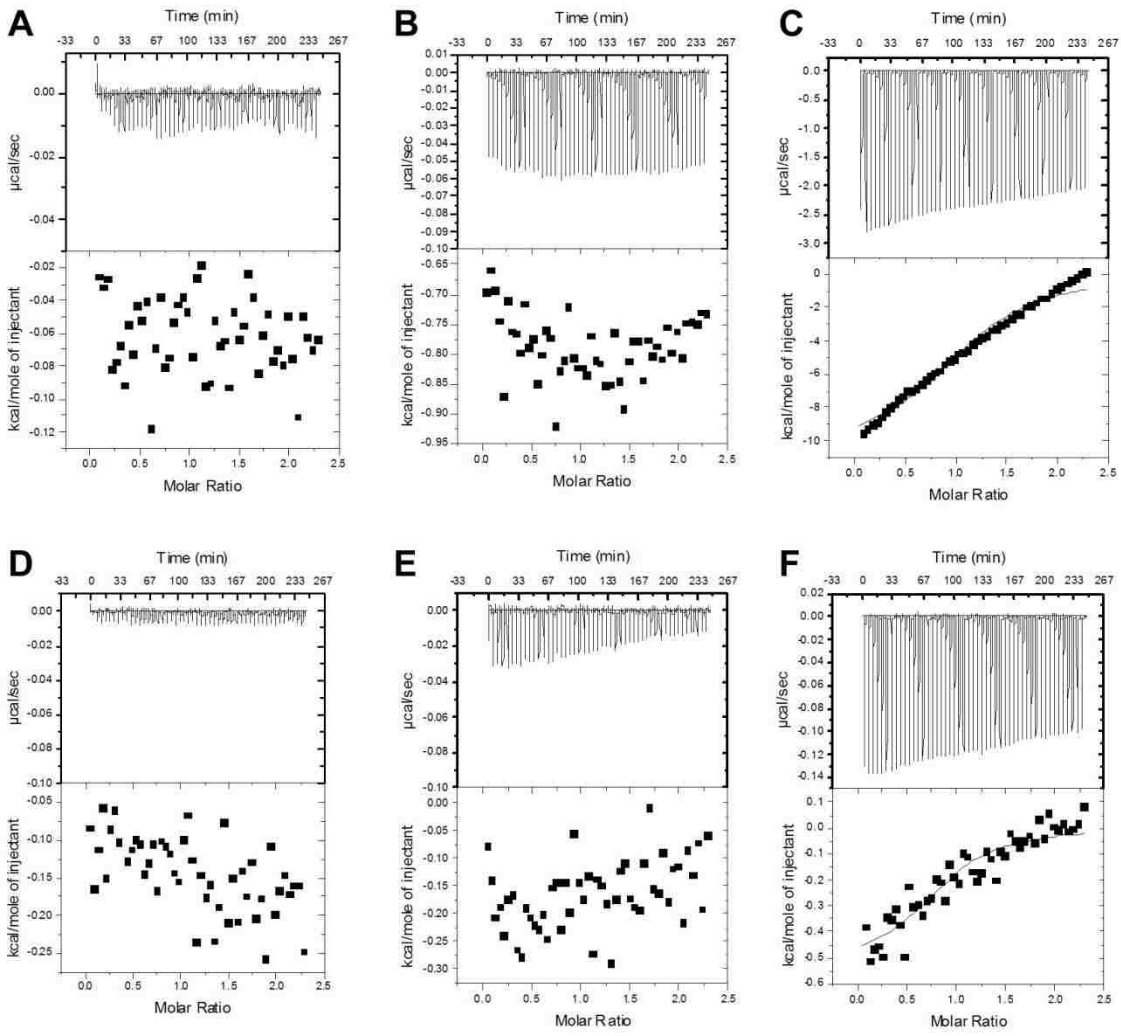

Figure A.1. Isothermal titration calorimetry investigation of the influence of glycerol in various buffers in buffer to buffer experiments.

ITC was conducted by injecting a specific buffer/glycerol formulation into a sample well containing the same buffer/glycerol formulation. Buffers were:
A) 10 mM phosphate,100 mM NaCl, 50 mM AMS, pH 6.5
B) 10 mM phosphate, 100 mM NaCl, 50 mM AMS, 2.5% glycerol (v/v), pH 6.5
C) 10 mM phosphate, 100 mM NaCl, 50 mM AMS, 5% glycerol (v/v), pH 6.5
D) ITC Buffer (Falk *et al.* (*3*)): 20 mM HEPES/NaOH pH 7.5, 200 mM NaCl, 2 mM MgCl2, 1 mM EDTA, 0.25 mM TCEP
E) ITC Buffer with 2.5% glycerol (Falk *et al.* (*3*)): 20 mM HEPES/NaOH pH 7.5, 200 mM NaCl, 2 mM MgCl2, 1 mM EDTA, 0.25 mM TCEP, 2.5% glycerol (v/v)
F) ITC Buffer with 5% glycerol (Falk *et al.* (*3*)): 20 mM HEPES/NaOH pH 7.5, 200 mM NaCl, 2 mM MgCl2, 1 mM EDTA, 0.25 mM TCEP, 5% glycerol (v/v)
Although polyols such as glycerol are frequently used to stabilize proteins, they cannot be assumed innocuous. Data obtained by Anna Daily.

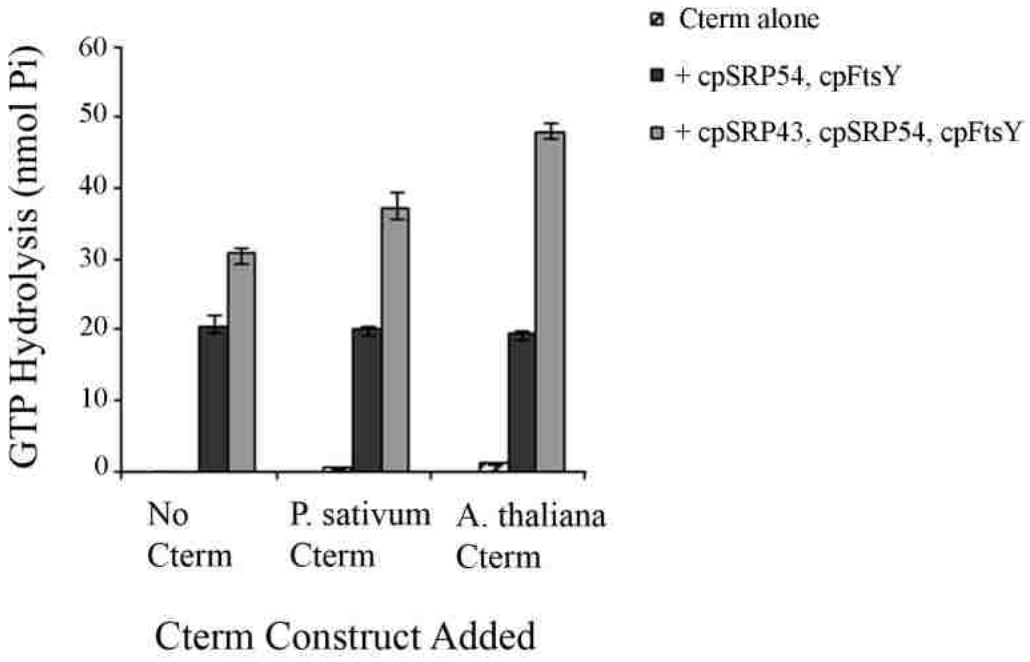

Figure A.2. Comparison of the ability of *Pisum sativum* and *Arabidopsis thaliana* Alb3-Cterm peptide to stimulate cpSRP43-dependent GTP hydrolysis by the cpSRP GTPases.

The effect of Alb3-Cterm on the GTP hydrolysis activity of cpSRP54 and cpFtsY was examined in the presence or absence of cpSRP43. Assays contained 150 pmol (1 μM final concentration) of cpSRP43, cpSRP54, and cpFtsY and 4000 pmol (27 μM final) of *P. sativum* or *A. thaliana* Alb3-Cterm as indicated with 2 mM GTP. GTPase activity resulting in the release of inorganic phosphate (Pi) was determined according to Gonzalez and Romo (*7*) using known phosphate standards. The average and standard deviation were calculated from three separate experiments. In conclusion, peptides corresponding to both *P. sativum* and *A. thaliana* are able to increase GTP hydrolysis in a cpSRP43-dependent manner, which is as expected given that the heterologous system has been repeatedly shown to be fully functional in reconstituting LHCP integration (see also Fig. A.3).

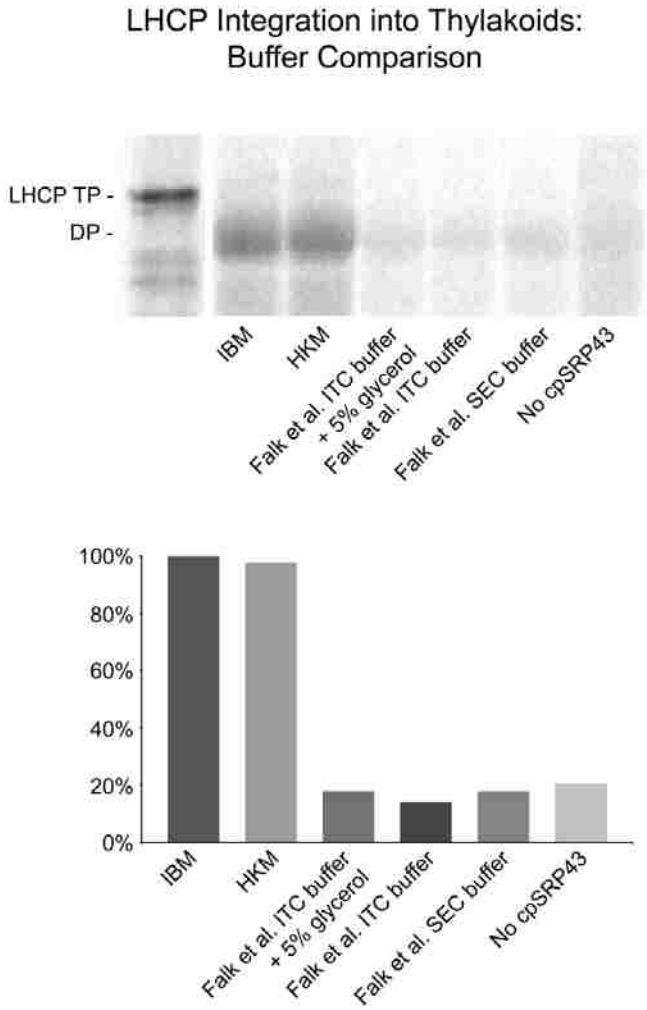

Figure A.3. Buffer influence on LHCP integration.

Salt-washed thylakoids in IBM were incubated with 5 mM ATP, 1 mM GTP, 12.5 µL of radiolabeled pLHCP translation product, and recombinant cpSRP43, cpSRP54, and cpFtsY (*2*). The final volume was brought to 150 µL in IBM or to 150 µL with a final concentration matching the buffer listed: **IBM:** 50 mM Hepes/KOH pH 8.0, 330 mM sorbitol, 10 mM MgCl2; **HKM:** 10 mM Hepes/KOH pH 8.0, 10 mM MgCl2; **ITC Buffer + 5% glycerol, Falk *et al.* (*3*):** 20 mM Hepes/NaOH pH 7.5, 200 mM NaCl, 2 mM MgCl2, 1 mM EDTA, 5% (w/v) glycerol, 0.25 mM tris(2-carboxyethyl)phosphine); **ITC Buffer, Falk *et al.* (*3*):** 20 mM Hepes/NaOH pH 7.5, 200 mM NaCl, 2 mM MgCl2, 1 mM EDTA, 0.25mM tris(2-carboxyethyl)phosphine); **SEC Buffer, Falk *et al.* (*3*):** 20 mM Hepes/NaOH pH 7.5, 200 mM NaCl, 2 mM MgCl2, 1 mM EDTA, 1 mM DTT. Reactions were incubated at 25 °C for 30 min under light. Membranes were collected by centrifugation at 3200 × g for 6 min at 4 °C and protease-treated with thermolysin. Protease-treated membranes were solubilized in SDS buffer, heated, and analyzed by SDSPAGE and phosphorimaging. IQ Solutions software (Molecular Dynamics) was used to quantify pLHCP degradation product (*DP*), which is indicative of properly inserted LHCP. Each integration assay was compared with integration in IBM (set to 100%). Integration in HKM, used by Lewis *et al.,* (*2*) for ITC and protein interaction/function assays, is equally efficient as IBM. Falk *et al.,* (*3*) buffers do not support integration.

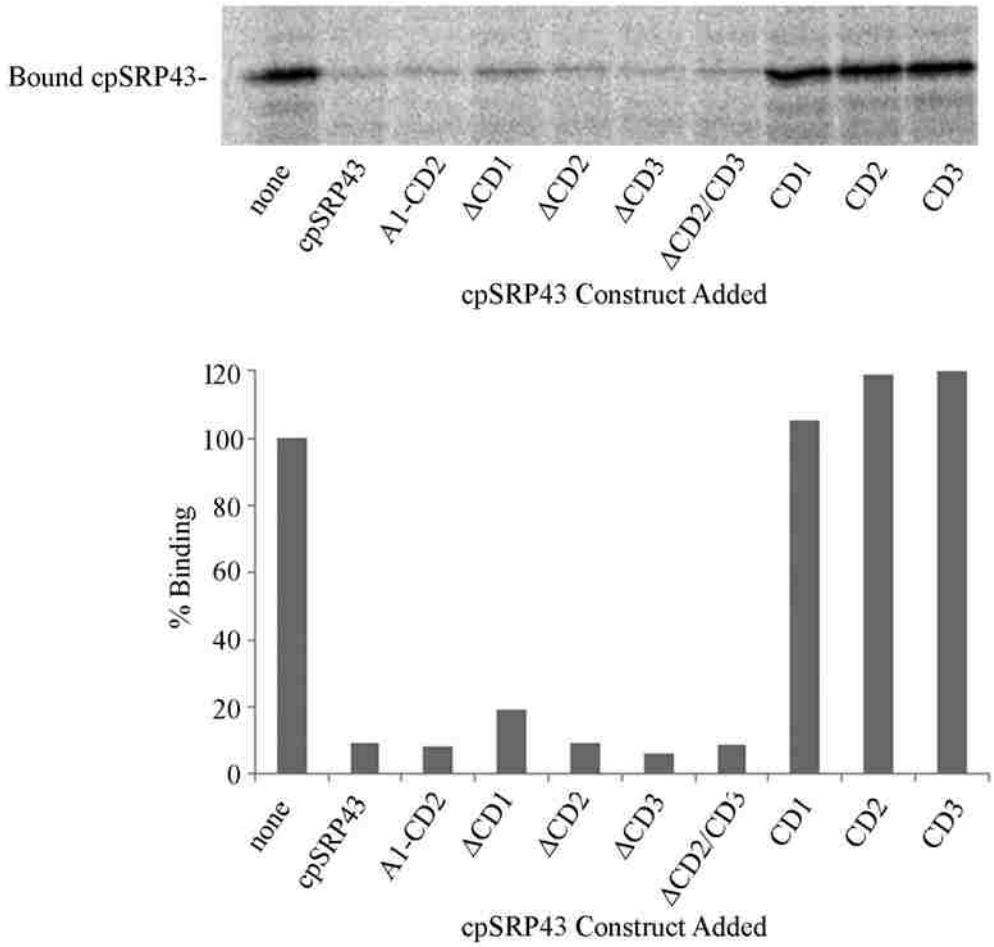

Figure A.4. Competition for cpSRP43 binding to the C terminus of Alb3 in salt-washed thylakoids.

Salt-washed thylakoids (equivalent to 75 μg of chlorophyll) and 8 nmol of recombinant cpSRP43 construct as indicated were incubated for 15 min at 25 °C in light. Equal amounts of radiolabeled cpSRP43 were added to each tube and incubated an additional 30 min under the same conditions. Samples were pelleted, washed, and analyzed via SDS-PAGE and phosphorimaging for radiolabeled cpSRP43. The graph depicts the amount of radiolabeled cpSRP43 bound to salt-washed thylakoids relative to the amount recovered when no recombinant protein was added. It has been previously demonstrated that cpSRP43 binding to salt-washed thylakoids takes place through a cpSRP43/Alb3-Cterm interaction (*2*). As shown, all of the ankyrin region-containing constructs (including cpSRP43 lacking CD2CD3) were able to prevent cpSRP43 binding to the C terminus of Alb3 in salt-washed thylakoids whereas chromodomains 1, 2, and 3 did not prevent cpSRP43 binding to thylakoids.

REFERENCES

1. Falk, S., and Sinning, I. (2010) The C Terminus of Alb3 Interacts with the Chromodomains 2 and 3 of cpSRP43, *Journal of Biological Chemistry 285*, le25-le26.

2. Lewis, N. E., Marty, N. J., Kathir, K. M., Rajalingam, D., Kight, A. D., Daily, A., Kumar, T. K., Henry, R. L., and Goforth, R. L. (2010) A dynamic cpSRP43-Albino3 interaction mediates translocase regulation of chloroplast signal recognition particle (cpSRP)-targeting components, *J Biol Chem 285*, 34220-34230.

3. Falk, S., Ravaud, S., Koch, J., and Sinning, I. (2010) The C terminus of the Alb3 membrane insertase recruits cpSRP43 to the thylakoid membrane, *J Biol Chem 285*, 5954-5962.

4. Goforth, R. L., Peterson, E. C., Yuan, J., Moore, M. J., Kight, A. D., Lohse, M. B., Sakon, J., and Henry, R. L. (2004) Regulation of the GTPase cycle in post-translational Signal Recognition Particle-based protein targeting involves cpSRP43, *Journal of Biological Chemistry 279*, 43077-43084.

5. Tzvetkova-Chevolleau, T., Hutin, C., Noel, L. D., Goforth, R., Carde, J.-P., Caffarri, S., Sinning, I., Groves, M., Teulon, J.-M., Hoffman, N. E., Henry, R., Havaux, M., and Nussaume, L. (2007) Canonical signal recognition particle components can be bypassed for posttranslational protein targeting in chloroplasts, *Plant Cell 19*, 1635-1648.

6. Milev, S., Bosshard, H. R., and Jelesarov, I. (2004) Enthalpic and Entropic Effects of Salt and Polyol Osmolytes on Site-Specific Protein−DNA Association: The Integrase Tn916−DNA Complex†, *Biochemistry 44*, 285-293.

7. Gonzalez-Romo, P., Sanchez-Nieto, S., and Gavilanes-Ruiz, M. (1992) A modified colorimetric method for the determination of orthophosphate in the presence of high ATP concentrations, *Anal Biochem 200*, 235-238.

III

USE OF MICROSCOPY AND LIPOSOMES TO STUDY MEMBRANE INTERACTIONS OF CHLOROPLAST SIGNAL RECOGNITION PARTICLE (CPSRP) TARGETING COMPONENTS

Parts of this research accepted for publication as:

Marty, N. J., Rajalingam, D., Kight, A. D., **Lewis, N. E.**, Fologea, D., Kumar, T. K. S., Henry, R. L., and Goforth, R. L. (2009) The Membrane-binding Motif of the Chloroplast Signal Recognition Particle Receptor (cpFtsY) Regulates GTPase Activity, *J. Biol. Chem. 284*, 14891-14903.

SUMMARY

The chloroplast thylakoid membrane is densely packed with proteins and hosts a variety of critical photosynthetic functions. Examining individual reactions of the chloroplast signal recognition particle (cpSRP) targeting pathway, particularly those taking place at the membrane, amidst this complexity is a difficult task. This work was aimed at studying the structure and arrangement of cpSRP membrane complex (composed of cpSRP54, cpSRP43, cpFtsY, and where applicable, Alb3) using advanced microscopy. Using confocal laser scanning microscopy (CLSM) and fluorescent nano-crystal labeling, we mapped the location and abundance of the cpSRP insertase Albino3 (Alb3) in intact thylakoids. Preliminary work was also done using cryo-Transmission Electron Microscopy (cryo-TEM) and Atomic Force Microscopy (AFM) to image thylakoid membranes and associated protein complexes. Further, we tested the ability of artificial membrane systems to support cpSRP targeting reactions with the possibility that liposomes would provide a less complex but physiologically relevant environment for studying targeting at the membrane. This work demonstrates that cpSRP complex formation and functions of the cpSRP receptor (cpFtsY) can be reconstituted on liposomes. The unique lipid composition of the thylakoid membrane was also considered and work was done to create thylakoid-mimicking liposomes.

INTRODUCTION

The ultimate purpose of post-translational chloroplast signal recognition particle (cpSRP) targeting is to localize LHCPs to the chloroplast thylakoid membrane in an integration-competent state and deliver said substrate to the pathway insertase for integration into the thylakoid membrane in a functional state (for a review of cpSRP targeting, see Chapter 1: Introduction). Thus, a significant portion of the cpSRP targeting pathway involves membrane-associated steps requiring interplay between soluble and membrane components. The soluble, substrate-loaded cpSRP transit complex (cpSRP54, cpSRP43, and LHCP) must bind the thylakoid membrane and dock with a membrane-partitioned receptor (cpFtsY). This complex must then target to the integral membrane insertase Alb3, which is composed of five transmembrane domains spanning the hydrophobic interior of the thylakoid membrane. Once docked, the LHCP substrate must be transferred to Alb3 and integrated into the lipid bilayer membrane for association with other photosynthetic components. Because much of the cpSRP pathway involves membrane-associated targeting steps, protein-lipid interactions and the thylakoid lipid environment are likely heavily involved in pathway coordination and arrangement. While much is known about the timing and nature of soluble protein interactions within the cpSRP pathway, understanding of basic membrane interactions and structural arrangements is comparatively lacking. For example, even the critical interaction between substrate LHCP and insertase Alb3, while assumed, has yet to be directly shown.

Thylakoids are vital biological systems that serve as the sites of photosynthesis in plants. To carry-out this critical function, thylakoids are densely packed with photosynthetic pigments, enzymes required for photoreactions, carriers for electron

transport, proteins involved in proton pumping for ATP synthesis, and many other essential components (*1-3*). This complexity, which greatly increases the difficulty in studying individual proteins or distinct protein pathways, is an essential component in gathering a full understanding of the cpSRP pathway in a truly relevant physiological setting because of the major influence the membrane has on the structure and function of many peripheral membrane proteins and nearly all intergral membrane proteins. To further understanding of cpSRP pathway membrane events, we employed various microscopy techniques to visualize the cpSRP components either individually or in a complex at the thylakoid membrane. Our goal was to identify cpSRP proteins through the use of nano-crystal labeling and use molecular-level imaging to visualize the arrangement and structure of said proteins in their native environment.

Currently, the primary techniques for high resolution structural determination of proteins are Nuclear Magnetic Resonance (NMR) and X-ray crystallography. These powerful techniques have improved dramatically in recent decades, both in terms of the types and numbers of proteins whose structures can be resolved as well as the level of molecular resolution obtainable. Although a primary drawback of X-ray crystallography is the requirement that one must be able to obtain protein crystals, x-ray structures now exist for a handful of membrane photosynthetic proteins (*4-5*). Likewise, strides have been made in overcoming traditional size limitations of NMR, and the upper limit is generally recognized to be around 30kDa (*6*). Structural determination of protein complexes and membrane proteins, on the scale of hundreds of kilo-Daltons, are now, in a very few cases, a possibility (*6-7*). However, unlike microscopy, both NMR and crystallography are indirect means of visualization, relying on diffraction patterns or

functional group maps to recreate protein structure. Furthermore, imaging of membrane proteins and membrane protein complexes in a membrane environment remains a daunting task.

Conventional optical microscopy techniques have been widely used for studying plant biology over the last several centuries (*8*). However these techniques have always suffered from the light diffraction phenomenon of the optical lens system, which greatly limits the resolution. The development of fluorescence microscopy coupled with staining techniques provided major advances in plant anatomy research (*8-9*), but still failed to provide sufficient resolution for imaging at the molecular level (*10-11*). Progress in microscopy techniques, especially electron based scanning and transmission microscopy, improved the resolution to nanometer and angstrom levels, respectively, primarily because of the shorter wavelengths of the electron beam used (*11*). Electron microscopy techniques have proven to be far superior compared to the optical based microscopy techniques in terms of resolution, but this has come at the cost of extensive and difficult specimen preparation (*11*). A primary challenge of these advanced microscopy techniques is maintaining samples in physiological relevant conditions while imaging. Most electron microscopes require samples to be held under vacuum and often dehydrated, conditions which obviously are not native to biological samples.

Scanning probe microscopy (SPM) techniques such as atomic force microscopy (AFM) provide superior vertical resolution. Although SPM methods yield high lateral resolution compared to optical techniques, electron microscopy techniques currently provide the highest level of lateral resolution. SPM's primary advantage over electron microscopy is the capability to maintain samples under physiologically relevant

conditions during imaging. AFM has been used extensively in biological fields for studies of cells, DNA, proteins, chloroplasts, etc (*12-14*). Those studies were carried out on dry or chemically fixed samples or in liquids. However, studies on chloroplasts and thylakoids have only been conducted in either dry or chemically fixed conditions (*12-14*).

The objective of the present research was to develop protocols for imaging thylakoids using AFM (under physiological conditions) as well as cryo transmission electron microscopy and compare the structural and morphological details obtained using both the techniques. These experiments would provide basic structural information of integral thylakoid membrane proteins and open pathways for developing new methodologies to extend the imaging techniques. Further, these studies will be widely useful in understanding membrane protein systems and nano-scale processes in biological systems. Once developed, we aimed to use these protocols in conjunction with nano-crystal labeling to identify and study cpSRP pathway components in various stages of membrane targeting.

A second approach we took to studying cpSRP membrane targeting was to develop a liposome-based system capable of supporting targeting steps. A cleaner system that incorporates lipid contributions while getting rid of other thylakoid proteins would provide an excellent substrate for the previously mentioned microscopic analyses. In addition, incorporating lipid membranes into protein-interaction and protein-function assays would provide a more *in vivo* like environment. Further, thylakoid-mimicking liposomes would be a valuable tool in determining what role, if any, lipids play in targeting and insertion.

Chloroplast membranes, including the thylakoid, have a unique lipid composition, containing a large amount of galactolipids (*3, 15*). The major lipid component, which makes up ~50 % or more of the thylakoid lipid content, is monogalactosyldiacylglycerol (MGDG), which has two polyunsaturated fatty acyl chains (*3*). Interesting, MGDG is a non-bilayer forming lipid, preferring a Hexagonal H_{II} phase. This preference is because the high degree of unsaturation gives the tail of the lipid a larger cross-section as compared to the head group. This produces an overall cone shape, as opposed to the cylindrical shape of most phospholipids, which prevents tight side-by-side packing necessary for a bilayer (See Fig. 3.1 for illustration) (*16*). The second most abundant thylakoid lipid (~25-35 %) is another rare galactolipid, digalactosyldiacylglcerol (DGDG). DGDG, like MGDG, has a high degree of unsaturation in its tail region, but unlike MGDG, has a larger head group and thus is cylindrically shaped and bilayer forming (*16*). Both of the major galactolipids are uncharged.

The third most abundant thylakoid lipid (~ 5-12 %) is a negatively charged sulfolipid, sulfoquinovosyldiacylglycerol (SQDG). SQDG is found in roughly the same amount as one of only two phospholipids in the thylakoid membrane, phosphatidylglycerol (PG) (*3, 15*). The second phospholipid, phosphatidylinositol (PI), is present in small amounts (~ 0.5-2 %) (*3, 15*). Small amounts of phosphatidylcholine (PC) are often reported to be a component of the thylakoid, but most believe this to be a contaminant from the outer chloroplast envelop (*17-18*). For an excellent review on the biogenesis and composition of the lipids comprising the thylakoid membrane see Douce and Joyard, 1996 (*3*).

Such a unique makeup hints at a role for the lipids in the various biological processes that take place at the thylakoid membrane. Work in this field has shown exactly that – both MGDG and DGDG, and to an extent the other thylakoid lipids, provide more than just the physical structure of the membrane, they have distinct functions in many critical thylakoid processes including protein transport and insertion (*19-20*), protein complex arrangement (*21-22*), and photosynthetic energy generation (*20, 23*). Specifically, D1, a core subunit of photosystem II, is rapidly degraded by high light (*24-25*) and must be quickly regenerated into thylakoid membranes in these conditions to avoid photoinhibition (*26*). It has been shown that successful D1 repair, and thus tolerance to high light, requires polyunsaturated lipids (*23*). Interestingly, DI is a substrate of a cpSRP54/cotranslation insertion pathway (*27*) and interacts with Alb3, which seems to serve a critical chaperone/assembly, but not insertase, function (*28*). However, the overall understanding of the lipid contribution to thylakoid biogenesis and function is still in its infancy compared to what is known about protein components. In this work, we explore the role of lipids in cpSRP targeting reactions and work towards development of a thylakoid-mimicking liposome system that could reconstitute the distinct contributions of thylakoid lipids on protein targeting. Further, this artificial thylakoid would provide a more *in vivo* like environment without the organelle complexity for use with advanced microscopic as well as traditional biochemical techniques.

MATERIALS AND METHODS

All reagents and enzymes used were purchased commercially. All primers were from Integrated DNA Technologies. The plasmid used for *in vitro* transcription/translation of pLHCP (psAB80XD/4) has been described (*29*). cpSRP43, cpFtsY, and cpSRP54 were prepared as described (*30-32*). Antibodies to the following proteins have also been described as follows: Alb3-Cterm (*33*), Alb3–50 amino acids (*34*), cpSRP43 (*35*), cpFtsY (*35*), and cpSRP54 (*35*). All cloned sequences were verified by sequencing.

Preparation of Salt-washed Thylakoids

Intact chloroplasts were isolated from 10- to 12-day-old pea seedlings (*P. sativum* cv. Laxton's Progress) and used to prepare thylakoids and stroma as described previously (*36*). Chlorophyll (Chl) content was determined as described previously (*37*). Thylakoids were isolated from lysed chloroplasts by centrifugation and salt-washed (SW) two times with 1 M potassium acetate in import buffer (IB: 50 mM Hepes-KOH, pH 8.0, 0.33 M sorbitol) and two times with IB with 10 mM MgCl2 (IBM) prior to use. Thylakoids were resuspended at 1 mg chlorophyll per 1 mL of IBM prior to use.

Sample preparation, Qdot tagging and CLSM Imaging

Salt washed thylakoids at 2X concentration (1 mg chlorophyll/mL IBM) were incubated with antibodies against the cpSRP insertase Alb3. Antibodies generated against the stromal exposed C terminus of Alb3 (Alb3-Cterm) and a stromal exposed 50 amino acid loop (50aa) have been described previously (*33-34*). Six µL of total antibody (3 µL αAlb3-Cterm, 3 µL α50aa) were added for every 1 µL of salt washed thylakoid.

Thylakoids and antibodies were incubated on ice for 30 minutes, centrifuged at 3600 × g for 6 min, washed once with IBM and then resuspended at 2X thylakoids in IBM. Thylakoid samples were then diluted with 6:1 with secondary antibody conjugated quantum dot solution (Invitrogen: Qdot® goat F(ab') 2 anti-rabbit IgG conjugate (H+L) 1 μM solution, highly cross-adsorbed, in pH 8.3 borate buffer). In Fig. 3.2 Qdots 605 were used, but similar images were generated using Qdot 525 and 585 (not shown). Before imaging, tagged thylakoids were diluted 1:50 in IBM and 20 μL was placed a standard glass microscope slide. Samples were mounted in ProLong Gold anti-fade reagent (Molecular Probes, Eugene, OR) and covered with 1.5 mm cover slips. Samples were analyzed on a Leica TCS SP2 AOBS laser-confocal microscope (Leica Microsystems, Heidelberg, Germany). Light detection was optimized for the specific fluorescent probes used. Excitation was set at 448 nm. Emitted fluorescence was collected between 590-620 nm in channel 1, which corresponds to Qdot 605, and between 620-700 nm for channel 2, which corresponds to chlorophyll autofluorescence. Chanel 3 is an overlay of channels 1 and 2. Images were obtained and analyzed using Leica confocal software. Colors shown in Fig. 3.2 were artificially assigned. Laser intensity and and detectors were optimized to minimize cross-talk between channels. Fig. 3.2 A shows representative images of SW thylakoids with Qdot-tagged Alb3. Thylakoids that were not incubated with Qdots showed either very faint or no fluorescence in the Qdot emission range (not shown). Due to the high cost of Qdots, the large volume necessary to observe sufficient tagging, and the variability of CLSM imaging, controls where Qdots were added in the absence of primary Alb3 antibody, or in the presence of a primary antibody against a non-thylakoid protein were not done. As an alternative control, Fig. 3.2 B shows a sample that was

imaged for an extended period of time, meaning prolonged exposure to laser pulses, which caused noticeable photobleaching of the chlorophyll autofluorescence (channel 2, moving left to right), while the Qdot fluorescence was not affected (channel 1, moving left to right).

Sample preparation and AFM Imaging

For liquid imaging, samples were significantly diluted using IBM. Results indicate an optimum dilution of 50:1 (50 parts IBM, 1 part salt washed thylakoids) for a final concentration of 0.02 mg chlorophyll/mL. Dilution of the samples proved crucial because of the opacity of the thylakoid suspension, which resulted in two major AFM operational problems. The first one is by affecting the laser signal; while the AFM tip was submerged in the liquid, the laser beam traversing through the liquid was obstructed by the suspended thylakoids and this lead to unstable AFM scans by causing the changes in laser signal intensity and thus the sum signal. In addition, thylakoids had a tendency to stick to the AFM probe, thereby causing inaccuracies by changing the tip response in the scanning process. Dilution of the thylakoid samples with IBM decreased the number of suspended molecules and thus helped in reducing the above problems.

For imaging purposes, ten microliters of diluted thylakoid sample were applied to freshly cleaved mica substrate. The surface charge of the freshly cleaved mica helps fix the thylakoids to the substrate and limits thylakoid movement during scanning. Samples were incubated on the mica for three to four minutes and subsequently washed with excess IBM to remove unfixed thylakoids. Three to four microliters of IBM solution was placed on the tip, which was on the liquid cell. Due to surface tension the liquid droplet

was held back while placing it on the scanning module. This ensured tip submersion in liquid buffer while scanning/imaging at room temperature.

For the present work, Veeco Nanoscope IV, Multimode AFM was used to image salt washed thylakoids. Imaging was done in buffer solution (IBM) using contact and tapping modes. The tips used for imaging were Veeco silicon nitride probes with four cantilevers. The resonance frequency of these tips in tapping mode in liquid was always close to 8 kHz.

Sample preparation and Cryo HRTEM imaging

Thylakoids prepared as before were diluted 20:1 using IBM. Quantafoil Cu grid with carbon film was used for sample preparation. Initially, the Cu grid was dipped into the diluted thylakoid solution and removed after a five second incubation. The grid was then placed on a filter paper for two seconds to remove excess solution. The Cu grid was placed on the cryo TEM stage and initially cooled to -25 °C with liquid nitrogen under ambient conditions. After insertion into the TEM the sample temperature was lowered to -185 °C before turning the electron beam on for imaging.

Cryo HRTEM studies were conducted on a JEOL 2100 cryo TEM. Spot size 4 was used during the entire imaging process. Accelerating voltage of the electron beam was 200 kV. The sample was exposed to the electron beam only after the temperatures reached ~ -185 °C.

Construction of cpFtsY F48A Clone

cpFtsY clones were designed to match the mature coding sequence of *Arabidopsis thaliana* cpFtsY starting with the predicted mature amino acid sequence CSAGPSGF and to include KpnI and XbaI sites, respectively, for ligation into pGEM-4Z. PCR

amplification was used to create the substitution mutant F48A with incorporation of a Kozak sequence (Met-Ala) and restriction sites for insertion into pGEM-4Z. Expression clones were created by subcloning into pET-32b. All cloned sequences were verified by DNA sequencing (Molecular Resource Laboratory, University of Arkansas for Medical Sciences, Little Rock, AR).

Liposome Preparation and Fluorescence Quenching Experiments

Soybean total extract lipids (Avanti Polar Lipids) were dissolved at 100 mg/ml in chloroform, dried under nitrogen, and vacuum-desiccated overnight. Lipid pellets were resuspended to 10 mg/ml (13 mM) in 10 mM HEPES-KOH (pH 7), 100 mM KCl, and 1 mM EDTA. The lipid solution was subjected to 15-s sonication/15-s rest cycles for 2 min. Liposomes were clarified by centrifugation at 11,700 × g for 10 min at 4 °C and stored at 4 °C for up to 1 month. Liposomes were sized (Avanti mini-extruder) by passing through polycarbonate filters seven times. Brominated lipids were obtained by bromine addition to the unsaturated carbons of the soybean phosphatidylcholine fatty acyl chain as described (15). Bromine was added in 5 μL drops to 2 mL of 25 mg/mL soybean PC in chloroform. After each addition, solution would become colorless signifying bromine incorporation into the lipid tails. Bromine was added until color loss subsided and solution remained weakly yellow. Unincorporated bromine and chloroform were evaporated under nitrogen and vacuum desiccation before lipid resuspension. The brominated lipid mixture was extruded through 80-nm polycarbonate membranes and homogenized via freeze/thaw cycles. Fluorescence quenching was measured using a SpectraMax Gemini XS spectrofluorometer (Molecular Devices) set for maximum sensitivity and 282-nm excitation/330-nm emission wavelengths. Ten μg of protein in 50

µl of 10 mM HEPES-KOH (pH 8) and 10mM MgCl2 and 0–50 µl of liposomes were mixed and equilibrated for 20 min at 25 °C, and the fluorescence was measured. For each concentration, six measurements of five separate samples were acquired. Fluorescence quenching was estimated as the normalized value of (*F*0-*F*)/*F*0, where *F*0 is the average fluorescence of the samples without liposomes, and *F* is the average fluorescence for each concentration.

Plant thylakoid lipids were purchased commercially from Lipid Products (Redhill, England). MGDG, DGDG, and SQDG were isolated from Spinach leaves. PG was from Kale. Lipids were stored in a methanol/chloroform solution under nitrogen until use. Thylakoid lipids were formed by mixing appropriate volumes of lipids in solution to closely match the percentage of each lipid in thylakoids (Fig. 3.5). Soy total lipid extract was added to the plant lipid mix to dilute the thylakoid lipids down to half the total lipid content. The addition of the soy extract was necessary to prevent MGDG from phase separating into the hexagonal H_{II} phase and forming a precipitate that was insoluble even in organic solvents (i.e. methanol, chloroform). Glass beads were added to the soluble lipid mixture in a round bottom flask to increase surface area and thus decrease the thickness of the lipid cake that formed after drying the solution under nitrogen, followed by vacuum-desiccation for at least 2 hours. Lipids were then rehydrated by vortexing/heating.

cpSRP membrane complex formation on liposomes

Volumes of cpSRP54, cpSRP43 and cpFtsY corresponding to 7 µg of protein were mixed with 55 µL of either 2X SW thylakoids, buffer, or liposomes at 10 µg/µL concentration. The non-hydrolyzable GTP analogue GMP-PNP was added for a final 0.5

mM concentration, and the entire reaction was brought to 100 µL in 10mM Tris-HCl (pH 8.0), 50 mM KCl, 1 mM EDTA and incubated for 30 min. at 25 °C. Each sample was centrifuged at 100,000 × g and washed with buffer three times. After final resuspension of pellet, SDS solubilization buffer was added and samples were analyzed by SDS-PAGE and Western blotting.

GTPase Assays

GTPase activity assays were conducted at 22°C and contained 100 nM cpFtsY or F48A, 0.5 µM [α-32P]GTP (400 Ci/mmol), and liposomes (0.2 mM to 1.0 mM as indicated in Fig. 3.7) in final volume of 5 µl buffer (50 mM Hepes, pH 8.0, 150 mM potassium acetate, 10 mM potassium chloride, 2 mM magnesium acetate, 0.01% octaethyleneglycol mono-N-dodecyl ether (C12 E8), and 2 mM DTT). Aliquots were removed at frequent time points and spotted onto PEI-cellulose thin layer plates as in (*38*).

RESULTS

Alb3 is concentrated in non-appressed regions of the thylakoid membarne

The goal of our work using CLSM was to visualize cpSRP complex arrangement at the thylakoid membrane. However, it became clear that achieving the magnification and resolution needed for this type of analysis was not possible because of instrumental and labeling limitations. Despite these limitations, the CLSM proved valuable in revealing the overall abundance and areas of concentration of Alb3 in the thylakoid membrane. This was an important finding—if sites of membrane complex assembly were rare, successfully imaging cpSRP components at the membrane using atomic level microscopy would be highly improbably due to difficulties in locating areas or interest. Numerical values of the number of Alb3 insertases per pea chloroplast (~650,000) have been published (*34*), but it is difficult to interpert those numbers when thinking at the level of a single protein within the vast membrane space of a thylakoid stack. Further, raw numbers do not provide details on the possibility that Alb3 could be more or less concentrated within the many microenvironments of the thylakoid membrane. This has already been shown to be the case with various thylakoid proteins and complexes including the LHCs, photosystem I and II, and ATP synthase (*2*, *39*), all of which are highly compartmentalized within the membrane. Based up images in Fig. 1A, Alb3 is an abundant thylakoid protein concentrated in the non-appressed regions (stroma lamellar domains, grana-end membranes, and/or grana margins; Fig. 3.2). The two images shown represent a pattern of Alb3 distribution that was reproduced across multiple samples.

AFM and cryo-TEM reveal the complexity of the thylakoid membrane

Fig. 3.3 shows AFM images of thylakoid stacks obtained using contact mode in IBM buffer solution. These micrographs show well resolved individual thylakoid structure. The size of thylakoids was measured to be ~ 470 nm, which is in close agreement with the values reported in the literature ~ 510 nm (*10, 14*) under dry condition. It has been argued that contact mode AFM causes sample and tip damage due to the forces exerted by the tip during scanning compared to the lesser forces of tapping mode. With soft samples such as biological materials, contact mode may lead to the sample damage, which is highly undesired.

Tapping mode operation in liquids is a challenging task. The damping effect of the liquid on the vibrating tip reduces resonance frequency of the cantilevers. In the present study the resonance frequency of silicon nitride probe tips was found to be close to 8 kHz in liquid compared to 60 kHz in air. The major challenges of tapping mode imaging in liquid are evaporation of liquid during imaging/scanning and impurities in the liquid sample that stick to the tip thereby affecting the resonance frequency. Fig. 3.3 A shows the micrograph of stacked thylakoids (or grana) obtained in liquid/buffer solution using tapping mode operation. In the amplitude error image (right), a stack of thylakoids could be clearly seen. The resolution and contrast in the amplitude error image is very clear compared to the height image (left), due to a large change in the height (~2.5 μm) within the scanned area, which contributes to the loss of information in the height image. Thus, it is intuitive for minimal changes in height, amplitude error images might lose contrast easily, and this was observed in the later stages of thylakoid stack imaging in liquids (data not shown). From these studies it is clear that while imaging in liquid, when

the height or morphology changes are very large (few microns), amplitude error images are useful for obtaining good morphology contrast.

Fig. 3.3 B shows the images of thylakoids in close up view. The right image renders the three dimensional view of the image shown on the left. In both cases, protrusions on the thylakoid surface could be easily seen. Fig. 3.3 C shows the topographic profile across the thylakoid surface in Fig. 3.3 B. It is clear that the topographic features on the thylakoid surface could be 10 to 20 nm in height. Since the thylakoid membrane houses numerous proteins, including those that take part in photosynthesis and in development of the proton gradient across the membrane, surface roughness of the membrane is expected.

Thylakoid images obtained by cryo-TEM are shown in Fig. 3.4. Approximate size of thylakoids is 400 – 500 nm and this is in close agreement with the literature as well as the AFM images obtained (*10, 14, 40*). The lipid bilayer membrane could be seen as a parallel track structure in Fig. 3.4 B. The globular surface protrusions fit expectations of different membrane and surface proteins and protein complexes. The size of these surface protrusions is around 10 – 25 nm, which is in close agreement with the surface protrusions observed in line profile of AFM images – shown in Fig. 3.3 B and C. This further substantiates the imaging of thylakoid proteins and protein complexes by AFM and TEM, which yield strikingly similar, but complimentary results.

While our data illustrate the high spatial resolution of solution-exposed protein complexes provided by both techniques, our results also point to the need for protein-specific labels to differentiate the identity of protein complexes. Unlike traditional optical labels, which provide a fluorescent colored tag, a new generation of labels are required

for use with nanometer-scale imaging of complex membrane systems by AFM and TEM. In this context, the integration of protein-specific antibodies with novel nanomaterials currently being developed may provide the labeling specificity and critical physical characteristics to distinguish one membrane protein from the other in a complex system. However, overall surface roughness of thylakoids would make identifying even a nano-tagged complex difficult. Alternatively, the placement of a single membrane protein complex into an artificial lipid bilayer (e.g. liposomes) could reduce the complexity associated with imaging biological membranes, thereby immediately increasing the utility of using AFM and cryo TEM to uncover nanometer scale structural details that underlay membrane protein function.

Liposomes support membrane complex formation in the absence of Alb3

Published results have shown that a cpSRP membrane complex composed of cpSRP (cpSRP54 and cpSRP43) and cpFtsY can form at the thylakoid membrane even in the absence of an available Alb3 insertase (*35*). Thus, if liposomes are to be a viable means for studying cpSRP targeting membrane steps, they should be capable of supporting formation of said complex. Fig. 3.6 shows that while not as efficient as on Alb3 containing thylakoids, cpSRP complex does form on liposomes at a level above nonspecific precipitation. However, the fact that cpSRP complex associates and pellets with liposomes does not answer the question of whether or not that association is a real function of the pathway or simply a non-specific association.

Liposomes support membrane binding function of cpFtsY

In contrast to SecY/FtsY interaction in the bacterial system (*41*), no proteinaceous thylakoid component is needed to provide a binding site for cpFtsY to the thylakoid

membrane (for a more in-depth discussion on the role of cpFtsY in cpSRP targeting, see Chapter 1: Introduction). We previously published that neither protease treatment of salt-washed thylakoids nor pretreatment of thylakoid membranes with antiserum against SecY or Alb3 prevents cpFtsY from partitioning to the thylakoid membrane (*35*). Taken together, these results suggest that cpFtsY is able to bind thylakoids through interaction with the lipid bilayer. We further identified a conserved phenylalanine residue in cpFtsY responsible for lipid binding (*42*). To determine if liposomes could support this membrane partitioning function of cpFtsY, soybean liposomes containing brominated acyl chains were used to examine the interaction of cpFtsY or the F48A mutant with lipid bilayers. Bromine quenching of cpFtsY Trp fluorescence served as an indicator of protein/bilayer interactions (*43*). As shown in Fig. 3.7 A, quenching of cpFtsY Trp fluorescence increased with the amount of brominated lipid in the assay. In contrast, brominated lipids exhibited a greatly reduced ability to quench Trp fluorescence of the F48A mutant, indicating impairment in lipid binding of F48A, which mirrors the loss of thylakoid binding. Together, these results suggest that soy liposomes are fully capable of supporting the natural membrane-binding function of cpFtsY.

Liposomes Stimulate GTP Hydrolysis by cpFtsY

In the presence of SRP, GTP hydrolysis by *E. coli* FtsY is stimulated by the addition of liposomes (*44*). Fig. 3.7 B shows that liposomes stimulated basal GTP hydrolysis by cpFtsY, but not by F48A, which lacks the ability to interact with the membrane. Importantly, F48A exhibited a GTP hydrolysis rate that was four times greater than cpFtsY in the absence of liposomes and did not respond to a rise in liposome concentration (Fig. 3.7 B). This corresponds to the earlier observations that lack of the

domain in *E. coli* FtsY increases basal hydrolysis rates (*44-45*). Taken together, these data confirm that Phe-48 is part of a structurally distinct, lipid-responsive domain. Interestingly, this lipid-responsive domain also appears to repress GTP hydrolysis when in solution, thereby limiting futile GTP hydrolysis by cpFtsY when not engaged in protein-targeting activities at the membrane. The ability to stimulate hydrolysis by cpFtsY shows that in addition to membrane binding, liposomes are able to support critical protein functions of the cpSRP pathway components.

DISCUSSION

This work explored ways to analyze steps in the cpSRP targeting pathway at the membrane interface. Current protein interaction assays are not suitable for understanding the organization and inter-complex interactions of the cpSRP components at the membrane. Further, traditional methods for determining protein structure are not well-suited to membrane analysis of a dynamic, multi-protein system. The use of modern microscopy techniques, namely AFM and TEM, offer the possibility of atomic-level imaging in a more native-like environment. Because of the relative newness of these technologies, protocols for imaging biological samples expectedly lag behind their use in materials sciences. In this work we developed necessary protocols while gaining valuable insight into the future difficulties that will need to be overcome to fully realize the goal of imaging protein-targeting events at the thylakoid membrane under physiological conditions.

We successfully imaged thylakoid stacks using CLSM and were able to tag and image the cpSRP membrane insertase Alb3 with fluorescent, antibody-conjugated Qdots. This data (Fig. 3.2) shows an abundant protein that seems to concentrate on the non-appressed regions of the thylakoid. This seems consistent with Alb3's role as an insertase, as the targeting and integration reactions likely could not physically take place in the limited space of the appressed regions. However, questions remain about the accuracy of the Qdot tagging process. It is not possible to know the tagging efficiency or the ratio of Qdots to Alb3, which makes observations about the actual number of insertases impossible. Additionally, we observed a tendency of Qdots to self-aggregate, which makes it difficult to relate fluorescence intensity in a given region to amount of

Alb3 present. As mentioned in the materials and methods section, controls need to be performed using a non-related primary antibody. Despite these questions, data generated by CLSM indicated that cpSRP pathway insertion sites were abundant enough to pursue imaging by AFM and TEM. In addition, the ability of Qdots to withstand photobleaching was a critical component in our ability to use CLSM with photosynthetic membranes.

Protocols for imaging thylakoids using AFM in liquid and cryo-TEM were successfully developed. AFM and cryo-TEM images show the surface roughness of thylakoids close to 10 to 25 nm and this can be attributed to the protruding protein structures and complexes embedded in the photosynthetic thylakoid membrane system. Further extension of these imaging methods and protocols could lead to high resolution imaging of protein structure, and thus aid understanding of biological processes at the nano-level. However, discrimination of individual proteins and systems on the molecular level will require more advanced labeling techniques. The use of nano-crystal labels was considered, but the unexpected level of surface complexity—literally the size and abundance of surface roughness—would make nano-crystals difficult if not impossible to locate.

An additional alternative to differentially labeling is use synthetic, thylakoid-mimicking liposomes. This would allow for cpSRP membrane analysis without the need to distinguish cpSRP components from other thylakoid constituents. To that end, we experimented with two different lipid compositions—a total soy lipid extract, which is quite different from the unique makeup of the thylakoid; and a combination of plant lipid extracts more closely mimicking the thylakoid. We have shown that even the soy total extract liposomes were able to support various cpSRP functions, membrane complex

formation, cpFtsY membrane partitioning, and cpFtsY GTPase stimulation; all critical to the proper functioning of the pathway *in vivo*. Further, we developed a protocol for the formation of thylakoid-like liposomes where half the lipid content mirrored the thylakoid but was diluted 1:1 with soy lipids. The presence of the readily bilayer forming soy lipids in conjunction with the lowered MGDG concentration and thinner lipid cake via the use of glass beads allowed for liposome formation with little to no separation into the hexagonal H_{II} phase, and thus precipitation, by MGDG. It is interesting to speculate what further roles these thylakoid-like liposomes could support. In addition to complex formation and GTP hydrolysis stimulation, would a more *in vivo* like microenvironment stimulate the known ability of the C terminus of Alb3 to cause LHCP release from transit complex (*46*)? Regardless, it is a tool that will give a more reliable depiction of the role of the thylakoid membrane lipids in cpSRP targeting.

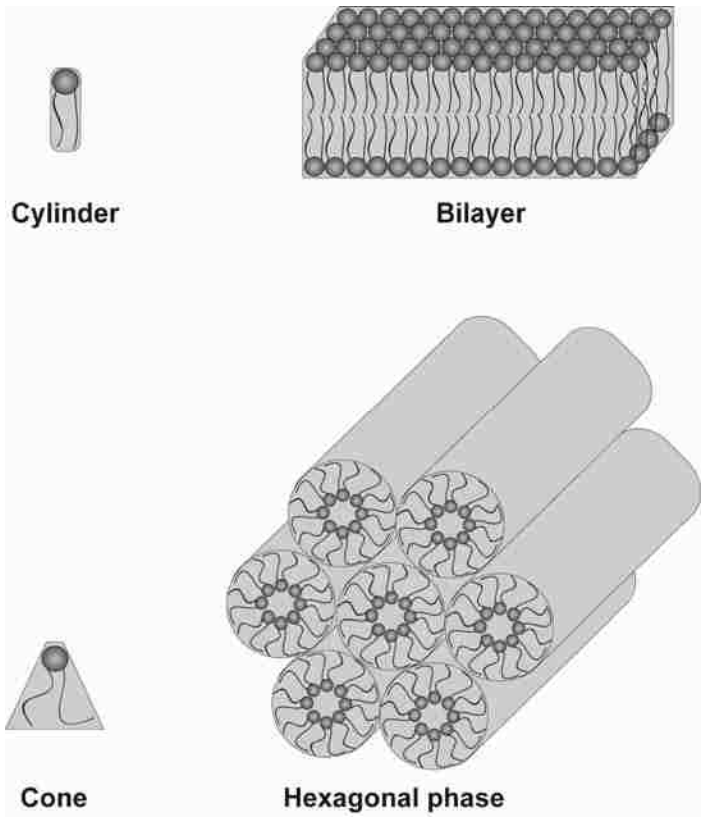

Figure 3.1. Representation of bilayer forming and non-bilayer forming lipids.

Bilayer forming lipids, such as phospholids and the thylakoid galactolipid DGDG, are represented in the upper images. The lipid head and tail region have a similar cross-sectional area, which gives the molecule a cylindrical shape and allows for packing in a bilayer structure. Non-bilayer forming lipids, such as MGDG, are represented in the lower images. These have a high degree of polyunsaturation in the lipid tails. This gives the tail region a larger cross-sectional area than the lipid head, resulting in a cone-shaped molecule that packs in the hexagonal H_{II} phase. Figure adapted from Lee 2000 (*16*).

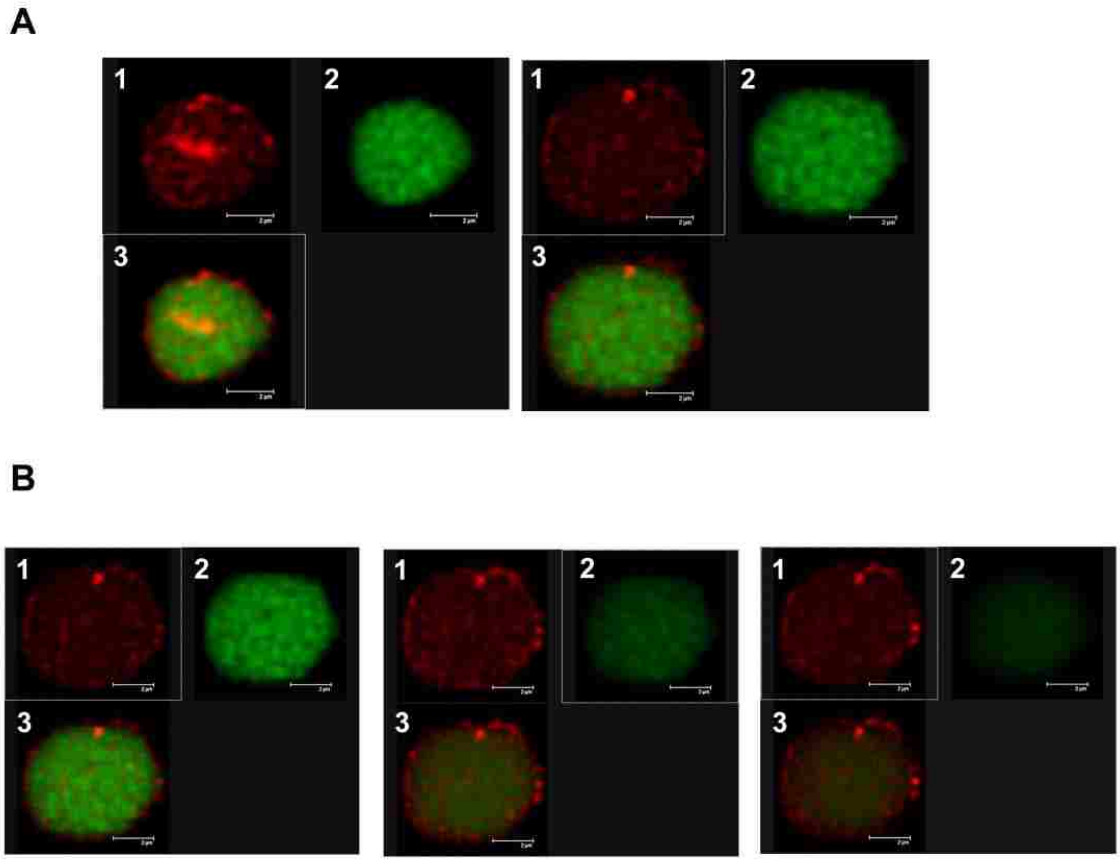

Figure 3.2. Thylakoid autofluorescence and Qdot 605 tagged Alb3 visualized by CLSM.

Thylakoids were tagged with antibodies against two regions Alb3 (the C terminus and a 50 amino acid loop) and then secondary antibodies conjugated to Qdot 605 fluorescent nano-crystals. All images were taken on a Leica TCS SP2 AOBS laser-confocal microscope (Leica Microsystems, Heidelberg, Germany). Excitation was set at 448 nm. Emission was collected between 590-620 (channel 1, Qdots 605) and 620-700 (channel 2, thylakoid autofluorescence). Chanel 3 is an overlay of channels 1 and 2. All colors are artificially generated. Scale bars equal 2 μm. **A)** Images of two different samples showing the distribution and abundance of Alb3 on the thylakoids. **B)** Time-course images showing longer laser exposure moving from left to right. Longer exposure corresponds to photobleaching and a reduction in intensity of thylakoid autofluorescence. Qdot fluorescence, however, is unchanged.

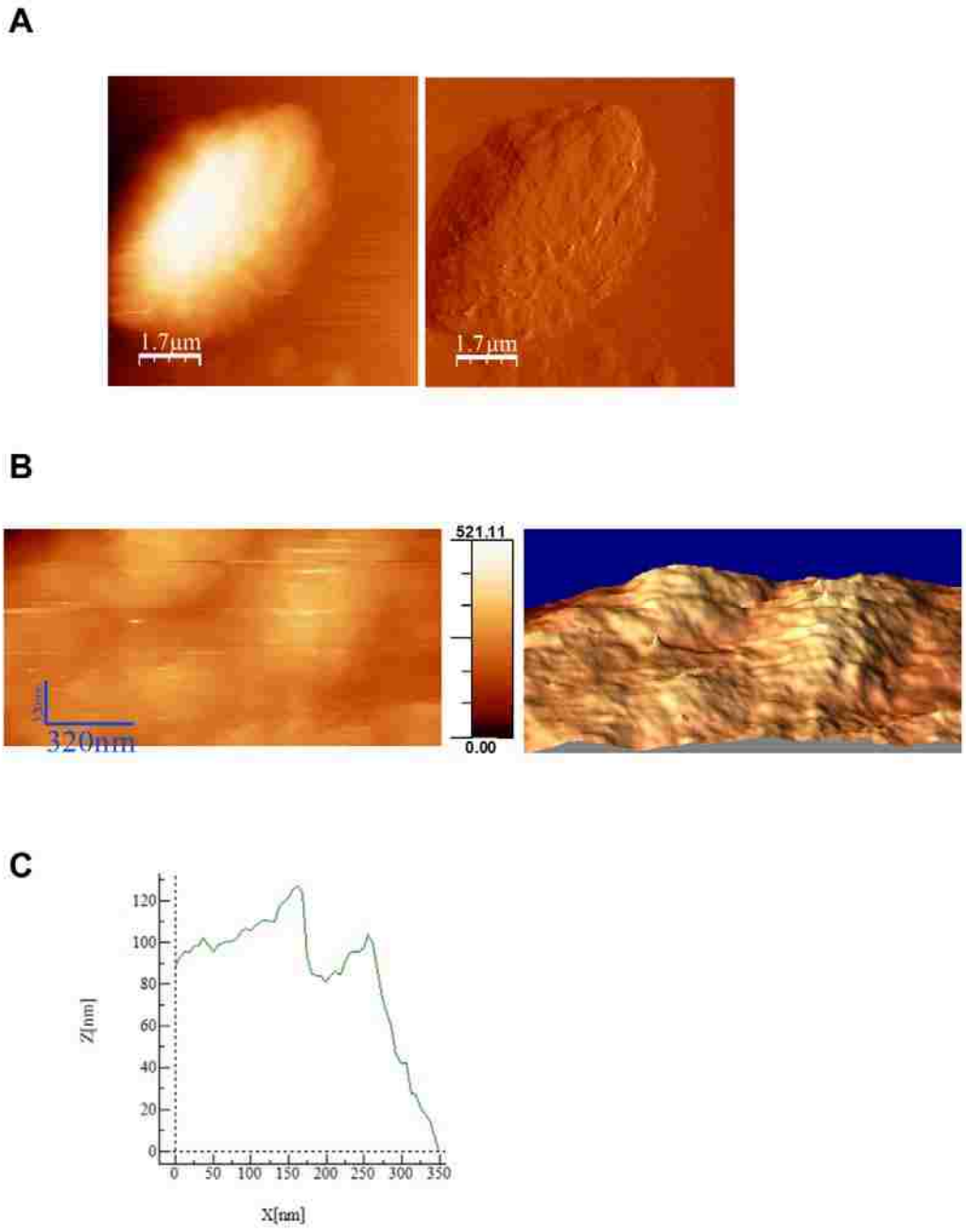

Figure 3.3. AFM analysis of thylakoid topography.

Thylakoids in IBM buffer were imaged using a Veeco Nanoscope IV, Multimode AFM in tapping mode. **A)** Large area scan shows thylakoid stacks (grana). Left is height image, right is amplitude error image. **B)** Small area scan shows thylakoid surface roughness. Left is height image, right is 3D image. **C)** Line profile cross-section of thylakoid surface. Data obtained by Ramesh Guduru N.E. Lewis.

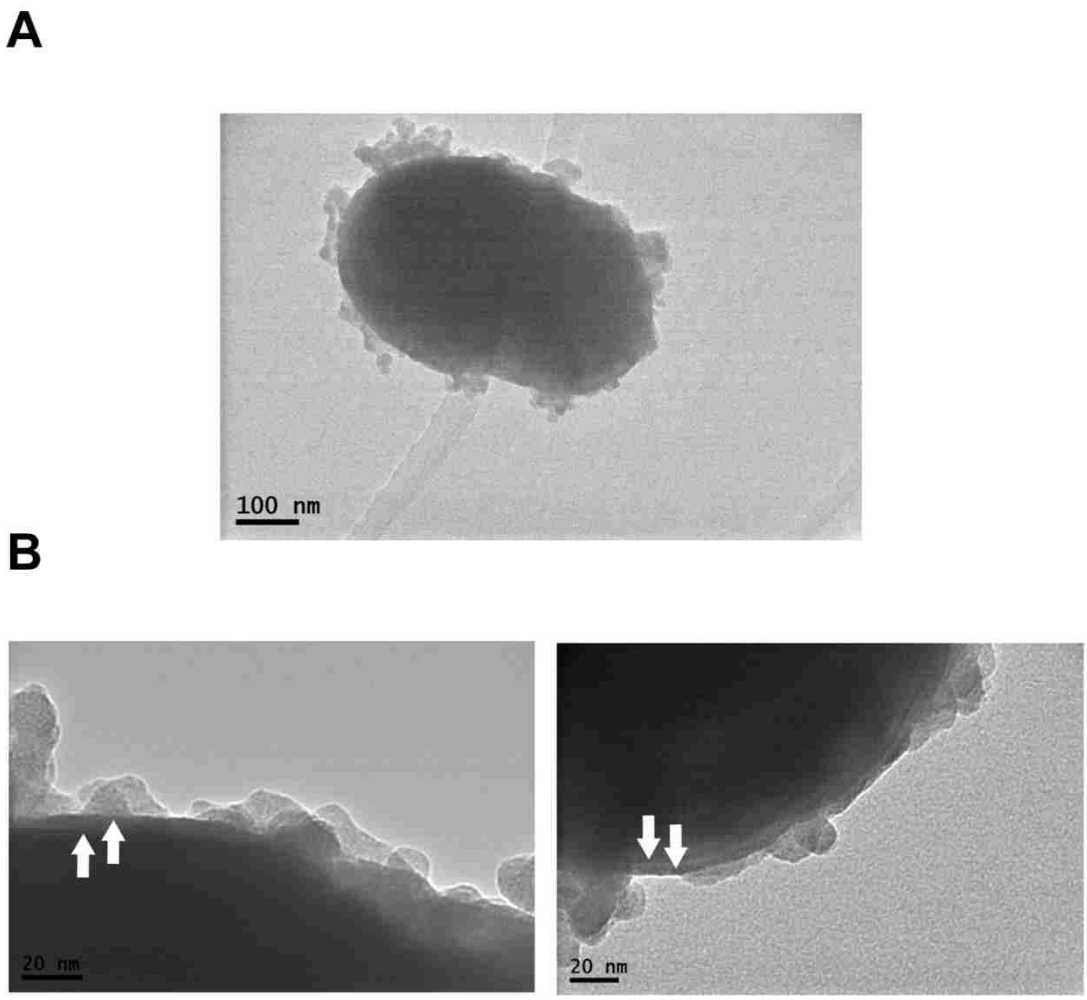

Figure 3.4. Cryo-TEM images of thylakoids.

Thylakoids in IBM were placed on a Quantafoil Cu grid with carbon film and cooled to ~-185 °C before imaging with a JEOL 2100 cryo TEM. **A)** Image of an entire thylakoid sample. **B)** Close-up view of different membrane sections of sample show in **A**. Arrows indicate parallel track lipid bilayer. Data obtained by Ramesh Guduru.

Lipid	Amount in Thylakoid (mol %)
Monogalactosyldiacylglycerol (MGDG)	~50
Digalactosyldiacylglycerol (DGDG)	~30
Sulfoquinovosyldiacylglycerol (SQDG)	~12
Phoshphatidylglycerol (PG)	~8
Phosphatidylinositol (PI)	~1

Lipid	Amount in Soy Total Extract (Avanti, mol %)
Phosphatidylethanolamine (PE)	18.06
Phosphatidylinositol (PI)	11.5
Phosphatidylcholine (PC)	24.0
Phosphatidic Acid (PA)	4.3
LPC	4.6
Other	37.0

Figure 3.5. Lipid content of the thylakoid membrane and of Avanti soy total extract. Charts comparing the lipid type and relative percentage of total lipid makeup for thylakoid membranes and commercially purchased soy total extract.

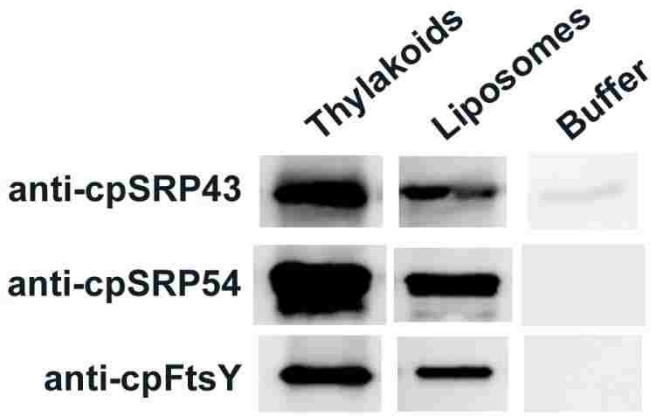

Figure 3.6. Liposomes support cpSRP membrane complex formation.
Equal µg amounts of cpSRP43, cpSRP54 and cpFtsY were incubated with either 2X SW thylakoids, 10 mg/ml soy extract liposomes or buffer in 10mM Tris-HCl (pH 8.0), 50 mM KCl, 1 mM EDTA for 30 min. at 25 °C. Each sample was centrifuged and washed three times before analysis by SDS-PAGE and Western blotting. Blots show ability of soy extract liposomes to support cpSRP membrane complex formation, albeit at a level reduced from thylakoids.

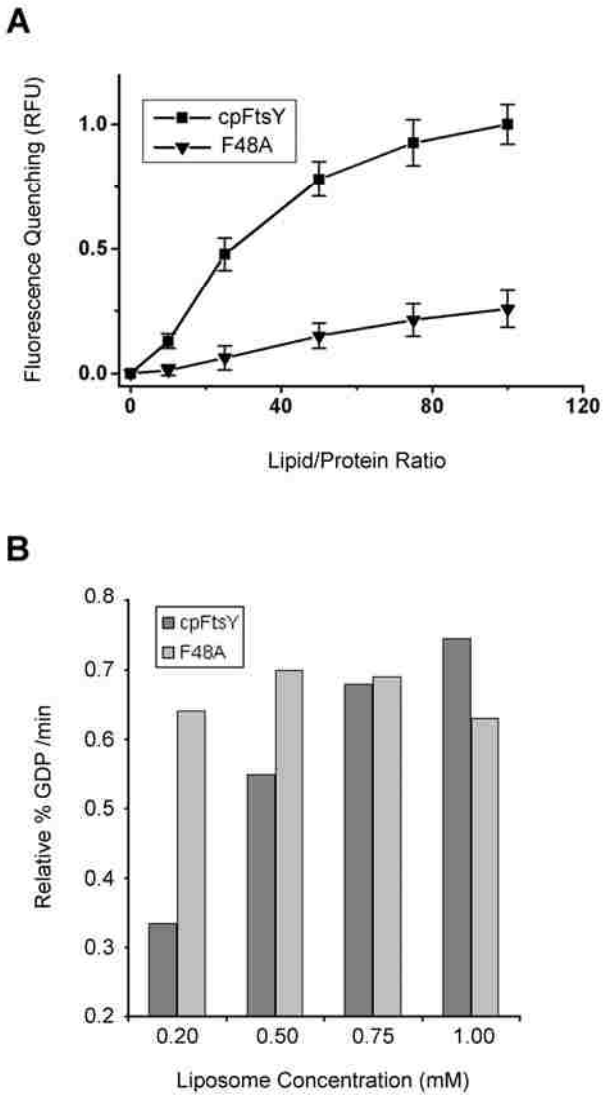

Figure 3.7. Liposomes support critical functions of cpFtsY.

A) Bromine was added to the fatty acyl chain of soybean phosphatidylcholine. 10 µg of either FtsY or F48A in 50 µl of 10 mM HEPES-KOH (pH 8) and 10mM MgCl2 and 0–50 µl of brominated liposomes were mixed and equilibrated for 20 min at 25 °C, and the fluorescence was measured. Fluorescence quenching was estimated as the normalized value of (*F*0-*F*)/*F*0, where *F*0 is the average fluorescence of the samples without liposomes, and *F* is the average fluorescence for each concentration. **B)** Either cpFtsY or F48A were incubated with 0.5 µM [α-32P]GTP and soy extract liposomes in final volume of 5 µl buffer (50 mM Hepes, pH 8.0, 150 mM potassium acetate, 10 mM potassium chloride, 2 mM magnesium acetate, 0.01% octaethyleneglycol mono-N-dodecyl ether (C12 E8), and 2 mM DTT). Samples at frequent time points were spotted onto PEI-cellulose thin layer plates. Liposomes stimulate hydrolysis of FtsY, but not F48A, which lacks membrane binding capacity.

REFERENCES

1. Staehelin, L. A., and Staay, G. W. M. (1996) Structure, Composition, Functional Organization and Dynamic Properties of Thylakoid Membranes, In *Oxygenic Photosynthesis: The Light Reactions* (Ort, D. R., Yocum, C. F., and Heichel, I. F., Eds.), pp 11-30, Springer Netherlands.

2. Albertsson, P. (2001) A quantitative model of the domain structure of the photosynthetic membrane, *Trends Plant Sci 6*, 349-358.

3. Douce, R., and Joyard, J. (1996) Biosynthesis of thylakoid membrane lipids, *Advances in Photosynthesis 4*, 69-101.

4. Jordan, P., Fromme, P., Witt, H. T., Klukas, O., Saenger, W., and Krauss, N. (2001) Three-dimensional structure of cyanobacterial photosystem I at 2.5 A resolution, *Nature 411*, 909-917.

5. Zouni, A., Witt, H.-T., Kern, J., Fromme, P., Krauss, N., Saenger, W., and Orth, P. (2001) Crystal structure of photosystem II from Synechococcus elongatus at 3.8 [angst] resolution, *Nature 409*, 739-743.

6. Luy, B. (2007) Approaching the Megadalton: NMR Spectroscopy of Protein Complexes, *Angewandte Chemie International Edition 46*, 4214-4216.

7. Tamm, L. K., and Liang, B. (2006) NMR of membrane proteins in solution, *Progress in Nuclear Magnetic Resonance Spectroscopy 48*, 201-210.

8. Cisek, R., Spencer, L., Prent, N., Zigmantas, D., Espie, G., and Barzda, V. (2009) Optical microscopy in photosynthesis, *Photosynthesis Research 102*, 111-141.

9. Hepler, P. K., and Gunning, B. E. S. (1998) Confocal fluorescence microscopy of plant cells, *Protoplasma 201*, 121-157.

10. Gradinaru, C. C., Martinsson, P., Aartsma, T. J., and Schmidt, T. (2004) Simultaneous atomic-force and two-photon fluorescence imaging of biological specimens in vivo, *Ultramicroscopy 99*, 235-245.

11. Vacha, F., Bumba, L., Kaftan, D., and Vacha, M. (2005) Microscopy and single molecule detection in photosynthesis, *Micron 36*, 483-502.

12. Lal, R., and John, S. A. (1994) Biological applications of atomic force microscopy, *American Journal of Physiology - Cell Physiology 266*, C1-C21.

13. Shao, Z., Yang, J., and Somlyo, A. P. (1995) Biological Atomic Force Microscopy: From Microns to Nanometers and Beyond, *Annual Review of Cell and Developmental Biology 11*, 241-265.

14. Kaftan, D., Brumfeld, V., Nevo, R., Scherz, A., and Reich, Z. (2002) From chloroplasts to photosystems: in situ scanning force microscopy on intact thylakoid membranes, *EMBO J 21*, 6146-6153.

15. Douce, R., and Joyard, J. (1990) Biochemistry and Function of the Plastid Envelope, *Annual Review of Cell Biology 6*, 173-216.

16. Lee, A. G. (2000) Membrane lipids: it's only a phase, *Curr Biol 10*, R377-380.

17. Dorne, A. J., Joyard, J., Block, M. A., and Douce, R. (1985) Localization of phosphatidylcholine in outer envelope membrane of spinach chloroplasts, *J Cell Biol 100*, 1690-1697.

18. Dorne, A. J., Joyard, J., and Douce, R. (1990) Do thylakoids really contain phosphatidylcholine?, *Proc Natl Acad Sci U S A 87*, 71-74.

19. Bruce, B. D. (1998) The role of lipids in plastid protein transport, *Plant Molecular Biology 38*, 223-246.

20. Aronsson, H., Schottler, M. A., Kelly, A. A., Sundqvist, C., Dormann, P., Karim, S., and Jarvis, P. (2008) Monogalactosyldiacylglycerol deficiency in Arabidopsis affects pigment composition in the prolamellar body and impairs thylakoid membrane energization and photoprotection in leaves, *Plant Physiol 148*, 580-592.

21. Zhou, F., Liu, S., Hu, Z., Kuang, T., Paulsen, H., and Yang, C. (2009) Effect of monogalactosyldiacylglycerol on the interaction between photosystem II core complex and its antenna complexes in liposomes of thylakoid lipids, *Photosynth Res 99*, 185-193.

22. Pali, T., Garab, G., Horvath, L. I., and Kota, Z. (2003) Functional significance of the lipid-protein interface in photosynthetic membranes, *Cell Mol Life Sci 60*, 1591-1606.

23. Tasaka, Y., Gombos, Z., Nishiyama, Y., Mohanty, P., Ohba, T., Ohki, K., and Murata, N. (1996) Targeted mutagenesis of acyl-lipid desaturases in Synechocystis: evidence for the important roles of polyunsaturated membrane lipids in growth, respiration and photosynthesis, *EMBO J 15*, 6416-6425.

24. Mattoo, A. K., Hoffman-Falk, H., Marder, J. B., and Edelman, M. (1984) Regulation of protein metabolism: Coupling of photosynthetic electron transport to in vivo degradation of the rapidly metabolized 32-kilodalton protein of the chloroplast membranes, *Proc Natl Acad Sci U S A 81*, 1380-1384.

25. Mattoo, A. K., Pick, U., Hoffman-Falk, H., and Edelman, M. (1981) The rapidly metabolized 32,000-dalton polypeptide of the chloroplast is the "proteinaceous shield" regulating photosystem II electron transport and mediating diuron herbicide sensitivity, *Proc Natl Acad Sci U S A 78*, 1572-1576.

26. Gaba, V., Marder, J. B., Greenberg, B. M., Mattoo, A. K., and Edelman, M. (1987) Degradation of the 32 kD Herbicide Binding Protein in Far Red Light, *Plant Physiol 84*, 348-352.

27. Nilsson, R., and van Wijk, K. J. (2002) Transient interaction of cpSRP54 with elongating nascent chains of the chloroplast-encoded D1 protein; 'cpSRP54 caught in the act', *FEBS Letters 524*, 127-133.

28. Ossenbuehl, F., Goehre, V., Meurer, J., Krieger-Liszkay, A., Rochaix, J.-D., and Eichacker, L. A. (2004) Efficient assembly of photosystem II in Chlamydomonas reinhardtii requires Alb3.1p, a homolog of arabidopsis ALBINO3, *Plant Cell 16*, 1790-1800.

29. Cline, K., Fulsom, D. R., and Viitanen, P. V. (1989) An imported thylakoid protein accumulates in the stroma when insertion into thylakoids is inhibited, *J Biol Chem 264*, 14225-14232.

30. Yuan, J., Kight, A., Goforth, R. L., Moore, M., Peterson, E. C., Sakon, J., and Henry, R. (2002) ATP stimulates signal recognition particle (SRP)/FtsY-supported protein integration in chloroplasts, *Journal of Biological Chemistry 277*, 32400-32404.

31. Goforth, R. L., Peterson, E. C., Yuan, J., Moore, M. J., Kight, A. D., Lohse, M. B., Sakon, J., and Henry, R. L. (2004) Regulation of the GTPase cycle in post-translational Signal Recognition Particle-based protein targeting involves cpSRP43, *Journal of Biological Chemistry 279*, 43077-43084.

32. Jaru-Ampornpan, P., Chandrasekar, S., and Shan, S.-o. (2007) Efficient Interaction between Two GTPases Allows the Chloroplast SRP Pathway to Bypass the Requirement for an SRP RNA, *Mol. Biol. Cell 18*, 2636-2645.

33. Woolhead, C. A., Thompson, S. J., Moore, M., Tissier, C., Mant, A., Rodger, A., Henry, R., and Robinson, C. (2001) Distinct Albino3-dependent and -independent pathways for thylakoid membrane protein insertion, *J Biol Chem 276*, 40841-40846.

34. Moore, M., Harrison, M. S., Peterson, E. C., and Henry, R. (2000) Chloroplast oxa1p homolog albino3 is required for post-translational integration of the light harvesting chlorophyll-binding protein into thylakoid membranes, *Journal of Biological Chemistry 275*, 1529-1532.

35. Moore, M., Goforth, R. L., Mori, H., and Henry, R. (2003) Functional interaction of chloroplast SRP/FtsY with the ALB3 translocase in thylakoids: substrate not required, *Journal of Cell Biology 162*, 1245-1254.

36. Cline, K., Henry, R., Li, C., and Yuan, J. (1993) Multiple pathways for protein transport into or across the thylakoid membrane, *EMBO J. 12*, 4105-4114.

37. Arnon, D. I. (1949) Copper enzymes in isolated chloroplasts. Polyphenoloxidase in Beta vulgaris, *Plant Physiol. 24*, 1-15.

38. Connolly, T., and Gilmore, R. (1993) GTP hydrolysis by complexes of the signal recognition particle and the signal recognition particle receptor, *J. Cell Biol. 123*, 799-807.

39. Hankamer, B., Barber, J., and Boekema, E. J. (1997) Structure and Membrane Organization of Photosystem Ii in Green Plants, *Annu Rev Plant Physiol Plant Mol Biol 48*, 641-671.

40. Dekker, J. P., and Boekema, E. J. (2005) Supramolecular organization of thylakoid membrane proteins in green plants, *Biochimica et Biophysica Acta (BBA) - Bioenergetics 1706*, 12-39.

41. Angelini, S., Boy, D., Schiltz, E., and Koch, H.-G. (2006) Membrane binding of the bacterial signal recognition particle receptor involves two distinct binding sites, *The Journal of Cell Biology 174*, 715-724.

42. Marty, N. J., Rajalingam, D., Kight, A. D., Lewis, N. E., Fologea, D., Kumar, T. K. S., Henry, R. L., and Goforth, R. L. (2009) The Membrane-binding Motif of the Chloroplast Signal Recognition Particle Receptor (cpFtsY) Regulates GTPase Activity, *Journal of Biological Chemistry 284*, 14891-14903.

43. Carney, J., East, J. M., Mall, S., Marius, P., Powl, A. M., Wright, J. N., and Lee, A. G. (2001) *Fluorescence Quenching Methods to Study Lipid-Protein Interactions*, John Wiley & Sons, Inc.

44. de Leeuw, E., te Kaat, K., Moser, C., Menestrina, G., Demel, R., de Kruijff, B., Oudega, B., Luirink, J., and Sinning, I. (2000) Anionic phospholipids are involved in membrane association of FtsY and stimulate its GTPase activity, *EMBO Journal 19*, 531-541.

45. Neher, S. B., Bradshaw, N., Floor, S. N., Gross, J. D., and Walter, P. (2008) SRP RNA controls a conformational switch regulating the SRP-SRP receptor interaction, *Nat Struct Mol Biol 15*, 916-923.

46. Lewis, N. E., Marty, N. J., Kathir, K. M., Rajalingam, D., Kight, A. D., Daily, A., Kumar, T. K., Henry, R. L., and Goforth, R. L. (2010) A dynamic cpSRP43-Albino3 interaction mediates translocase regulation of chloroplast signal recognition particle (cpSRP)-targeting components, *J Biol Chem 285*, 34220-34230.

IV

THE C TERMINUS OF ALBINO3 INTERACTS WITH THE RIBOSOSOMAL PROTEIN L23

SUMMARY

The chloroplast thylakoid membrane protein Alb3 is a member of the Oxa1/YidC/Alb3 family responsible for membrane insertion of proteins in mitochondria, bacteria, and chloroplasts, respectively. Both Oxa1 and YidC function co-translationally and have been shown to interact with the ribosome during peptide synthesis/insertion. Alb3 is known to function as an insertase in the post-translational cpSRP pathway. Here, we show that the stromal-exposed C-terminal region of Alb3 interacts with the *Arabidopsis thaliana* ribosomal protein L23. This novel finding opens the possibility that Alb3 functions in both post- and cotranslation protein insertion, with the C terminus playing a critical role in both pathways.

INTRODUCTION

Oxa1, YidC, and Alb3 are a conserved family of proteins that function in membrane biogenesis in mitochondria, bacteria, and chloroplasts, respectively. This relatively recently discovered group of proteins serve multiple functions within its particular membrane system. New findings into the molecular mechanisms of this protein family has continually expanded their functions, which now includes insertase, translocase, chaperone, and assembly factor activities [for review see Wang and Dalbey (*1*)]. These related but distinct roles allow the proteins to function within different pathways utilizing different substrates.

The mitochondrial inner membrane protein Oxa1 was the first member of this family discovered. Initially, Oxa1 was shown to serve as a translocase essential for the assembly of the cytochrome c oxidase complex (*2-5*). Future studies showed Oxa1 is essential for the proper insertion/assembly of many proteins and complexes involved in respiratory energy production (*6-7*). The most well studied role of Oxa1 involves assembly of the cytochrome oxidase (COX) complex. Oxa1 cotranslationally inserts COX subunits, which are mitochondrially encoded, into the inner membrane (*7*). In this cotranslational pathway Oxa1 not only acts as the insertase, but also serves directly as a ribosome receptor (*8*). This ribosome interaction requires the matrix-exposed C terminus of Oxa1 (*9*). Further, Mrp20, a component of the large ribosomal subunit which is homologous to L23, cross-links to Oxa1. In addition to cotranslational insertion of COX subunits, Oxa1 plays a role in the biogenesis of the F_1F_0-ATP synthase (*6, 8*). Unlike the COX subunits, however, Oxa1 null mutants show a greatly reduced, but still present, level of functional F_1F_0-ATP synthase (*6-8*). Formation of the multisubunit F_1F_0-ATP

synthase complex, not insertion of individual subunits, was disrupted by Oxa1 deletion (*10*). Further, Oxa1 forms a stable complex with the Atp9 subunit of F_1F_0-ATP synthase and can be copurified with the fully functional F_1F_0-ATP synthase complex. This data shows Oxa1 seems to serve a post-translational chaperone/assembly function for subunits of the F_1F_0-ATP synthase.

Similarly to Oxa1, the bacterial member of the protein family, YidC, can serve a variety of functions in bacterial membrane biogenesis. From its initial discovery, YidC has been shown to operate as an integrase/chaperone in conjunction with the Signal Recognition Particle-SEC pathway and as a SEC-independent insertase (*11-13*). Both YidC pathways are thought to be cotranslation, but a post-translational role has not been ruled out (*14*). Like Oxa1, YidC interacts with the ribosomal subunit L23, even though YidC lacks a large C terminus (*15*). Both Alb3 and Oxa1 can functionally replace YidC in bacteria (*16-17*). YidC can likewise functionally replace Oxa1, however it requires the ribosome-binding C terminus of Oxa1 (*18*). Gram positive bacteria contain a second YidC (YidC2/YdjG), which is more homologous to chloroplast Alb3 than gram negative YidC (*18*) and which has a large C terminus, similar to both Oxa1 and Alb3. Interestingly, *S. mutans* YidC2 requires no addition to functionally replace Oxa1 due to its large C-terminal domain which is competent in ribosome binding (*19*).

Compared to family members Oxa1 and YidC, relatively little is known about Alb3, particularly outside of its insertase role in post-translational chloroplast Signal Recognition Particle (cpSRP) targeting of light-harvesting chlorophyll-binding proteins (LHCP) to the thylakoid membrane (for a more in depth discussion on the role of Alb3 in cpSRP targeting, see Introduction). Similar to YidC, Alb3 has been shown to associate

with the SEC translocon (*20*). However, we have previously demonstrated that the SEC translocon is not required for cpSRP/Alb3 insertion of LHCP. Regardless, it seems quite likely that Alb3, like YidC, may perform an additional assembly/chaperone function in conjunction with the SEC translocon, but this has not been shown.

Alb3 has been speculated to play a role in assembly of D1 into photosystem II. D1 is a chloroplast-encoded protein that is cotranslationally targeted to the SEC translocon for insertion into the thylakoid membrane (*21-22*). This targeting is likely assisted by cpSRP54, but not cpSRP43, bound to the ribosome, as cpSRP54 has shown to bind D1 as a nascent chain emerging from the chloroplast ribosome (*23*). Interestingly, in the *Chlamydomonas reinhardtii* alb3 knockout, D1 is integrated but not efficiently assembled into the PSII complex, hinting at a role for Alb3 post-insertion (*24*). Still, much is unknown about the likely alternative functions of Alb3 outside of LHCP insertion.

To this end, we aimed to investigate the possibility of an interaction between the ribosome and Alb3, which would hint at a cotranslational function for Alb3. Oxa1 and YidC (and YidC2) function cotranslationally and both have been reported to interact with the ribosomal protein L23 (*15*), which is located on the large subunit along the peptide exit tunnel. In addition, much evidence exists that the cpSRP54 homolog SRP54/Ffh binds L23 during cotranslational SRP targeting (*25-27*). In chloroplasts, however, cpSRP targeting is post-translational, utilizing the unique cpSRP43 molecule as a functional ribosome replacement (*28*). But outside of cpSRP targeting, the possibility exists that Alb3 may, like Oxa1 and YidC, function in ribosome binding. If this interaction does take place, the most attractive and probably binding site would be the C terminus of Alb3. The C terminus of Alb3 has shown to interact with cpSRP43, which targets the

cpSRP complex to and docks with the Alb3 insertase (*29-30*), a role traditionally fulfilled by the ribosome. In addition, it is the C-terminal extension in both Oxa1 and YidC2 that interacts with the ribosome in cotranslational targeting (*9, 19*). On the ribosomal side, both Oxa1 and YidC interact with the ribosomal subunit L23, among others (*9, 15*).

In this work we explore the possibility of an interaction between Alb3 and the ribosome. We further characterize this interaction by narrowing it to a specific domain of Alb3 and a particular ribosomal subunit. Finally, we discuss the implications and future possibilities of said interaction.

MATERIALS AND METHODS

Chloroplast and Stromal Extract Isolation

Intact chloroplasts were isolated from 10- to 12-day-old pea seedlings (*Pisum. sativum* cv. Laxton's Progress) and used to prepare thylakoids and stroma as described previously (*31*). Chlorophyll (Chl) content was determined as described previously (*32*). Chloroplast stromal extract (SE) was isolated by suspending freshly isolated chloroplasts at 2 mg chlorophyll/mL HKM (10 mM Hepes-KOH, pH 8.0, 10 mM $MgCl_2$) and incubating for 5 min on ice. Lysed chloroplasts were centrifuged at 3000 x g for 5 min, and the supernatant transferred to a new tube and spun 42000 × g for 30 min to remove membrane components. The resulting SE was aliquoted, flash frozen in liquid N2, and stored at -80°C until needed.

Construction of Alb3-Cterm Clones

Production of a recombinant peptide corresponding to the C-terminal 124-amino acids of PPF1 (defined as Alb3 in *P. sativum*, Alb3-Cterm) was as according to Lewis et al (*29*). Final products were an Alb3-Cterm peptide containing a six-histidine tag and either a Flag-tag or an Stag located at the N terminus of the peptide (His-Flag-Alb3-Cterm or His-Stag-Alb3-Cterm). Alb3-Cterm constructs were purified over Talon® Superflow metal affinity chromatography and either desalted into HKMK (HKM with 100 mM KCl) buffer or further purified by cation exchange over Resource S (binding: 20 mM Hepes, pH 8, 10 mM KCl, and elution: 20 mM Hepes, pH 8, 1 M KCl) and then desalted into HKMK buffer. For full details on cloning, expression, and purification of Alb3-Cterm, see Chapter II: A Dynamic cpSRP43-Albino3 Interaction Mediates

Translocase Regulation of Chloroplast Signal Recognition Particle (cpSRP)-Targeting Components (Materials and Methods section).

Construction of L23 Clones

A ribosomal protein L23 clone was obtained by RT-PCR from *Arabidopsis thaliana* total RNA using a OneStep RT-PCR Kit (Qiagen). Forward and reverse primers matching the sequence for L23 (accession # 000932) were designed to include NdeI and XhoI sites, respectively, for ligation into similarly restricted pET-15b. In addition to the XhoI site, the reverse primer included a Strep-tag and stop codon, resulting in the following plasmid following ligation: His-L23-Strep-pET-15b. This plasmid was transformed into BL21 Star (Invitrogen) and used for IPTG induced expression of His-L23-Strep.

An *in vitro* transcription/translation L23 clone was produced using primers designed with an EcoR1 site and Kozak sequence so that the translated protein begins MDGIK and ends RKKRT with a stop codon and HindIII site. The resulting PCR product was restricted and ligated into pGEM-4Z to generate the plasmid L23-pGEM-4Z.

In vitro transcription and translation

Capped L23 RNA was produced by *in vitro* transcription of L23-pGEM-4Z DNA using SP6 RNA polymerase (GE Healthcare). L23 RNA was translated using a wheat germ system (*33*) in the presence of ^{35}S methionine to produce radiolabeled protein (*34*). Translation product was diluted two-fold in 100 mM Hepes-KOH (pH 8.0), 0.66 M sorbitol and 60 mM unlabeled methionine before use.

Recombinant L23 Purification

L23 was purified from *E. coli* by slightly modifying a procedure used for the purification of *maize* L23 expressed in *E. coli* (*35*). *E. coli* (~ 5 g) expressing his-L23-Strep were lysed using sonication (3 sets of 25 one-second bursts with 1min rest in between sets at level 8 with a Branson Sonifier 150 probe tip sonicator). Lysate was then centrifuged at 30,000 × g for 30 min at 4 °C. The resulting pellet was resuspended in 25 mL of 1 % Triton X-100 by slow stirring for 15 min at room temperature and subsequently centrifuged at 30,000 × g for 30 min at 4 °C. The inclusion body pellet was washed twice by addition of 25 mL of 50 mM Tris-HCl (pH 8.1), 100 mM NaCl, 10 mM EDTA, 5 mM DTT, 500 μM PMSF, and 2 % Na-deoxycholate and stirring for 20 min at room temperature. The pellet was then washed once with 25 mL of 5 mM DTT, 500 μM PMSF. The washed inclusion bodies were then dissolved in 20 mL of 6 M guanidine-HCl, 100 mM NH_4-acetate (pH 5.2), 5 mM DTT, 500 μM PMSF and then applied to a HiPrep^{TM} 26/10 Desalting Column (GE Healthcare) equilibrated in the same buffer. L23 fractions were combined and renatured by overnight dialysis against ~1 L 50 mM NH_4-acetate (pH 5.2), 5 mM DTT, 500 μM PMSF using a Slide-A-Lyzer Dialysis Cassette (3500 MWCO, Pierce). L23 was then concentrated using a Vivaspin protein concentrator (5000 MWCO, Sartorius) to ~ ¼ original volume and quantified by SDS-PAGE.

Size Exclusion Chromatography (SEC)

SE was thawed on ice and concentrated to ~ half volume by centrifugation in a Vivaspin 5000 MWCO to an ~ 8X SE final. Concentrated SE was loaded at 0.5 mL/min onto a HiPrep Sephacryl S-300 16/60 SR gel filtration column prequilibrated in HKM. Fractions were collected in 96 well plates and analyzed for the presence of chloroplast

ribosomes by Western blotting for cpSRP54, which is known to bind ribosomes and function in cotranslational chloroplast targeting (*21, 23*). cpSRP54 was found in two distinct pools, cpSRP54-ribosome (~47 mL flow volume) and cpSRP54-cpSRP43 (~61 mL flow volume). High molecular weightcpSRP54 fractions were pooled and incubated with His-Flag-Alb3-Cterm for 10 min on ice. The sample was then centrifuged at 42000 × g for 1 hour. Supernatant was concentrated to 600 µL using Vivaspin 5000 MWCO and then loaded at 0.5 mL/min on HiPrep Sephacryl S-300 16/60 SR gel filtration column equilibrated in HKM. Fractions were collected and analyzed for the presence of cpSRP54 and Alb3-Cterm by Western blotting. Alb3-Cterm co-eluted with cpSRP54 (ribosomes) at 46.5-54 mL flow volume. An equal volume of Alb3-Cterm, in the absence of SE, loaded onto the column under the same conditions eluted at 100-105 mL flow volume as determined by Western blotting.

Protein Binding Assays

His-Stag-Alb3-Cterm equal to 800 pmols in 100 µL of import buffer (IB: 50 mM Hepes-KOH, pH 8.0, 0.33 M sorbitol) with 10 mM MgCl2 (IBM) was incubated with 30 µL of a 50 % S-protein agarose slurry in HKM for 15 min at room temperature. Following incubation, 50 µL of radiolabeled L23 translation product was added and reactions were incubated at 4°C for 30 min under gentle agitation. Samples were washed six times with 0.1 % Maltoside in IB and three times with IB using 0.8 mL centrifuge colums (PIERCE). Proteins were eluted by adding 30 µl SDS-PAGE solubilization buffer (10 % glycerol, 5 % β-mercaptoethanol, 2 % SDS) and incubating for 30min at room temperature. Eluted proteins were analyzed by SDS-PAGE.

Either 500 pmols of recombinant His-L23-Strep or an equivalent volume of buffer were mixed with 30 µL Streptactin resin, brought to 150 µL with 50 mM NH4-Acetate (pH 7.5) and incubated for 15 min at room temperature. Either 500 or 1000 pmoles of HSCterm were added for a second 15 minute incubation at room temperature with gently shaking. Reactions were transferred to spin columns and washed three times with 50 mM NH4-Acetate (pH 7.5). Proteins were eluted by addition of 30 µL solubilization buffer and analyzed by SDS-PAGE.

Analysis of Samples

A portion of each sample from each assay was analyzed by SDS-PAGE followed by Coomassie Blue staining, Western blotting, or phosphorimaging. GE Healthcare image analysis software (ImageQuant) was used for quantification of radiolabeled protein from phosphorimages obtained using a Typhoon 8600. Horseradish peroxidase-labeled mouse IgG (Southern Biotech) was used as secondary antibody, and blots were developed with SuperSignal® West Pico chemiluminescent substrate (Pierce). Western blots were imaged using an Alpha Innotech FluorChem IS-8900 using chemiluminescent detection. AlphaEase FC Stand Alone software (Alpha Innotech) was used for quantification. SDS-PAGE standards (Invitrogen) were used to calculate molecular weights (MagicMark™ XP Western Standard for Western blots; Benchmark™ Protein Ladder for Coomassie-stained gels). Protein concentrations were estimated by Coomassie Blue staining. Primary antibodies to the following proteins have been described previously: cpSRP54 (*36*), Alb3-Cterm (*37*).

RESULTS

Alb3-Cterm interacts with chloroplast ribosomes

Using SEC, we studied the retention time of Alb3-Cterm alone and in the presence of pooled ribosomal/cpSRP54 fractions (*21, 23*). The retention time of Alb3-Cterm on the column was dramatically reduced (from ~100 mL to ~47 mL) when preincubated with a cpSRP54-ribosome fraction isolated from chloroplast SE. This preliminary works suggests an interaction between the C terminus of Alb3 and the chloroplast ribosome. Future work includes the use of sucrose gradient centrifugation to isolate ribosomal fractions for SEC chromatography. In addition to confirming the presence of cpSRP54 (via Western blotting) in isolated ribosomal fractions, we will also confirm the presence of RNA by gel electrophoresis and EtBr staining. Currently we have demonstrated the ability to isolate ribosomal fractions by sucrose gradient centrifugation and confirm the presence of RNA and cpSRP54. Ideally, an antibody that is reactive with chloroplast ribosomal proteins will be identified for use as a final confirmation of the isolation procedures. Alternatively, we may consider making an antibody to *A. thaliana* L23. The sequence identity between *A. thaliana* and *P. sativum* is 80 %, so we would expect cross reactivity with chloroplast ribosomes isolated from *P. sativum.*

Alb3-Cterm interacts with the ribosomal subunit L23

In trying to uncover the ribosome binding site for Alb3-Cterm, one strong possiblity was the ribosomal protein L23. L23 is known to interact with Alb3 family members Oxa1 and YidC L23 (*9, 15*). To this end, we produced two L23 clones, an *in vitro* produced peptide for radiolabeling and a recombinant peptide with two affinity tags. Recombinant expression and purification of *Arabidopsis* L23 had, to our knowledge,

never been accomplished and presented unique challenges. L23 expressed in *E. coli* was found, almost exclusively, in insoluble inclusion bodies. Traditional methods of isolating inclusion bodies (multiple sucrose washes and eventual solubilization in either 8 M urea or solubilization buffer) proved unsuccessful. However, adaptation of a published method for purification of maize L23 (*35*) was successful in purifying large quantities of soluble L23 from inclusion bodies (Fig. 4.1). This procedure yielded ~ 3 mg of protein per 1 L of expression. However, protein quantity was much lower than is likely possible due to loss of a significant amount of sample during desalting. This error is easily fixed and future purifications should yield much greater quantities of L23. While some residual contaminants remain, purity level of L23 should be sufficient of antibody generation.

Radiolabeled L23 was copurified using an Stag on Alb3-Cterm and S-protein agarose resin to isolate His-Stag-Alb3-Cterm and all copurifying proteins. The amount of L23 copurified was significantly above the level of background binding to the resin (Fig. 4.2 A). Further, the reverse of this experiment was done using Streptactin reisn to isolate recombinant His-L23-Strep. Fig. 4.2 B shows that Alb3-Cterm copurifies to a level significantly above background binding of Alb3-Cterm to the resin alone. Taken together, results in Figs 4.2 show that the C terminus of Alb3 is involved in an interaction with the chloroplast ribosome, which minimally involves the large ribosomal subunit protein L23.

DISCUSSION

Although much has been learned about the role of Alb3 in post-translational targeting by the cpSRP pathway in the past several years, it continues to be an ongoing area of study (*29-30, 36-40*). In contrast, while often speculated upon, little evidence exists for a cotranslational role of Alb3, either in insertion or assembly. The fact that Alb3 exists both independently and associated with the chloroplast Sec translocon (*20*), in addition to the cotranslational roles of Oxa1 and YidC, hints at the possibility of alternative functions for Alb3. Work done here focused on uncovering data that would not only further the notion of Alb3 operation in a cotranslational pathway, but also discover specific interactions that would facilitate such a function. While preliminary, our results have identified an interaction between the C terminus of Alb3 and the chloroplast ribosome. Specifically, we have identified an interaction between Alb3-Cterm and the ribosomal protein L23. While interesting, possibly the most significant aspects of this finding are the questions it raises as well as the future research possibilities it opens. For instance, what chloroplast encoded protein is the ribosome delivering to Alb3? Currently, LHCP is the only known substrate of Alb3. The Sec pathway inserted substrate D1 is a possible substrate of co-translationally active Alb3 where Alb3 may act in an assembly role (*24, 41*). However, significantly more work is needed to fully understand what if any link there is between Alb3 and D1. If Alb3 is required for efficient D1 assembly into PSII, it seems unlikely that Alb3 would interact with the ribosome when chaperoning/assembling a protein integrated by the Sec translocon. Regardless of the substrate, other important questions remain. Does Alb3 act independently in cotranslational targeting, or is it associated with the Sec translocon? Further, as is the

case with D1, is cpSRP54 involved in targeting the ribosome to Alb3? Our SEC results suggest that the presence of cpSRP54 on the ribosome does not hinder the interaction, but clearly more work is needed to determine if it is required or if the pathway operates independent of cpSRP components. *In vivo* studies of LHCP targeting in *Arabidopsis* mutants lacking both cpSRP54 and cpFtsY indentified a cpSRP43 only pathway for efficient targeting of LHCP to Alb3 (*42*). This is supported by findings that cpSRP43 can interact with Alb3-Cterm in the absence of cpSRP54 (*29-30*). Thus, neither the presence nor absence of cpSRP54 in cotranslational targeting to Alb3 would be surprising. Finally, it is interesting to speculate that competition exists between cpSRP43 (post-translational) and the ribosome (cotranslational) for binding to the C terminus of Alb3. While not successful as of yet, work is underway to determine if Alb3-Cterm binding to L23 inhibits an interaction with cpSRP43, or if the reverse, prebinding of cpSRP43 to Alb3-Cterm inhibits L23 interaction, is true. Determining the affinity of the ribosome (L23) for Alb3-Cterm would be useful for comparing to the affinity of cpSRP43 for Alb3-Cterm and possibly hint at how the C terminus regulates Alb3's participation in post- or cotranslational targeting.

These questions, which mostly require *in vivo* analysis, are difficult to address in the chloroplast system. The most common method for identification of interaction partners with Oxa1 and YidC has been *in vivo* crosslinking, which is a method that should be pursued for future research into the alternative functions of Alb3. However, crosslinking followed by immunoprecipitation of Alb3 or chloroplast ribosome isolation is not likely to be clear cut and will present difficulties both in deciphering and indentifying true data among non-specific artifacts. The positive of this approach is that it

has the ability to reveal interacting partners ranging from ribosomal proteins and nascent polypeptide substrates to neighboring translocons or other assembly factors. However, until such work is done, any statement about the meaning of this Alb3-L23 interaction is speculative at best.

To this end, we have developed a very early model of Alb3 functioning as both a post- and cotranslational insertase (Fig. 4.3). In our model, the C terminus regulates binding of Alb3 to cpSRP43 or the chloroplast ribosome by a yet unknown mechanism. As shown, the C terminus of Alb3 binding to the ribosome is mediated by L23, although other ribosomal proteins are likely involved, as is the case with both Oxa1 and YidC (*15, 43*). Further, our model does not rule out the possibility of other integral membrane proteins assisting Alb3 in this function, as indicated. While peripheral membrane proteins and soluble targeting factors are not shown, they obviously cannot be ruled out at this point.

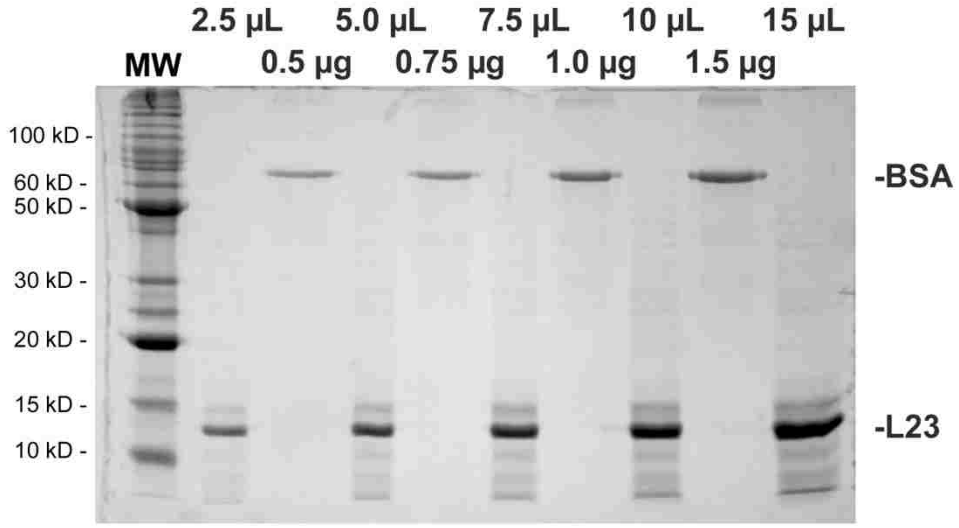

Figure 4.1. Quantification of purified, recombinant L23.

Recombinant L23 was purified and concentrated as described in Materials and Methods. Gel shows increasing volumes of a L23 (diluted 1:20 in SDS solubilization buffer) and increasing quantity of known BSA standard on the same gel. Top row of numbers indicates µL volume of diluted L23 loaded in corresponding lane. Bottom row of numbers indicates µg amount of BSA standard loaded in corresponding lane. Concentration of L23 was calculated using AlphaEase Fluorchem software (Alpha Innotech) by comparing band density to BSA standards.

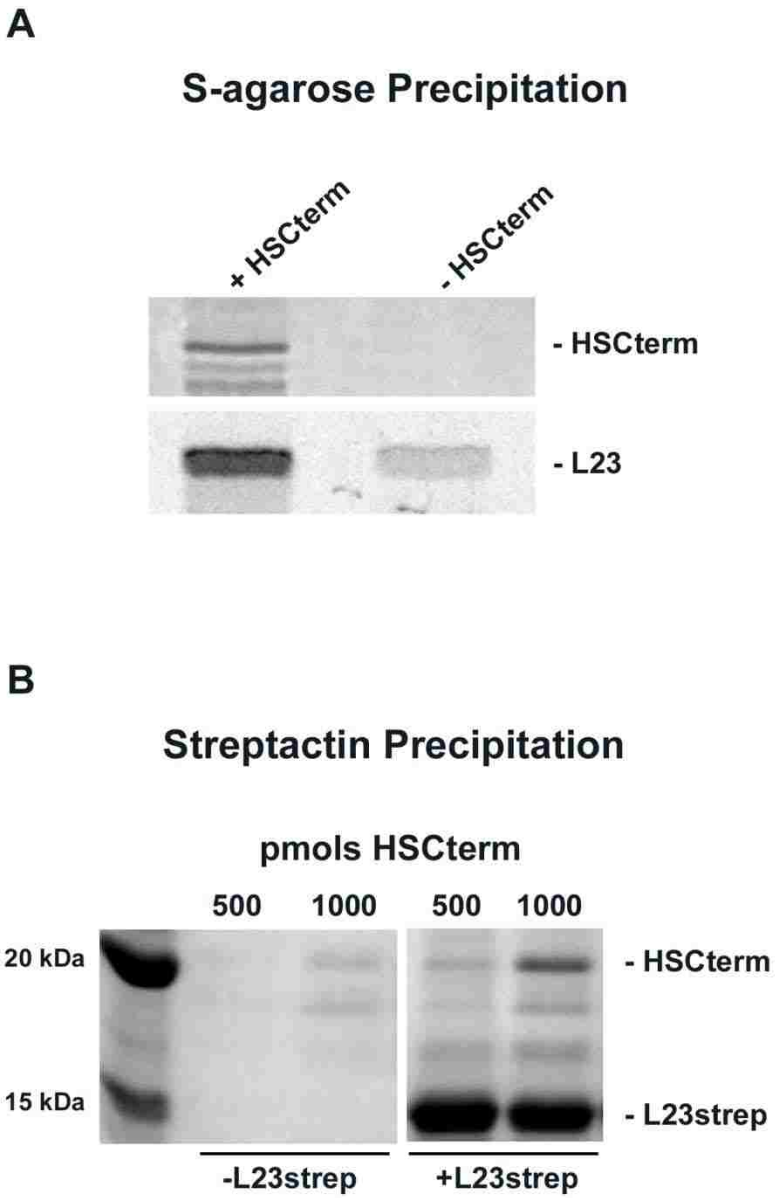

Figure 4.2. The ribosomal protein L23 and Alb3-Cterm coprecipitate.

A) Either 800 pmols of HSCterm or an equal volume of buffer alone were incubated with S-protein agarose, then radiolabled L23 translation product. Samples were washed six times with 0.1 % Maltoside in IB and three times with IB. Copurifying proteins were eluted with SDS sample buffer and analyzed by SDS-PAGE. Data obtained by Jennifer Rogers. **B)** Streptactin resin was incubated with either His-L23-Strep or buffer and then added to either 500 or 1000 pmols of HSCterm. After three buffer washes, proteins were eluted with SDS sample buffer and analyzed by SDS-PAGE

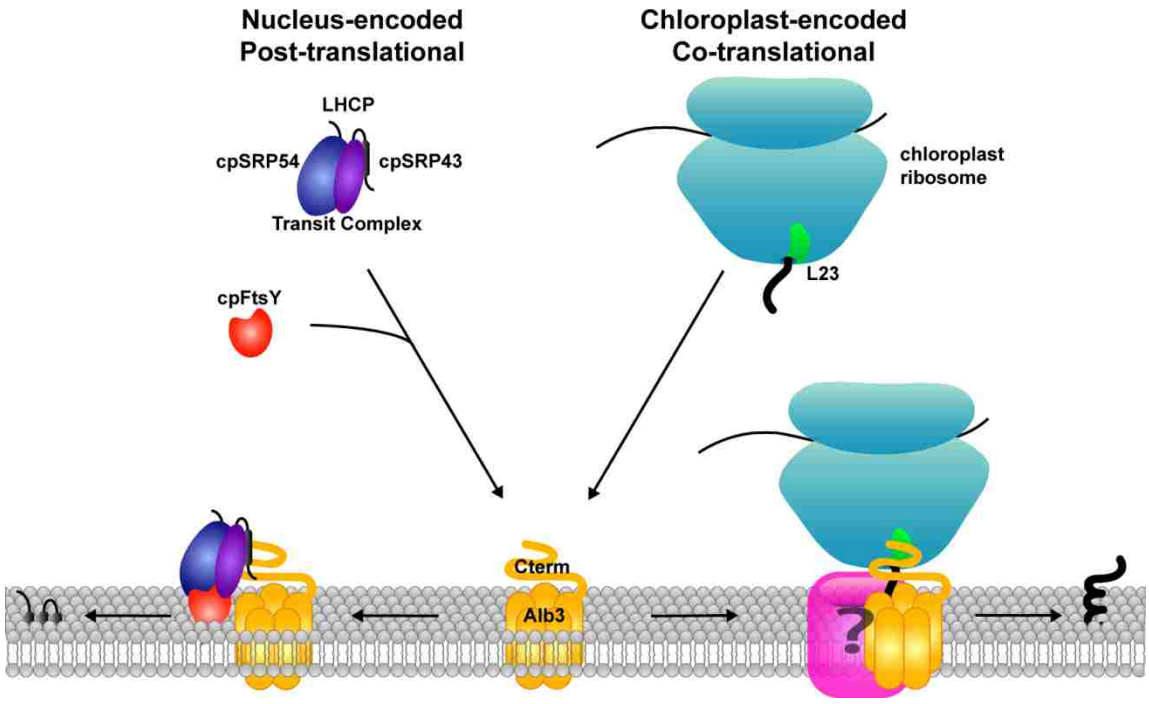

Figure 4.3. Model of post- and cotranslational targeting to Alb3.
Alb3 functions in the post-translational insertion of LHCP by the cpSRP pathway. This model depicts a second, cotranslational function of Alb3 that involves the C terminus binding to the ribosomal protein L23. The possibility of the Sec translocase, or another unknown membrane protein, assisting in insertion/assembly is indicated by the unlabeled pink molecule.

REFERENCES

1. Wang, P., and Dalbey, R. E. (2010) Inserting membrane proteins: The YidC/Oxa1/Alb3 machinery in bacteria, mitochondria, and chloroplasts, *Biochimica et Biophysica Acta*.

2. Bauer, M., Behrens, M., Esser, K., Michaelis, G., and Pratje, E. (1994) PET1402, a nuclear gene required for proteolytic processing of cytochrome oxidase subunit 2 in yeast, *Mol Gen Genet 245*, 272-278.

3. Bonnefoy, N., Chalvet, F., Hamel, P., Slonimski, P. P., and Dujardin, G. (1994) OXA1, a Saccharomyces cerevisiae nuclear gene whose sequence is conserved from prokaryotes to eukaryotes controls cytochrome oxidase biogenesis, *J Mol Biol 239*, 201-212.

4. He, S., and Fox, T. D. (1997) Membrane translocation of mitochondrially coded Cox2p: distinct requirements for export of N and C termini and dependence on the conserved protein Oxa1p, *Mol Biol Cell 8*, 1449-1460.

5. Hell, K., Herrmann, J., Pratje, E., Neupert, W., and Stuart, R. A. (1997) Oxa1p mediates the export of the N- and C-termini of pCoxII from the mitochondrial matrix to the intermembrane space, *FEBS Lett 418*, 367-370.

6. Altamura, N., Capitanio, N., Bonnefoy, N., Papa, S., and Dujardin, G. (1996) The Saccharomyces cerevisiae OXA1 gene is required for the correct assembly of cytochrome c oxidase and oligomycin-sensitive ATP synthase, *FEBS Lett 382*, 111-115.

7. Hell, K., Neupert, W., and Stuart, R. A. (2001) Oxa1p acts as a general membrane insertion machinery for proteins encoded by mitochondrial DNA, *EMBO Journal 20*, 1281-1288.

8. Szyrach, G., Ott, M., Bonnefoy, N., Neupert, W., and Herrmann, J. M. (2003) Ribosome binding to the Oxa1 complex facilitates co-translational protein insertion in mitochondria, *EMBO Journal 22*, 6448-6457.

9. Jia, L., Dienhart, M., Schramp, M., McCauley, M., Hell, K., and Stuart, R. A. (2003) Yeast Oxa1 interacts with mitochondrial ribosomes: the importance of the C-terminal region of Oxa1, *EMBO Journal 22*, 6438-6447.

10. Jia, L., Dienhart, M. K., and Stuart, R. A. (2007) Oxa1 directly interacts with Atp9 and mediates its assembly into the mitochondrial F1Fo-ATP synthase complex, *Mol Biol Cell 18*, 1897-1908.

11. Scotti, P. A., Urbanus, M. L., Brunner, J., de Gier, J. W., von Heijne, G., van der Does, C., Driessen, A. J., Oudega, B., and Luirink, J. (2000) YidC, the Escherichia coli homologue of mitochondrial Oxa1p, is a component of the Sec translocase, *EMBO Journal 19*, 542-549.

12. Samuelson, J. C., Chen, M., Jiang, F., Moller, I., Wiedmann, M., Kuhn, A., Phillips, G. J., and Dalbey, R. E. (2000) YidC mediates membrane protein insertion in bacteria, *Nature 406*, 637-641.

13. Stuart, R. A., and Neupert, W. (2000) Making membranes in bacteria, *Nature 406*, 575, 577.

14. Kiefer, D., and Kuhn, A. (2007) YidC as an essential and multifunctional component in membrane protein assembly, *Int Rev Cytol 259*, 113-138.

15. Kohler, R. B., Daniel; Greber, Basil; Bingel-Erlenmeyer, Rouven; Collinson, Ian; Schaffitzel, Christiane; Ban, Nenad (2009) YidC and Oxa1 form dimeric insertion pores on the translating ribosome, *Molecular Cell 34*, 344-353.

16. Jiang, F., Yi, L., Moore, M., Chen, M., Rohl, T., Van Wijk, K. J., De Gier, J. W., Henry, R., and Dalbey, R. E. (2002) Chloroplast YidC homolog Albino3 can functionally complement the bacterial YidC depletion strain and promote membrane insertion of both bacterial and chloroplast thylakoid proteins, *Journal of Biological Chemistry 277*, 19281-19288.

17. van Bloois, E., Nagamori, S., Koningstein, G., Ullers, R. S., Preuss, M., Oudega, B., Harms, N., Kaback, H. R., Herrmann, J. M., and Luirink, J. (2005) The Sec-independent function of Escherichia coli YidC is evolutionary-conserved and essential, *J Biol Chem 280*, 12996-13003.

18. Preuss, M., Ott, M., Funes, S., Luirink, J., and Herrmann, J. M. (2005) Evolution of mitochondrial oxa proteins from bacterial YidC. Inherited and acquired functions of a conserved protein insertion machinery, *J Biol Chem 280*, 13004-13011.

19. Funes, S., Hasona, A., Bauerschmitt, H., Grubbauer, C., Kauff, F., Collins, R., Crowley, P. J., Palmer, S. R., Brady, L. J., and Herrmann, J. M. (2009) Independent gene duplications of the YidC/Oxa/Alb3 family enabled a specialized cotranslational function, *Proc Natl Acad Sci U S A 106*, 6656-6661.

20. Klostermann, E., Droste Gen Helling, I., Carde, J. P., and Schunemann, D. (2002) The thylakoid membrane protein ALB3 associates with the cpSecY-translocase in Arabidopsis thaliana, *Biochemical Journal 368*, 777-781.

21. Nilsson, R., Brunner, J., Hoffman, N. E., and van Wijk, K. J. (1999) Interactions of ribosome nascent chain complexes of the chloroplast- encoded D1 thylakoid membrane protein with cpSRP54, *EMBO Journal 18*, 733-742.

22. Zhang, L., Paakkarinen, V., Suorsa, M., and Aro, E. M. (2001) A SecY homologue is involved in chloroplast-encoded D1 protein biogenesis, *Journal of Biological Chemistry 276*, 37809-37814.

23. Nilsson, R., and van Wijk, K. J. (2002) Transient interaction of cpSRP54 with elongating nascent chains of the chloroplast-encoded D1 protein; 'cpSRP54 caught in the act', *FEBS Letters 524*, 127-133.

24. Gohre, V., Ossenbuhl, F., Crevecoeur, M., Eichacker, L. A., and Rochaix, J.-D. (2006) One of two Alb3 proteins is essential for the assembly of the photosystems and for cell survival in Chlamydomonas, *Plant Cell 18*, 1454-1466.

25. Halic, M., Becker, T., Pool, M. R., Spahn, C. M., Grassucci, R. A., Frank, J., and Beckmann, R. (2004) Structure of the signal recognition particle interacting with the elongation-arrested ribosome, *Nature 427*, 808-814.

26. Gu, S. Q., Peske, F., Wieden, H. J., Rodnina, M. V., and Wintermeyer, W. (2003) The signal recognition particle binds to protein L23 at the peptide exit of the Escherichia coli ribosome, *RNA 9*, 566-573.

27. Ullers, R. S., Houben, E. N., Raine, A., ten Hagen-Jongman, C. M., Ehrenberg, M., Brunner, J., Oudega, B., Harms, N., and Luirink, J. (2003) Interplay of signal recognition particle and trigger factor at L23 near the nascent chain exit site on the Escherichia coli ribosome, *J Cell Biol 161*, 679-684.

28. Goforth, R. L., Peterson, E. C., Yuan, J., Moore, M. J., Kight, A. D., Lohse, M. B., Sakon, J., and Henry, R. L. (2004) Regulation of the GTPase cycle in post-translational Signal Recognition Particle-based protein targeting involves cpSRP43, *Journal of Biological Chemistry 279*, 43077-43084.

29. Lewis, N. E., Marty, N. J., Kathir, K. M., Rajalingam, D., Kight, A. D., Daily, A., Kumar, T. K., Henry, R. L., and Goforth, R. L. (2010) A dynamic cpSRP43-Albino3 interaction mediates translocase regulation of chloroplast signal recognition particle (cpSRP)-targeting components, *J Biol Chem 285*, 34220-34230.

30. Falk, S., Ravaud, S., Koch, J., and Sinning, I. (2010) The C terminus of the Alb3 membrane insertase recruits cpSRP43 to the thylakoid membrane, *J Biol Chem 285*, 5954-5962.

31. Cline, K., Henry, R., Li, C., and Yuan, J. (1993) Multiple pathways for protein transport into or across the thylakoid membrane, *EMBO J. 12*, 4105-4114.

32. Arnon, D. I. (1949) Copper enzymes in isolated chloroplasts. Polyphenoloxidase in Beta vulgaris, *Plant Physiol. 24*, 1-15.

33. Cline, K., Henry, R., Li, C., and Yuan, J. (1993) Multiple pathways for protein transport into or across the thylakoid membrane, *EMBO Journal 12*, 4105-4114.

34. Chu, F., Shan, S. O., Moustakas, D. T., Alber, F., Egea, P. F., Stroud, R. M., Walter, P., and Burlingame, A. L. (2004) Unraveling the interface of signal recognition particle and its receptor by using chemical cross-linking and tandem mass spectrometry, *Proc Natl Acad Sci U S A 101*, 16454-16459.

35. Bubunenko, M. G., Schmidt, J., and Subramanian, A. R. (1994) Protein substitution in chloroplast ribosome evolution. A eukaryotic cytosolic protein has replaced its organelle homologue (L23) in spinach, *J Mol Biol 240*, 28-41.

36. Moore, M., Goforth, R. L., Mori, H., and Henry, R. (2003) Functional interaction of chloroplast SRP/FtsY with the ALB3 translocase in thylakoids: substrate not required, *Journal of Cell Biology 162*, 1245-1254.

37. Woolhead, C. A., Thompson, S. J., Moore, M., Tissier, C., Mant, A., Rodger, A., Henry, R., and Robinson, C. (2001) Distinct Albino3-dependent and -independent pathways for thylakoid membrane protein insertion, *J Biol Chem 276*, 40841-40846.

38. Bellafiore, S., Ferris, P., Naver, H., Gohre, V., and Rochaix, J. D. (2002) Loss of Albino3 leads to the specific depletion of the light-harvesting system, *Plant Cell 14*, 2303-2314.

39. Moore, M., Harrison, M. S., Peterson, E. C., and Henry, R. (2000) Chloroplast oxa1p homolog albino3 is required for post-translational integration of the light harvesting chlorophyll-binding protein into thylakoid membranes, *Journal of Biological Chemistry 275*, 1529-1532.

40. Sundberg, E., Slagter, J. G., Fridborg, I., Cleary, S. P., Robinson, C., and Coupland, G. (1997) ALBINO3, an Arabidopsis nuclear gene essential for chloroplast differentiation, encodes a chloroplast protein that shows homology to proteins present in bacterial membranes and yeast mitochondria, *Plant Cell 9*, 717-730.

41. Ossenbuhl, F., Gohre, V., Meurer, J., Krieger-Liszkay, A., Rochaix, J. D., and Eichacker, L. A. (2004) Efficient assembly of photosystem II in Chlamydomonas reinhardtii requires Alb3.1p, a homolog of Arabidopsis ALBINO3, *Plant Cell 16*, 1790-1800.

42. Tzvetkova-Chevolleau, T., Hutin, C., Noel, L. D., Goforth, R., Carde, J.-P., Caffarri, S., Sinning, I., Groves, M., Teulon, J.-M., Hoffman, N. E., Henry, R., Havaux, M., and Nussaume, L. (2007) Canonical signal recognition particle components can be bypassed for posttranslational protein targeting in chloroplasts, *Plant Cell 19*, 1635-1648.

43. Jia, L., Kaur, J., and Stuart, R. A. (2009) Mapping of the Saccharomyces cerevisiae Oxa1-mitochondrial ribosome interface and identification of MrpL40, a ribosomal protein in close proximity to Oxa1 and critical for oxidative phosphorylation complex assembly, *Eukaryot Cell 8*, 1792-1802.

V

SUMMARY

Signal Recognition Particle (SRP)-dependant protein targeting is a conserved system for the localization of proteins to their specific sites of function within the cell. Over the past 30 years, much work has been done to uncover the components associated with SRP targeting and to understand the function of those components within the pathway. This work has led to a detailed understanding of many facets of SRP targeting, and the nature of protein targeting in general, in both pro- and eukaryotes. Results from both structural and functional studies have clarified the picture so that knowledge of protein-protein interactions, critical functional domains of targeting components, and means of pathway regulation exist for many of the targeting steps. However, much mystery remains surrounding certain aspects of SRP targeting, particularly membrane-associated events where understanding greatly lags behind soluble targeting steps.

The research presented here was focused on events at the membrane interface of the chloroplast signal recognition particle (cpSRP) targeting pathway. We aimed to gain a better understanding of the role of both the thylakoid lipid environment and the cpSRP insertase Albino3 (Alb3). This required the development of new tools to better study targeting events in a very complex environment. Using these tools, we made new discoveries and added increasing clarity to the model of cpSRP targeting.

We developed tools for studying cpSRP targeting on a less complex liposome membrane system. We showed liposomes made using soybean extract lipids were capable of supporting formation of a cpSRP membrane complex containing cpSRP54, cpSRP43, and cpFtsY at a level close to that observed for isolated thylakoids. We further showed the ability of soy liposomes to support more advanced functions of cpSRP components. Using brominated liposomes, we were able to quench tryptophan

fluorescence of chloroplast FtsY (cpFtsY) (*1*). This is a strong indicator of membrane binding and possibly partial insertion into the lipid bilayer. Confirmation of these results came from the dramatic decrease in quenching of fluorescence from a previously developed mutant of cpFtsY, which lacks the membrane-binding motif (*1*). Thus, cpFtsY is specifically able to bind liposomes using the same mechanism involved in binding to isolated thylakoid membranes. In addition, artificial liposomes stimulated GTP hydrolysis by the cpSRP GTPases – cpSRP54 and cpFtsY (*1*). Taken together, these results show that liposomes competently function in place of the thylakoid membrane in multiple cpSRP pathway steps. In addition, we developed liposomes with a lipid content much closer to the unique thylakoid membrane than our original soybean total extract liposomes. By doping a mixture of lipids mimicking the thylakoid membrane with soy lipids, we successfully generated liposomes, despite the presence of non-bilayer forming thylakoid lipids. These tools will be valuable in future studies on cpSRP membrane interactions, with the ultimate goal of reconstituting cpSRP targeting on liposomes.

As an alternative to traditional biochemical assays, we used three different microscopes – confocal laser scanning microscope (CLSM), atomic force microscope (AFM), and transmission electron microscope (TEM) – to visualize cpSRP components. Using a combination of antibody-nanocrystal labeling and CLSM, we were able to visualize the abundance and localization of the insertase Alb3 in the thylakoid membrane. Images of isolated thylakoids were captured using AFM and TEM, which gave a visual understanding of the complexity of the protein-rich thylakoid membrane. While we were not successful in imaging cpSRP targeting steps, the protocols developed here could

prove helpful in accomplishing that goal or others pertaining to thylakoid membrane visualization.

In addition to the lipid environment of the thylakoid membrane, this research focused on the cpSRP insertase Alb3. We showed two key interactions involving the C-terminal domain of Alb3 (Alb3-Cterm) using both recombinant and in vitro translated peptides corresponding to this domain. Using a combination of copurification assays and isothermal titration calorimetry (ITC), we showed a high affinity interaction between the cpSRP subunit cpSRP43 and Alb3-Cterm (*2*). We narrowed down the site of this interaction, using a combination of copurification assays, ITC, and GTP hydrolysis assays, to the ankyrin repeat region of cpSRP43 (*2*). We further showed the functional relevance of this interaction in cpSRP membrane targeting steps. Using a GTP hydrolysis assay, we showed that the C terminus of Alb3 stimulates GTP hydrolysis of the cpSRP GTPases (cpSRP54 and cpFtsY) in a cpSRP43-dependant manner (*2*). In addition, as visualized by non-denaturing PAGE, we found that the addition of Alb3-Cterm to soluble cpSRP transit complex (cpSRP54-cpSRP43-LHCP) caused LHCP to separate from the cpSRP heterodimer (*2*). Taken together, these results add clarity to the role of Alb3 in cpSRP targeting membrane events and advance the overall understand of the pathway. It appears that the cpSRP54-cpSRP43 bound with LHCP substrate interacts with cpFtsY at the thylakoid membrane. This complex then targets to Alb3 via an interaction between the ankyrin repeat region of cpSRP43 and the C terminus of Alb3. This cpSRP43-Alb3 interaction serves as a sensor of localization to the insertase and triggers appropriate events to advance the cpSRP targeting cycle. These events, the order of which is not known, are 1) release of LHCP substrate from the cpSRP heterodimer, presumably to

Alb3 and 2) hydrolysis of GTP by cpSRP54 and cpFtsY, presumably for release and recycling of cpSRP components.

A second interaction we identified is between the C terminus of Alb3 and the chloroplast 50S ribosomal protein L23 (*Arabidopsis thaliana*). Using size exclusion chromatography, we showed a shift in the elution profile of Alb3-Cterm following incubation with a cpSRP54-ribosome complex. L23 was identified as one of the ribosomal subunits responsible for the interaction with Alb3-Cterm using copurification assays. This interaction strongly hints at a role for Alb3 in co-translational protein targeting, as opposed to the traditional role of Alb3 in post-translational insertion of LHCP. Since the C terminus of Alb3 interacts with both cpSRP43 (post-translational targeting) and L23 (cotranslational targeting), future studies into the regulation/coordination of Alb3 participation in these distinct pathways by its C terminus will be interesting. We propose that cpSRP43 and the chloroplast ribosome might compete for interaction with Alb3-Cterm; however this proposition is purely speculative.

REFERENCES

1. Marty, N. J., Rajalingam, D., Kight, A. D., Lewis, N. E., Fologea, D., Kumar, T. K. S., Henry, R. L., and Goforth, R. L. (2009) The Membrane-binding Motif of the Chloroplast Signal Recognition Particle Receptor (cpFtsY) Regulates GTPase Activity, *J of Biol Chem 284*, 14891-14903.

2. Lewis, N. E., Marty, N. J., Kathir, K. M., Rajalingam, D., Kight, A. D., Daily, A., Kumar, T. K., Henry, R. L., and Goforth, R. L. (2010) A dynamic cpSRP43-Albino3 interaction mediates translocase regulation of chloroplast signal recognition particle (cpSRP)-targeting components, *J Biol Chem 285*, 34220-34230.